邦文概要

Fundamental Research on Human-friendly Motion Control

（人間親和型モーションコントロールに関する基礎研究）

呉 世訓

この学位論文は人間親和型モーションコントロールの確立を目指している。近頃様々な福祉機器が注目を浴びているが、制御工学的な観点からそれらの機器をどのように制御するかというソリューションを与えることを目的に、以下の三つの対策を本研究では行った。

(1) 人間親和型モーションコントロールに必要な条件を提案する。

(2) フィードバック制御を人間親和型モーションコントロールの観点から再考する。

(3) パワーアシスト車椅子を具体的な適用例として用いて様々な人間親和型コントロールを適用する。

この人間親和型モーションコントロールは人間に快適感と安心感を与える動きを取り扱っていて、人間が行っている制御とも深い関係がある。それは、人間のような筋肉と神経システムを必要としているということでもある。適切に制御しているモータを筋肉システムに、また制御器の中のオブザーバを神経システムとして利用することができるのである。ということで、本論文ではフィードバック制御とオブザーバ設計に関する研究を行う。

モータを人間親和的に動かすためフィードバック制御設計をインピーダンス制御の観点から見直し、インピーダンス制御が多数のフィードバック制御（位置制御、速度制御、力制御）の一般化した形であることを示した後、その観点から制御器をどう設計するかということを考察した。さらに、フィードバック制御における新しい二つのトピック、非整数次インピーダンスと二関節筋モデルのモーションコントロールへの応用を人間親和型的モーションコントロールの観点から紹介した。

これらの考えに基づき、いくつかのアドバンスト制御をパワーアシスト車椅子に適用した。

まず、車椅子の運転状況をモニタリングするオブザーバを設計した。前述したように、車椅子を安全に走らせるために神経システムが必要であり、そのため多数のセンサーを用いることも考えられる。しかし、必要なだけセンサーを利用するということは合理的でないだけでなく、そのセンサーが直接必要な情報を提供しない限り、またセンサー自体が弱点を持っているときに正確な情報を得るにも不十分である。この問題を解決するためにオブザーバ設計をベースとしたセンサーフュージョン手法を提案した。この手法は人間親和型モーションコントロールに必要なセンサー（神経）システムを改善する方法になる。

車椅子運転に必要な情報を定義し、それを得るためのオブザーバを設計した。この提案する運転状況オブザーバはエンコーダ、ジャイロスコープ、加速度計を利用し、前後方向の速度、車体の傾き角度、そして外乱を観測する。このオブザーバはジャイロスコープのド

リフト現象と低速における速度観測の問題点などを克服したものであり、その有効性が実験によって確かめられた。得られた情報を利用し、外乱抑制制御器を設計した。産業応用のためには多数の外乱抑制制御器が利用されているが、それらは外乱を完全に抑制するのを目的としており、そのまま福祉機器に利用するのは難しい。乗り物に乗っている人間は前後方向には速度制御に、左右方向には力制御に慣れている。この特徴を車椅子のような乗り物の外乱抑制制御を設計するとき考慮すべきである。これを考慮し、車椅子のための二種類の外乱抑制制御をインピーダンスの概念を利用して設計した。前後方向の速度ベースの外乱抑制制御と左右方向の力ベース外乱抑制制御がそれである。これらの制御器は実験によってその有効性が確かめられた。人間親和型モーションコントロールのもう一つのトピックは外乱増幅制御である。人間自体がモータの制御から見た場合には外乱となるので、もし強い外乱抑制制御が人間の身近で利用される機器に利用されると人間の動作に反する方向でモータが動くことになり、とても危険な状況を招くことになる。この理由で時には人間の力を増幅する制御が必要になるのである。この外乱増幅制御もインピーダンス制御の観点から実現することが可能で、その例として車椅子用のトルクセンサーレスパワーアシスト制御器を設計し、実験を行った。

最後に人間親和型制御器設計例として時変インピーダンス制御器を設計した。自分の動作を見ていると人間は時変制御を行っていることが簡単にわかる。車椅子の片手漕ぎ制御器を時変制御器の例として設計した。左右方向のインピーダンスが一つ変数を持って変えられるフィードフォワード制御とフィードバック制御を提案し、車椅子の方向がその変数によって決められるようにした。このインピーダンスを決める変数は人間の力の勢いを入力とするシグモイド関数によって決められるようにし方手漕ぎを実現した。

この論文で提案した制御例は、一つのシステムを統合的に人間親和的に設計することができることを見せるためパワーアシスト車椅子に焦点を合わせているが、同一な考え方を他の福祉機器に拡張して応用することも可能なのである。

なお、本文は英語により記述されていることを付記する。

Abstract

This dissertation aims at the establishment of human-friendly motion control. To provide a solution to the need for emerging advanced welfare tools in terms of control design, three measures are taken in this dissertation.

(1) The requirements for human-friendly motion control are suggested.

(2) The feedback control is reconsidered in the viewpoint of human-friendly motion control.

(3) A power-assisted wheelchair is adopted as an application, and various human-friendly motion control designs are applied to the wheelchair.

This human-friendly motion control deals with the motion that makes a human user feel comfortable and at ease, and is related to the human-like motion control, which means it needs to have the muscular and sensory systems, too. The motors with controllers can work as the muscular system, and observer in the controller can work as the sensory system. From this viewpoint, the design of feedback controllers and an observer is studied here.

To control a motor in a human-friendly way, feedback control design is scrutinized and it is found out that the impedance control provide a general way to describe various kinds of feedback control - position control, velocity control, force control - and an insight to adjust the design of a controller to make it human friendly. Moreover, two novel topics on the feedback control design - design of fractional order impedance and application of the biarticular muscle to motion control - are introduced.

Based on this idea, several advanced controllers are designed for a power-assisted wheelchair.

At first, an observer is developed to monitor the driving state of a wheelchair. The sensory system, as mentioned above, is necessary to control a wheelchair in a safe way, for that reason, various sensors may be employed. However, just using as many sensors as necessary is not rational nor enough to obtain correct information when sensors cannot provide the direct value of necessary information, or have drawbacks. To cope with this problem, a sensor-fusion method based on the observer theory is proposed here, and this is a solution that can improve the sensory system necessary for human-friendly motion control.

Necessary information for control of wheelchair driving is defined and an observer is designed to acquire that information. The proposed driving state observer for a wheelchair uses an encoder, a gyroscope, and an accelerometer to produce the longitudal velocity, body-inclination angle, and external disturbance. This observer can overcome the drift phenomenon in the gyroscope and the difficulty in acquisition of velocity at low speed, which is verified by experiments.

Using the obtained information, disturbance attenuation control for a wheelchair is devel-

oped. A number of disturbance attenuation controllers are used in industry. Nevertheless, they need to be modified when adopted in welfare tools as industrial control applications are adjusted to reject all disturbances completely. A human rider in a vehicle is accustomed to the velocity control in the longitudal direction, and the force control in the lateral direction. These characteristics should be included in the design of human-friendly disturbance attenuation control for a vehicle such as a wheelchair. Taking this into considerations, two kinds of disturbance attenuation controllers are designed based on the impedance concept: velocity based disturbance attenuation for the longitudal direction and force based disturbance rejection control for the lateral direction. These controllers are experimented and the effectiveness is verified.

Another topic for human-friendly motion control is disturbance amplification control. A human operator itself is a disturbance from the viewpoint of motion control so that strong disturbance rejection control, if it is employed for a tools used nearby people, is dangerous for it operates a motor in a way against human user. For this reason, the force exerted by a human operator occasionally needs to be amplified. This disturbance amplification control also can be realized using the impedance concept and as an example of this control, torque-sensor-less power-assist control for a wheelchair is proposed and experimented in this dissertation.

Lastly, time-varying impedance control is developed as a human-friendly motion control design. It is easily known from our own motion that a human adopts time-varying control for his own behavior. One-hand propulsion control of a power-assisted wheelchair is proposed as an example of this time-varying control. By the proposed feedforward power-assist control, and feedback power-assist control, where the impedance for the lateral direction is be changed by one variable, the direction of the wheelchair will be determined by the variable. This impedance-determining variable is altered via the sigmoid function with the momentum generated by one hand as the input, and this enables the rider to propel the wheelchair with one hand.

All the applications suggested in this dissertation are focused on a power-assisted wheelchair to present that a controller for one system can be wholly designed in a human-friendly way, however, the basic ideas that are applied for the design of the wheelchair control can also be employed for other welfare tools.

Sehoon Oh
(sehoon@horilab.iis.u-tokyo.ac.jp)

Acknowledgement

First of all, I should thank God still wondering this dissertation is worth starting with this thanks to God. I want to thank God for Him to allow me to do this research, and if there is some noticeable wisdom or knowledge, it must come from Him.

I cannot thank enough my supervisor, Prof. Yoichi Hori for his valuable advice on this work and all the supports he gave me. It has been over 8 years since he taught me. He taught me many things not only what to my research and how to research, but also how engineering and a researcher should be. His practical insight into motion control stimulates me and helps me constructing my knowledge on motion control. Apart form this academic guidance, I also owe a great deal of thanks for his helps that has supported my student life in Japan. I am very grateful for and proud of being a member of his laboratory.

I owe a great deal to the former and current members of Hori laboratory. Mr. Toshiyuki Uchida, the technical staff, helped me both in the technical and official work, and also Ms. Ochi, the secretary, helped me with lots of official work. Prof. Yeonghan Chun and Dr. Kyungwhan Kim in Korea, Dr. Shinichiro Sakai, Dr. Hiroshi Fujimoto, Dr. Fumiyasu Suzuki, Dr. Hichirosai Oyobe and Dr. Hirokazu Seki and all other members who spent they time with me for last 8 years taught me a lot of things during their student time. Especially Dr. Shinichiro Sakai and Dr. Hiroshi Fujimoto frequently advised me on my way of research after they graduated. They were role models for me.

I also appreciate all my colleagues. Dr. Chengbin Ma, Dr. Nobutaka Bando and Dr. Naoki Hata were good colleagues. I thank them for the helpful discussions, support, comradeship and entertainment. Especially, Dr. Hata gave me great helps to set up the experimental wheelchair. Discussion with him stimulated me and helped me in finding out some topics in this research. I also wish to thank Byunghoon Chang, Hou Ka, Yoshifumi Aoki, Kiyotaka Kawashima, Wei Li, Syousei Ryu, Lu Wu and other present members of Hori laboratory.

Special thanks to all the members in the office (including COE office) of the electrical engineering department of the University of Tokyo for assisting me in scholarship and dormitory applications and many other different things. Ms. Yagyu, Ms. Ohno, Ms. Tanaka, Ms. Fukano and Ms. Shigihara deserve special mention.

I have been supported financially by the 21st century COE program in Electrical Engineering and Electronics of the University of Tokyo and The Honors Scholarship for Privately financed International Students. For this assistance, I am very grateful.

Finally, I am forever indebted to my mother. She is the reason why I am.

Contents

List of Figures

List of Tables

Chapter 1

Introduction

1.1 Introduction of Human-friendly Motion Control

Advanced technologies will play an important role in the coming aging society. Among those technologies, information related technology seems to be most highlighted nowadays. However, it only provides informative and virtual support and cannot physically support human behavior.

The function of human is getting worse as he gets older. If he can find a satisfying mechanical substitute for his lost, it would be a best help to him. For those who lost their function, power assistance by motors and its appropriate control are more important and necessary technologies.

Moreover, not for those handicapped people but also for healthy people, extension of human power by mechanics is considered as an important technology and has been one of scientists' dream. We can see a large number of those examples in sci-fi movies. Let us call this kind of tools as power assistance or power assist devices. This dissertation aims at suggestion of a viewpoint for design of control which makes the power assist devices work satisfactorily.

What we should note in considering how to design a controller, is that these devices are usually located near a man or attached to one's body, and amplify human power. This operational environment makes the control design difficult, and this is a problem unique to these devices. For an example, power assist devices should move in such a way that the user does not feel it uncooperative or clumsy because human has a variety of sensors and thus is very sensitive to external force. This contact with the user is a main problem in the development of power assist devices.

In this dissertation, a new concept, human-friendly motion control is suggested as a general form of solution to this problem.

1.1.1 Requirements for the Human-friendly Control

What characteristics are required for the human-frinedly motion control? The following four characteristics can be suggested as the requirements.

Adaptation to the environment

(a) HAL by Sankai Lab.

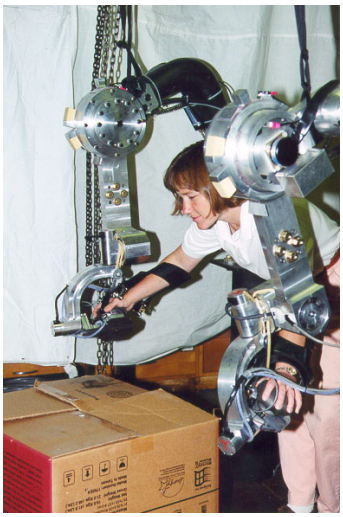

(b) Extender by U.C.B

(c) ASIMO by Honda

Figure 1.1: Various devices which help human activities

The range of human activities is large. Power assist devices used to support these human activities should adapt to various environment.

Excellent Manipulability

Power assist devices are located near a man. Every movement of the devices will affect user's sense directly. So as not to make user feel uncomfortable, the controller should present excellent operational performance.

Elaborate response to disturbance

Disturbance is defined as exerted force which is not produced from the controller. In this meaning, human power is a disturbance to the controller, and strict rejection of this disturbance can make dangerous situation or awkward operation. Response to this disturbance should be designed elaborately

Useful evaluation of control

There are little established standard that can be used for the evaluation of how human-friendly the controller is. It is due to the difficulty in description of the performance in mathematical way. In other words, if this evaluation is established, design of human-friendly control becomes easier.

Solutions to each problem will establish the human-friendly control. Contents explained in the following chapters are related to these four requirements.

Figure 1.2 shows some solutions to these requirements that are provided in this dissertation. These are not the only solutions but it is suggested through these solutions that the advanced control theories can be applied to power assist devices if it is designed adequately. A viewpoint necessary for the design of the human-friendly control, and examples of that design are provided in this dissertation.

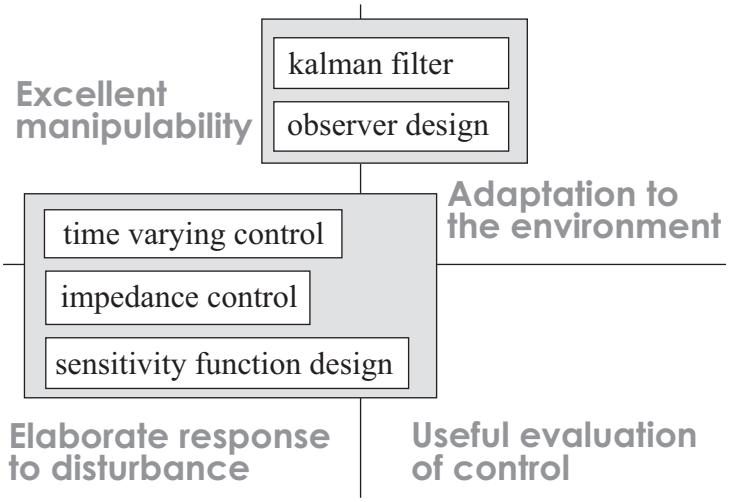

Figure 1.2: Proposed solutions in this dissertation for the human-friendly motion control

1.2 Why Power-assisted Wheelchairs?

Walking or mobility is the basic function of a human body and should be indeed excellently supported. The wheelchair has been a most successive solution. It has helped lots of handicapped people during the last 100 years. The success of the wheelchairs throughout the industrialized world has rendered the wheelchair almost universally recognized and a cultural symbol representing all disabled people.

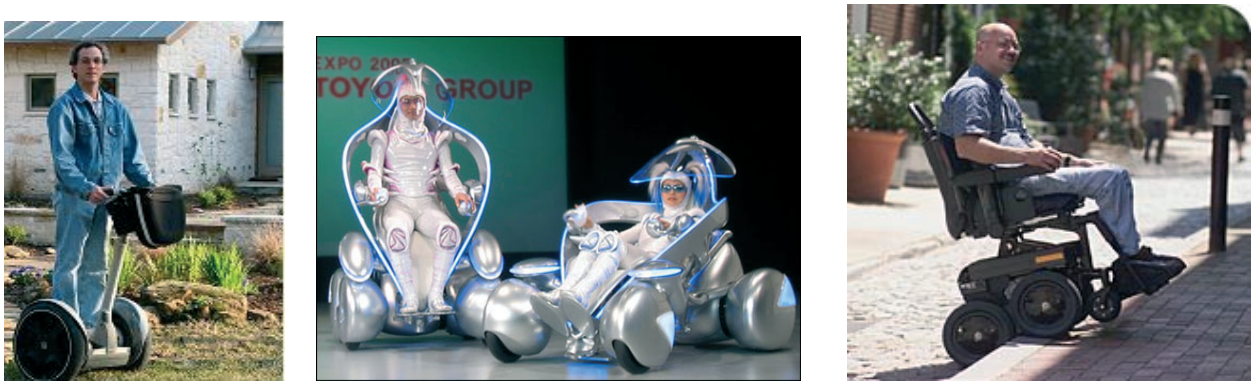

(a) Segway^{TM} (b) I-unit ©Toyota (c) iBOT^{TM} ©INDEPENDENCE

Figure 1.3: Walking assistive devices with wheels

Development of modern technology is changing this situation. Recently, advances in engineering enable various kinds of mobility assistive devices. Figure 1.3 and 1.4 show those advanced devices. The devices in Figure 1.3 have wheels for mobility and the wheels are driven by motors. Figure 1.4 are walking assistive devices that have legs.

Devices with legs are still under development and cannot yet give sufficient assistance: they are quite slow and have problems in their safety. In spite of their outstandingly wide rage of locomotion, these imperfections are great obstacles to establish this type of

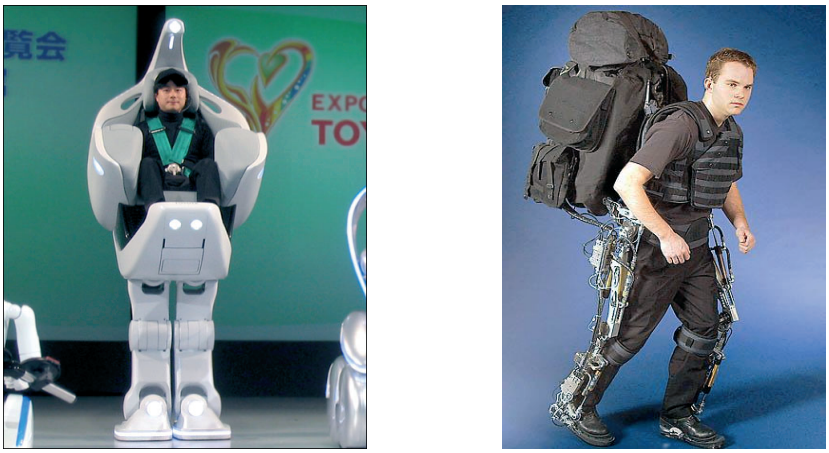

I-foot by Toyota　　Berkeley Lower Extremity Exoskeleton

Figure 1.4: Walking assistive devices with legs

assistance.

Figure 1.5 shows the characteristics of these walking assistive devices. Realization of wide range of locomotion, fast velocity, and stability still has lots of problems to solve. The mechanical legs can provide wide range of locomotion, but the control still has stability problems, thus it can not provide fast velocity. On the other hand, the electric powered wheelchairs use vehicle technologies which are already established, and give sufficient stability and velocity. However, the interface between the wheelchair and the user is restricted to a joystick, which will work only in restricted ways and allows only narrow range of locomotion.

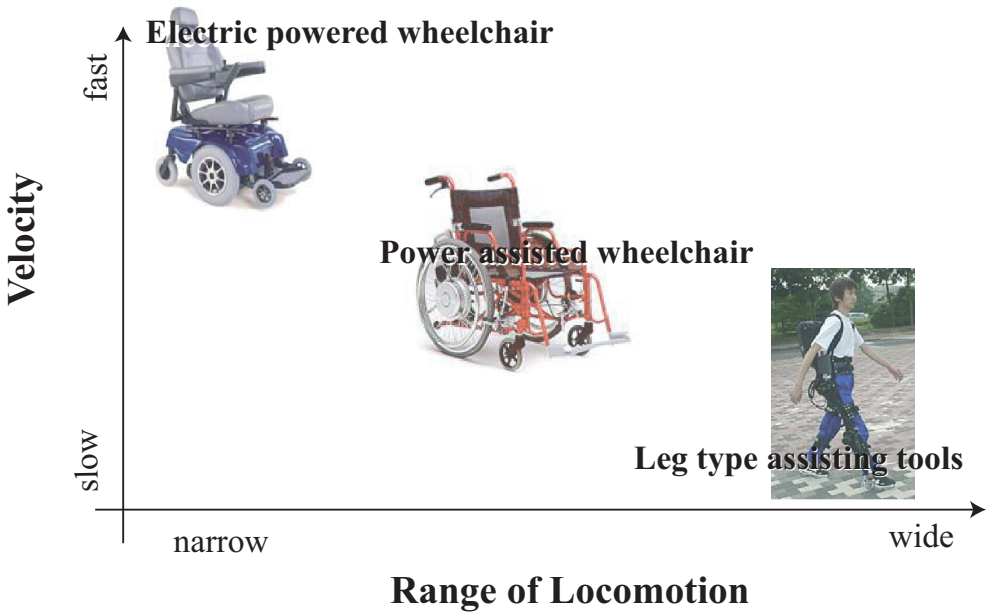

Figure 1.5: Diagram showing characteristics of walking assistive devices

Here, the power-assisted wheelchair is adopted as an application which needs the human-

friendly motion control. This power-assisted wheelchair presents good stability characteristic with wheels, and also provides good manipulability. The system is a kind of human-machine interaction system, thus it needs sophisticated control. This is the reason this power-assisted wheelchair is selected as an application of the human-friendly motion control.

1.3 Power-Assisted Wheelchairs Now

In Japan, there are few commercial power-assisted wheelchairs. Figure 1.6 shows one of the power-assisted wheelchairs that is available in Japan: JW II produced by YAMAHA.

Figure 1.6: Power-assisted wheelchair as an example of power assist device(YAMAHA JW II)

Power assistive control implemented in this wheelchair is depicted in Figure 1.7. JW II has a torsional sensor between a rim and a wheel and it can measure the torque exerted by a rider (T_{human} in Figure 1.7). Then the assisting motor provides assisting torque

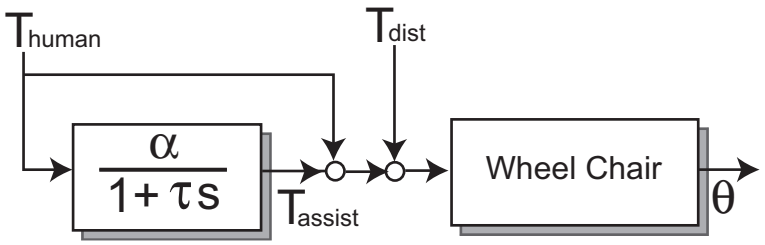

Figure 1.7: Power assist control in conventional power-assisted wheelchairs

(T_{assist}) according to the measured torque (T_{human}). The relationship between T_{human} and T_{assist} can be described as

$$\frac{\alpha}{\tau s + 1}, \tag{1.1}$$

where α is an assist ratio and τ is a time delay.

This is a feedforward control and does not feedback any information of the wheelchair. Consequently this controller has some problems. On a slope, the assisting torque works as a torque that makes the wheelchair tip over instead of as the torque drive the wheelchair forward. Also on downward hills, the assisting torque should decrease the acceleration by the gravity to make the wheelchair safe. However, this feedforward control does not decelerate the wheelchair; on the contrary, it works in the same direction with the gravity and endangers the rider. Figure 1.8 illustrates these dangerous situations.

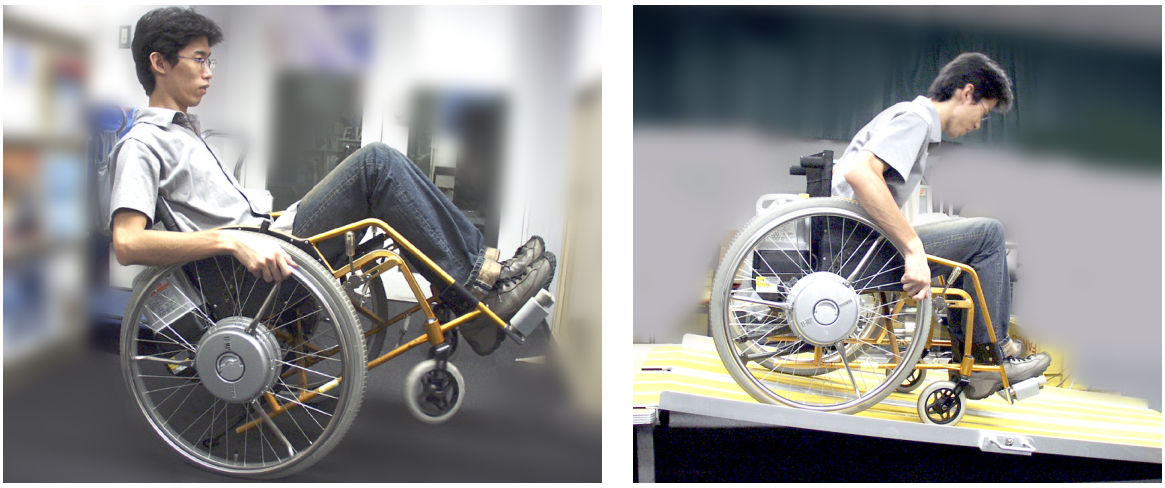

(a) Tipping over of a wheelchair (b) On downward hill

Figure 1.8: Dangerous operational conditions

1.4 Outline of the Dissertation

First in Chapter 2, various kinds of control design methods are redescribed based on one structure. To design a controller in a human-friendly way, how the controller works or what meaning each parameter in the controller has should be scrutinized. From the viewpoint of human-friendly control, the kind of physical value controlled by the controller is important; There are force control, velocity control, and position control to control force, velocity, and position. In Chapter 2, these controllers are generalized in the form of impedance control which has been regarded as one kind of force control. This viewpoint enables us progress control design in some interesting ways.

In Chapter 3, an operational state observer for a power-assisted wheelchair is provided. Estimation of velocity and inclination angle is one of well-known problems in humanoid robots. The power-assisted wheelchair also has the same problem because its body can tip over when excessive torque is applied to the wheels. Furthermore, the angle of slope on which a wheelchair is located works as a dominant factor in identifying the environment, and should be estimated correctly. This topic is studied in the Chapter 3.

In Chapter 4, two disturbance or external force attenuation controllers are designed.

Two-dimensional disturbance to a wheelchair is considered here: the front direction and the lateral direction. For each direction, different control strategy is necessary, since the way that the user will feel in each direction is different. The viewpoint explained in Chapter 2 is used and applied in the design of two disturbance attenuation controllers.

Chapter 5 solves force-sensor-less power assist problem without force sensor. In power assist control, force sensor is utilized to obtain the exerted force by a user, but this causes inconvenience since it restricts the place where the user's force should be applied. This controller can be designed also using the viewpoint explained in Chapter 2. Power assistance can be translated as soft impedance. This is the strategy in the design in this chapter.

Human-friendly motion control can have time-varying characteristics to be human-friendly. Chapter 6 tries this time-varying control for human-friendly motion control. A fuzzy way that transmits a user's intention is adopted and experimented. This chapter insists that motions which are somewhat complicated can be controller with a simple parameter depending on the way a controller is designed. If that dominant parameter is changed according to a specific law, the actuator can work in a complicated but human-friendly way.

Chapter 2

Generalization of the Feedback Control for the Human-friendly Control Design

In establishing of human-friendly motion control, a question "what kind of control is necessary for the human-friendly motion control?" can be important. Instead of answering this question, answers to a question "what function does control can do?" is studied in this chapter.

A solution to the design of human-friendly motion control is provided by suggesting various impedances that will be realized by feedback controllers

2.1 Impedance Control as a Solution to Human-friendly Motion Control

What should we consider in designing human-friendly motion control? At first, let us take up an example of humanoid robot control. The purpose of this control is to make a robot behave in a more human-like way. However, this control of a robot in a human-like way is a quite complicated problem. That kind of control is something different from making of an animation movie of robots where the tracking of position is most important. In robot control, more than an accurate position control is necessary: especially force which is invisible should be considered. This view clarifies what we should focus on in design of human-friendly motion control, since human-friendly motion control is strongly related to human-like control.

Conventional industrial controls tend to regard the accuracy as the most important factor. On the other hand, in human-friendly motion control, that accuracy is not so important factor. Human being controls his position, velocity and force less accurately. More important point is that human being continuously changes his target of control. This brings us a good insight to human-friendly control. The impedance control which has been considered as one kind of force control, is a good candidate for a solution to this human-friendly motion control because it is a general form of position, force, and velocity controls.

2.1.1 Disturbance Rejection Used in Conventional Controllers

As we explained in Section 1.1.1, design of the disturbance response plays very important role in human-friendly motion control. Power assist devices compensate for human forces against external force. Human force, however, itself can be a disturbance or external force when it is seen from the controller. This is a noticeable point in the design of human-friendly motion control. For this disturbance response design in a human-friendly way, impedance control is adopted in this dissertation. Before analyzing this impedance control, the disturbance observer is explained here for comparison.

The disturbance observer in Figure 2.1 is a typical method of the disturbance rejection in industrial motor controls. This disturbance observer can estimate external forces and modeling error as disturbance, and remove them with the feedback of estimated disturbance. This aims at robust and perfect disturbance rejection up to high frequency ranges. As discussed before, this strong disturbance rejection is not suitable for the power assist control. Disturbance in power assist devices can be related to human forces itself in many cases. Stiff rejection of disturbance can worsen the operational performance and even make dangerous situation. The adjustable parameters in the disturbance observer, however, are only suitable for the stiff rejection, and do not provide enough degree of freedom for the flexible disturbance attenuation. In order to render disturbance response more human-friendly, more variety in adjustable elements in control design is necessary, and it would be better if those elements have physical meaning.

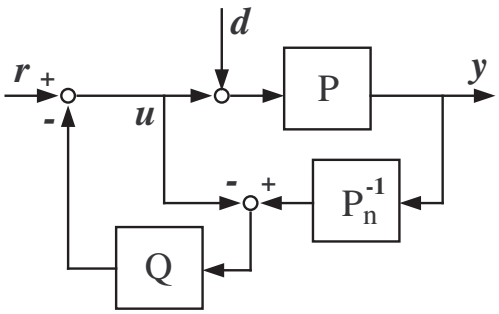

Figure 2.1: Structure of the disturbance observer

Q in Figure 2.1 is the adjustable parameter the disturbance observer has. With this Q, the output of y is given as

$$y = \frac{P}{1 + Q\left(P_n^{-1}P - 1\right)}r + \frac{P\left(1 - Q\right)}{1 + Q\left(P_n^{-1}P - 1\right)}d. \tag{2.1}$$

As is well known, when $P_n = P$ then the disturbance d is estimated correctly and removed according to $1 - Q$. If Q is 1, the disturbance is rejected to zero and this yields the output $y = P_n r$, which means the reference response is nominalized; that is, this parameter Q is a parameter for the stiff disturbance rejection not adequate for detailed configuration of the disturbance response.

To study this characteristic for detail, $Q(s)$ is given as the equation (2.2) which is used most generally. This results in y in the equation (2.3).

$$Q(s) = \frac{K}{\tau s + 1} = \frac{1 - \Delta K}{\tau s + 1} \tag{2.2}$$

$$y = Pr + \frac{\tau s + \Delta K}{\tau s + 1} Pd \tag{2.3}$$

Figure 2.2 shows the bode diagram of the transfer function from d to y where P is a first order delay system.

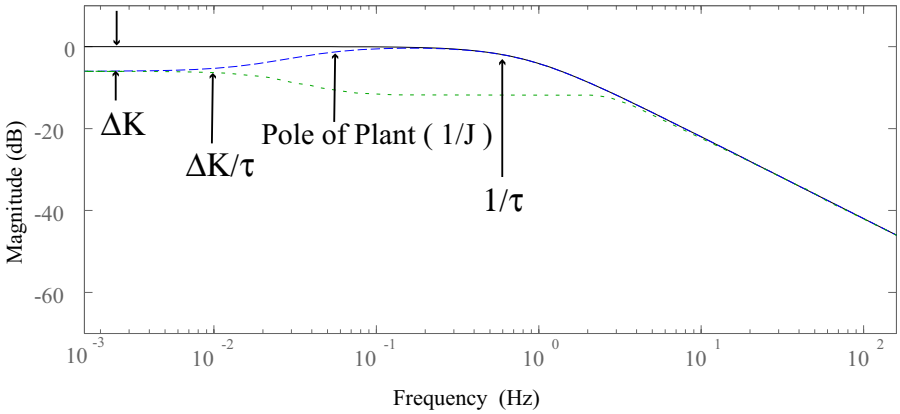

Figure 2.2: Disturbance response by the disturbance observer

K (or ΔK) determines the extent of rejection in low frequency band and τ determines the frequency bandwidth. This is an explanation using a frequency viewpoint and the parameters have less physical meaning. However, impedance control has parameters that will physically account for the disturbance response.

2.1.2 Equivalency of Impedance Design and Sensitivity Function Design

Here, the relationship between reaction force by a motor and the impedance that a man will feel when he applies his force to the motor is revealed. The disturbance response has the same meaning of impedance or the reaction force by a controller. Figure 2.3 illustrates this viewpoint.

If an external force F_e is applied to the plant by a man, the position y is changed from the original reference position y_r. In addition, when a motor is controlled by a feedback controller, it will produce F_m based on Δy or F_e. This F_m is the reaction force that the man who applies the force F_e will feel.

Under a feedback control, Δy is decided not only by the disturbance force F_e but also the motor force F_m; that is, the position will be moved, after applying F_e, to the equilibrium point where F_e and F_m (according to Δy) makes a balance. This leads to an equation

$$F_m(\Delta y) \simeq F_e \tag{2.4}$$

a) Reference position (y') is changed according to the external force(F_e).

b) Motor torque (F_m) is changed according to the displacement (Δy).

Figure 2.3: Equivalency of impedance design and sensitivity function design

It is true that in the transient process, two forces are not equivalent. Nevertheless, the assumption as the equation (2.4) is effective; when the two forces have a large difference the position y will reach the equilibrium point quite shortly and if the transient process takes long time, it means the two forces have almost same values. This viewpoint tells us the equivalency of the impedance design and the sensitivity function design. The reaction force decided by the impedance control is equivalent to the rejection force decided by the sensitivity function.

Equation (2.5) and (2.6) represent the relationship between the deviated positon Δy and the external force F_e or the control force F_m by a motor.

$$\Delta y = \frac{1}{M_d s^2 + B_d s + K_d} F_e \tag{2.5}$$

$$F_m = \left(M_d \Delta\ddot{y} + B_d \Delta\dot{y} + K_d \Delta y\right). \tag{2.6}$$

In impedance control, $M_d s^2 + B_d s + K_d$ in Equation (2.5) is called as impedance and means the relationship between the applied external force(F_e) and the deviated position errorΔy. Mostly this relationship is realized by changing the reference position y_r, which is illustrated in figure 2.3 (a). The impedance control uses measured force F_e and calculates Δy according to the equation (2.5) and then the modified reference $y'_r = y_r + \Delta y$ is provided to a position controller.

Sensitivity function decides the reaction force F_m which is provided by a motor according to Δy. Equation (2.6) shows the reaction force design based on Δy. Under the assumption (2.4), this control design is equivalent with the reference design in Equation (2.5).

In the following sections, the impedance is defined the transfer function from the external force F_e to the deviated velocity $\Delta\dot{y}$. By this definition, the impedance described in Equation 2.5 is rewritten as

$$\frac{s}{M_d s^2 + B_d s + K_d}. \tag{2.7}$$

The reason for this definition will be explained in Section 2.2.2

2.2 Sensitivity Function Design as a Specification of Human-friendly Control

2.2.1 Design of a Feedback Control using the Impedance Concept

From the viewpoint explained in the last section, the feedback control which has the structure in Figure 2.4 can be translated as an impedance controller. The difference between the real output and the nominal output will be Δy in Figure 2.3 and the reaction force F_e is created through the C filter.

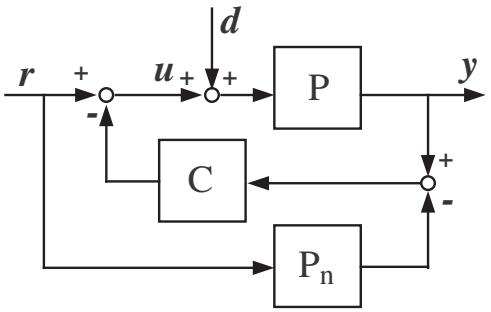

Figure 2.4: Basic structure of impedance control proposed in this research

This impedance control block diagram is interpreted as a two degree-of-freedom control. By this control, the response of the plant will be:

$$y = P\left(\frac{1+CP_n}{1+CP}r + \frac{1}{1+CP}d\right). \tag{2.8}$$

The reference response from r to y will be P if P_n is P, and the disturbance response will be given as $\frac{P}{1+CP}$. This respective responses are the feature of the two-degree-of-freedom (TDOF) control [12]. Conventional TDOF control design such as [12] uses the disturbance observer for the design of the disturbance response with an object of stiff disturbance rejection. In the human-friendly motion control, on the other hand, design of this $\frac{P}{1+CP}$ should be done more carefully. What this dissertation insist, is this disturbance response be designed using the impedance concept explained in the last section because this $\frac{P}{1+CP}$ can work in the same way with $\frac{1}{M_d s^2+B_d s+K_d}$ in Equation(2.5) if C is a properly designed.

The passive adaptive control in [13] has the same structure with Figure 2.4. The literature [13] adopted βP_n^{-1} as C, which resulted in a disturbance response as

$$T_{yd} = \frac{1}{\beta+1}P \tag{2.9}$$

under the assumption $P = P_n$. If β is large, the effect of a disturbance is suppressed strongly with the gain $\frac{1}{\beta+1}$ over a wide frequency range. Because of this purpose of design, the passive adaptive control is different from the approach taken in the dissertation even though it has the same structure.

Figure 2.5 shows two design examples which will be adopted in the following chapters. The feedback control in the figure 2.5 (a) named as velocity based impedance has no stiffness

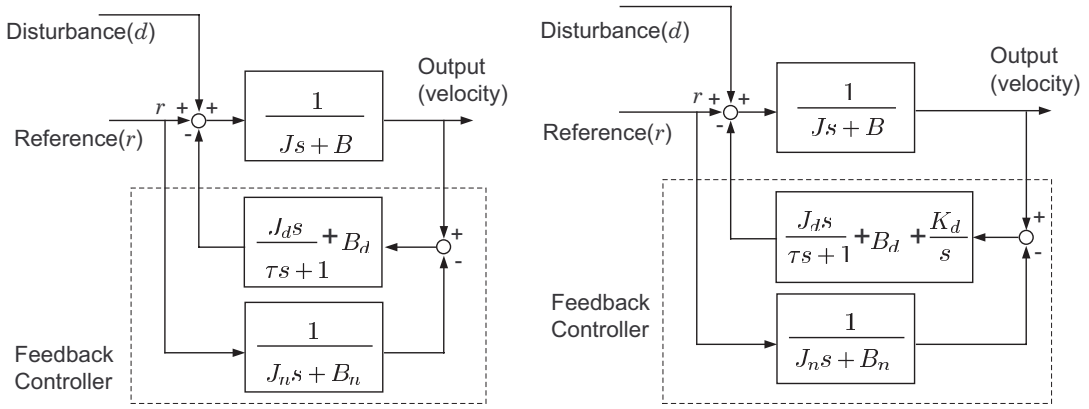

(a) velocity based impedance (b) position based impedance

Figure 2.5: Various types of impedance control

term. Its impedance is given as

$$\frac{1}{(J+J_d)s+(B+B_d)}. \tag{2.10}$$

The reaction force and the motion provided by this control are illustrated in Figure 2.6 (a). This plant has no stiffness term so that is not restricted to a certain position and the final position will be changed by the external force; in other words, the position will not go back to the original position after the disturbance dies. In addition, the hand, or the one who applies the external force to the plant will feel the reaction force mostly proportional to the moving velocity.

On the other hand, the control described in Figure 2.5 (b) has position based impedance or a stiffness term. The impedance is given as

$$\frac{s}{(J+J_d)s^2+(B+B_d)s+K_d}, \tag{2.11}$$

when the plant itself has no stiffness against the external force. A plant controlled by this controller works in the way illustrated in Figure 2.6 (b). The position is restricted and if the disturbance is taken away, the position will restore to the original position. Consequently, the hand in Figure 2.6 (b) feels the reaction force mostly proportional to the changed position. This analysis can be also explained using the bode diagram, too.

Figure 2.7 is bode diagrams of this two impedances. Transfer functions from the disturbance to the velocity output are described by these diagrams. Compared with the disturbance observer (Figure 2.1 and 2.2), the parameters J_d, B_d, K_d in the impedance control have physical meanings and it is also presented in the bode diagrams. J_d, B_d and K_d decide the characteristics of high frequency, middle frequency, and low frequency bandwidth respectively. Values of J_d, B_d and K_d represent the extent of rejecting force against the disturbance in each frequency bandwidth and it also represents the magnitude of the

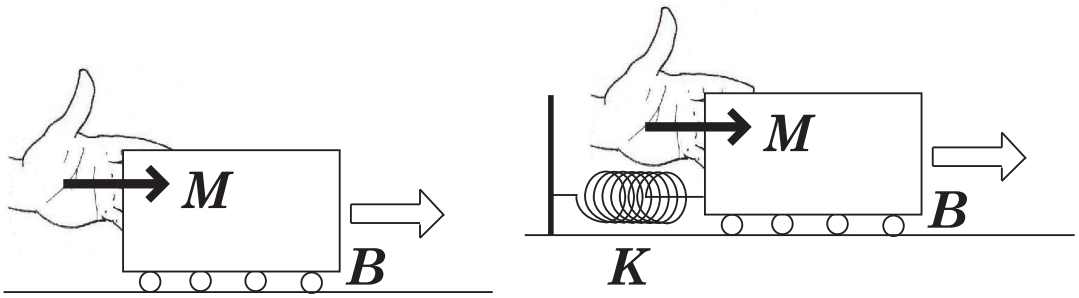

(a) velocity based impedance (b) position based impedance

Figure 2.6: Illustration of the difference between the two types of impedance

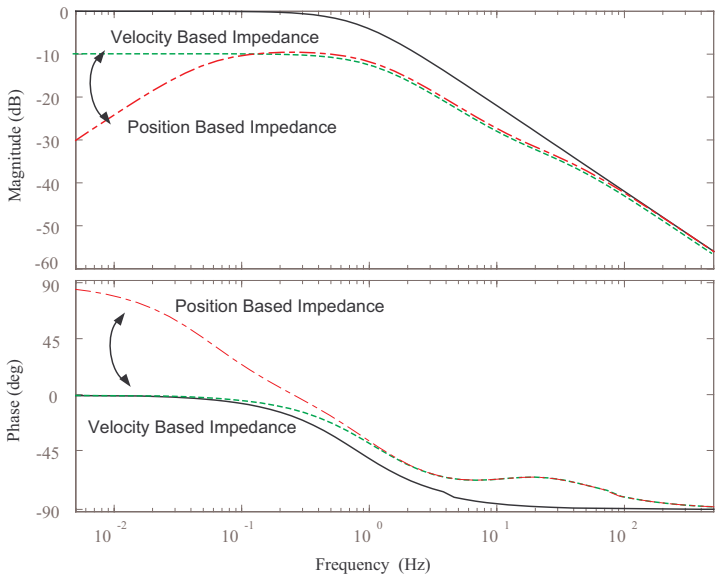

Figure 2.7: Difference between the two types of impedance described in bode diagram

reaction force to the disturbance. It should be noticed that the characteristics of the low frequency determines in which way a plant moves: (a) or (b) in Figure 2.6.

This viewpoint helps us design a sensitivity function in the human-friendly motion control.

2.2.2 Unification of Position, Velocity, and Force Control

More interesting point this impedance-control viewpoint explains is that it is a generalized form which can describe a force control, velocity control, position control and even the disturbance observer at the same time. To discuss this point more in detail, the definition of each control should be redefined. This redefinition may be different from that used in conventional ways; however, it is definition necessary in terms of the human-friendly motion control.

position control control to make the position of a plant track the reference position, feedbacks position information.

velocity control control to make the velocity of a plant track the reference position, feedbacks velocity information.

force control control to make a plant react in a specific way to the external force, feedbacks force information.

Figure 2.8 is block diagrams of position control (a) and force control(b), which are used in the literature [1] but is modified here.

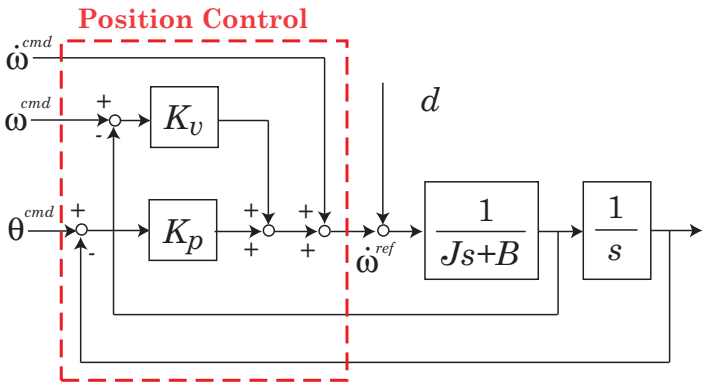

(a) Position control block diagram

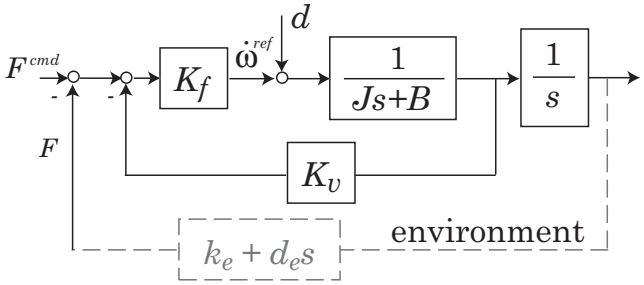

(b) Force control block diagram

Figure 2.8: Block diagrams of two different controllers

In Figure 2.8 (a), the position output (θ) is fed back and is controlled to track the reference position (θ_{cmd}) and in (b) the force applied externally is fed back. The above definition tells us that the position based impedance control is categorized into the last section is included in position control and the velocity based impedance control is categorized into velocity control. Force control feedbacks force information of the plant, but is somewhat different from the other two controls because its purpose is not tracking. Another interesting point in force control is that the disturbance observer is categorized into force control because it feedbacks the estimated force.

One of the purposes is to eliminate applied external force; the disturbance observer (Figure 2.9) works for this purpose so that it completely removes the estimated disturbance. The other purpose of the force control is to change the reference position of a plant according

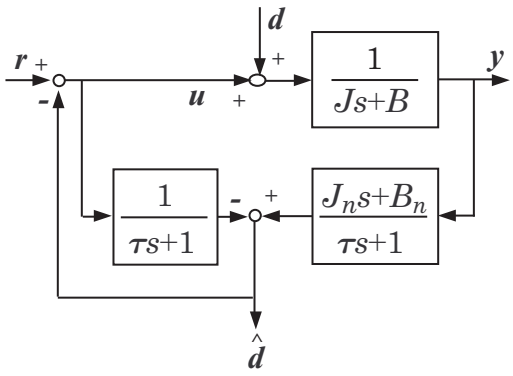

Figure 2.9: Disturbance observer as a force controller

to external force so that it can make specific reaction force to the disturbance. This is the way the impedance control works. It changes the position of the plant according to the external force. These two different force controls result in different reaction forces. Elimination of the external force provides the same force as the external force, which means the disturbance or the hand in Figure 2.6 feels extremely strong reaction force, while the impedance control provides somewhat weak or flexible reaction force. In spite of these differences, the two force controls can be considered in the same way and the difference just result from the difference of some parameters. And furthermore even position control and velocity control also can be considered in the same structure. This analysis was roughly reported in the literature [1], but here it will be examined in more detail.

Figure 2.10 shows the block diagram of impedance control. This is the general form of feedback controllers that can unify position control, velocity control and force control.

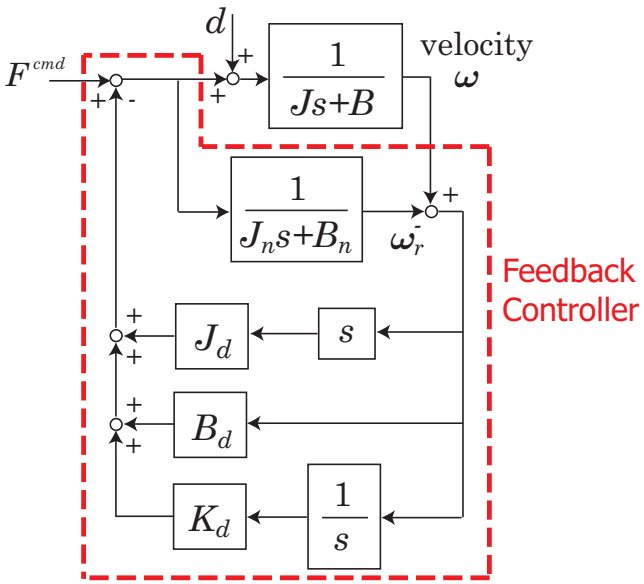

Figure 2.10: Impedance control as general motion control

Following explanation is done under the assumptions $J_n = J, B_n = B$. Velocity of the plant is used as output of the plant because it is the dimension located between force and position. The output error e is driven by the disturbance d, the external force.

$$e = \omega_r - \omega = \frac{1}{Js + B} d \tag{2.12}$$

It is clear that the output error has information on the external force. Using this error, the feedback control input is decided as

$$u_{fb} = \left(J_d s + B_d + \frac{K_d}{s} \right) e \tag{2.13}$$

How to decide these J_d, B_d and K_d determines the type of a controller: position control, velocity control, force control. Basically, a controller with nonzero K_d is a position controller because the position error is fed back and the position of the plant will track the reference position. J_d and B_d are used to improve the speed of response in position control. In force control, however, J_d, B_d and K_d have quite different meanings but the same function; that is, J_d, B_d and K_d are the elements of impedance in force control. With the feedback of equation (2.13), the transfer function from the external force to the position of a plant is given as

$$T_{pd} = \frac{1}{(J + J_d)s^2 + (B + B_d)s + K_d} \tag{2.14}$$

Now we can see that the gains J_d, B_d and K_d have dual meaning according to the viewpoints whether the controller is position control or force control. K_d is the position gain and also stiffness to the external force. B_d means damping in both control. J_d is the acceleration gain but it has a special meaning in force control, especially in the disturbance observer.

Figure 2.11 shows force control and position control re-described in the form of impedance control.

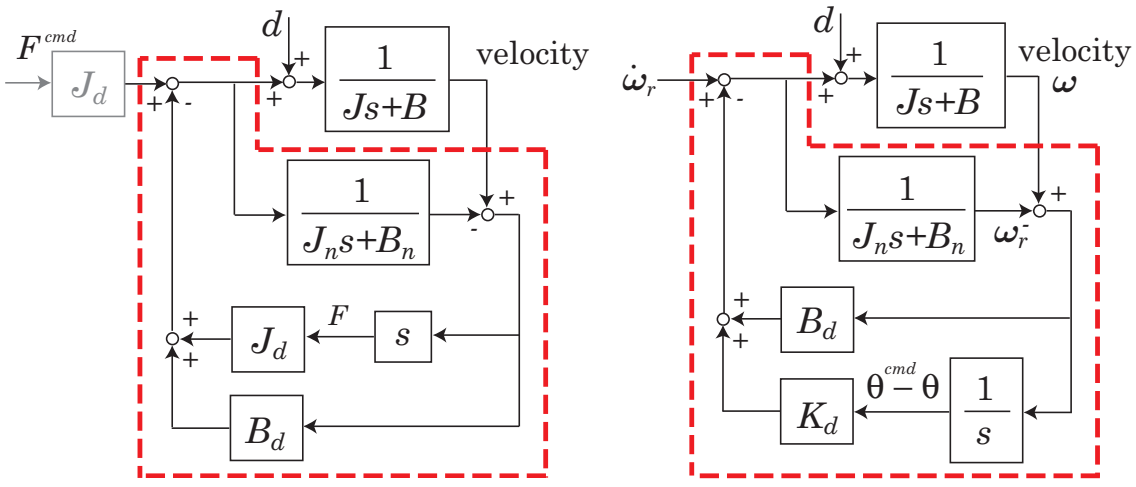

(a) force control type (b) position control type

Figure 2.11: Block diagrams of various control types

To eliminate the steady-state position error, two approaches are usually adopted: position control with integrator and disturbance observer. These two approaches also can be

analyzed from the impedance-control viewpoint. The disturbance observer has special parameters. J_d and B_d is set as J_n and B_n (which is illustrated in Figure 2.12), which makes the sensitivity function in Equation (2.14) zero and makes the plant totally insensitive to the disturbance. To achieve position control with integrator, a second order integration of velocity error will be added to Figure 2.10. This approach is subject to a time delay because the integration takes time. On the other hand, the disturbance observer rejects the disturbance force, and this results in the quite fast reduction of the steady-state error. This is why the disturbance observer is preferred in the industrial control design.

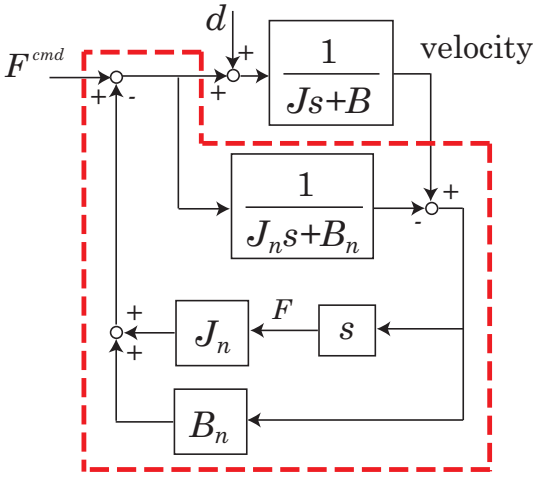

Figure 2.12: Disturbance observer described in the proposed form

This unifying viewpoint gives us an insight into human-friendly control design. Human switches his control strategy, position control and force control, according to the environment. This combination of control types looks complicated, but from the proposed viewpoint, it is nothing but the changes of parameters. As a man changes his control strategy according to the environmental conditions, we can change some gains in the same way.

In Chapter 4, two kinds of disturbance attenuation controller are provided based on this consideration. Furthermore, another novel design can be realized by modifying factors in the impedance. This idea is examined in the following section.

2.2.3 Extension to the Disturbance Amplifying Control

Existing power assist devices use force sensors to measure the force to amplify. This costs expensive and restricts the assistance because the force should be applied to the specific places where the force sensor is installed to obtain assistance. The impedance concept in control design can help this problem, too. Amplification of human power can be interpreted as decrease in the impedance of a plant. This is the approach taken here to achieve a power assist control without force sensor.

Figure 2.13 is the simplest structure of impedance reducing controller.

This feedback controller works as a power assist control by setting the gains J_A, B_A to

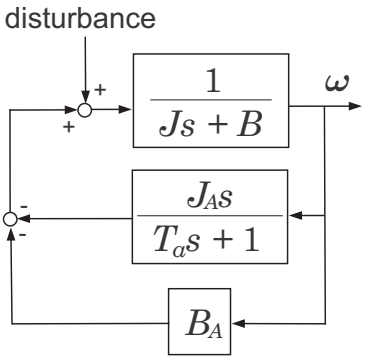

Figure 2.13: Simplest impedance reducing control

some negative values. However, the negative gain is dangerous in terms of stability. This possible instability is not acceptable for the human-friendly motion control.

Hori[18] suggested an inertia control which can simulate the inertia value of motor using disturbance observer. It is another way to reduce the impedance. Here the modified version of this inertia control is proposed. Hori's inertia control[18] only adjust inertia value in low frequency band. Adding damping factor into this control provides enough parameters that can adjust sensitivity function more precisely. Figure 2.14 describes the proposed power assist control.

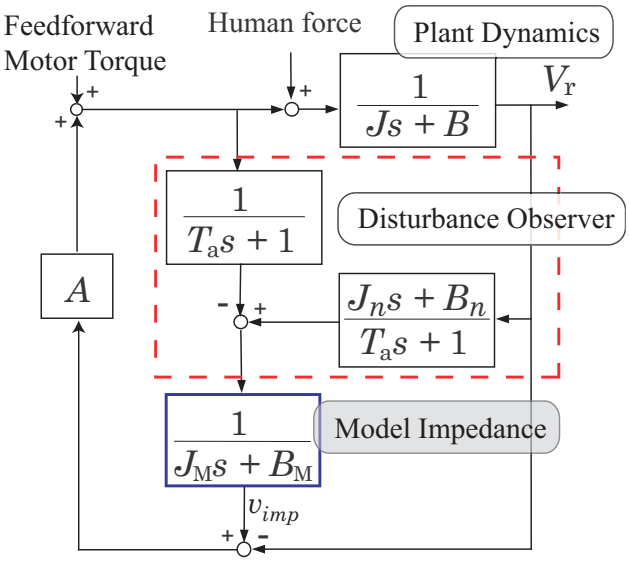

Figure 2.14: Block diagram of proposed disturbance amplifying control design

First, the external manipulating force is observed using the disturbance observer and then the controller calculates a reference velocity based on the observed manipulating force. $\frac{1}{J_M s+B_M}$ is a filter to calculate the reference velocity. J_M and B_M is set smaller than J and B. This results in reduction of the impedance after feedback control. Real velocity is controlled to track this reference velocity by feedback with the gain A. With this control

system, the transfer function from human force to velocity is:

$$T_{\text{assisted}}(s) = \frac{1}{Js + B + A}\left(\frac{J_M s + B_M + A}{J_M s + B_M}\right) \tag{2.15}$$

In section 5.4.2, we will relate these parameters with some assistance performance index.

2.2.4 Realization of Fractional Order Impedance

To achieve human-friendly motion control, we need to examine the human control of his muscle. However, the control of muscle activity is so complicated that it would be better to obtain so more degrees of freedom than the three gains J_d, B_d and K_d. Here, as this new adjustable parameter, the order of differentiation is suggested.

Fractional order differentiation has come to be applied in control design [27]. Those kinds of design are called fractional order control (FOC), however, they are still used in terms of industrial applications such as for vibration suppression.

When the fractional order differentiation is employed in the proposed impedance control, fractional order impedance can be realized. Figure 2.15 shows this realization.

The kind of impedance whether it has K_d or not has quite important meaning in the reaction force design and steady-state error reduction as is explained before. What is notable is that the order of integration itself can be an adjustable factor when adopting the fractional order differentiation.

This fractional order impedance can be a promising control design and enables more sophisticated control that will make a plant more human friendly. Nevertheless, it still has some problems; the perfect calculation of fractional differentiation is not available yet. Some calculation methods are explained in Chapter A. All of them realize the fractional order differentiation in a limited frequency bandwidth. It is impossible to continue that fractional-order characteristics throughout all frequencies so that realization of the impedance illustrated in Figure 2.15 (b) is impracticable. Figure 2.16 is feasible fractional order impedance. However, if the frequency band where the fractional order impedance is achieved matches with the most sensitive frequency bandwidth for human, it will be enough for a reaction force generation necessary for the human-friendly motion control.

Development of realization method for the fractional-order differentiation is still undergoing.

2.3 Analysis of Impedance Control of Human Muscle

2.3.1 Varying Impedance of Human Muscle

The understanding of how the muscle impedance works will help us design a human-friendly control. Dowben [5] showed the length-tension and force-velocity relation of the contracting skeletal muscle, and Ito and Tsuji [6] discussed this relationship and presented a visco-elastic muscle model by their experiments. Kumamoto [7] adopts this model and expanded it to the biarticular muscle model.

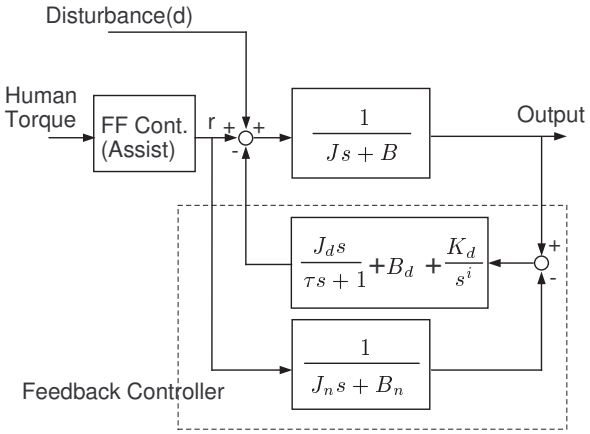

(a) Structure of fractional impedance control

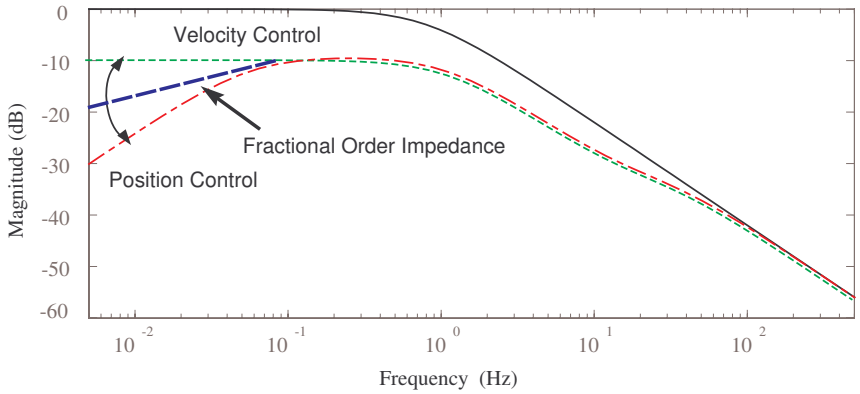

(b) Bode diagram of fractional order impedance

Figure 2.15: Fractional order impedance models

Figure 2.17 is the model of muscle used in [7]. The output force of a muscle consists of these three force elements: u is the contractile force of a muscle, $K(u)$ is the elastic force, and $B(u)$ is the viscous force. $K(u)$ and $B(u)$ can also be modeled as ku and bu with a elastic coefficient k and a viscosity coefficient b. Finally, we can get the model of output force given as Equation (2.16).

$$F = u - K(u)x - B(u)\dot{x} = u - kux - bu\dot{x} \tag{2.16}$$

2.3.2 Robust and Fast Disturbance Suppression using Antagonistic Structure

It is interesting, the impedance of a muscle is changed according to the contractile force (u) of the muscle. Furthermore, there is another remarkable point in the impedance of muscle. Muscle has the antagonistic structure described in Figure 2.18.

This antagonistic structure of muscle shows remarkable points in terms of disturbance suppression control. With one actuator to a plant in 2.19 (a), the force that suppresses

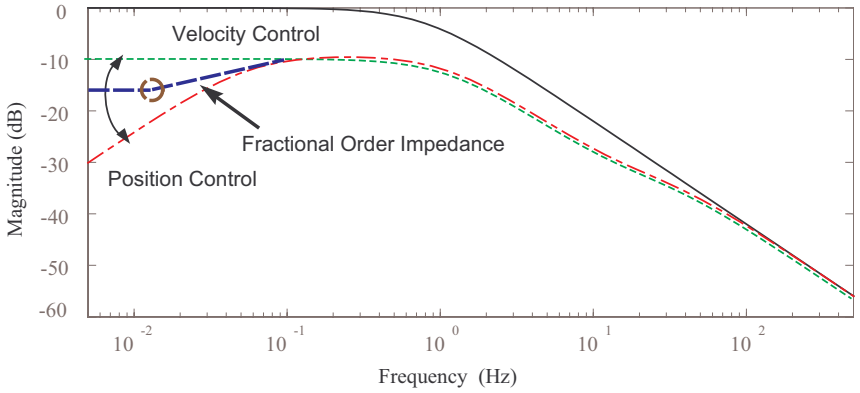

Figure 2.16: Bode diagram of feasible fractional order impedance

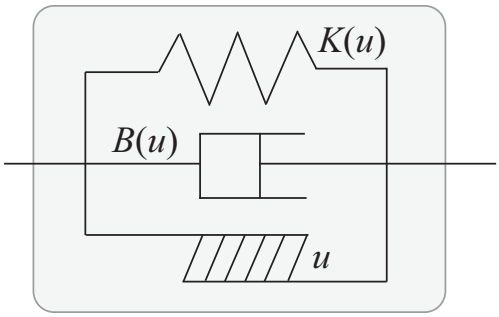

Figure 2.17: Visco-elastic muscle model

a disturbance should be added after the disturbance force is applied to the plant. The force for disturbance suppression will induce the unexpected motion of the plant if there is no disturbance force; that is, disturbance suppression should be done in a feedback way. However, two actuators with antagonistic structure in Figure 2.19 (b) is different.

The antagonistic structure can increase the input force of two actuators without changing the position of the plant because the two forces cancel out each other. Moreover, the increased force will raise the impedance of the plant according to Equation (2.16). For instance, let us look at the actions of a hand in Figure 2.20.

When a hand is clenching, the contractile forces of muscles along with elasticity and viscosity are increased making the hand robust to disturbances. This is what we, humans do to react any disturbance in advance; that is, this disturbance suppression is done before a disturbance occurs. However, due to the antagonistic structure, the increased force does not affect the position of hand. This is the feature of human control strategy; disturbance suppression without feedback. It is true that human also feedbacks his sensing of forces, however, that feedback control is additional one.

Human beings control their actions by generation of force pattern; that is in a feedforward way. This antagonistic structure of muscles is one of the reasons why that human control can work well without feedback control. With this feedforward force pattern generation, human beings can deal with large disturbances, for instances, weight lifting in Figure 2.21.

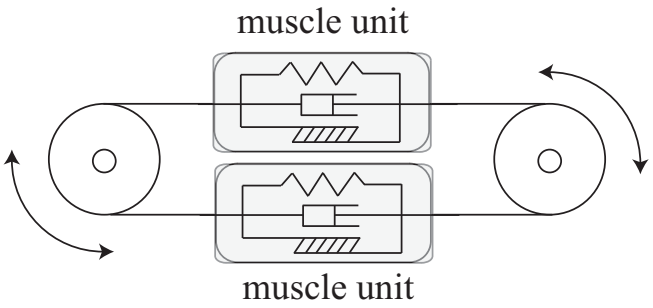

Figure 2.18: Antagonistic structure in human muscles

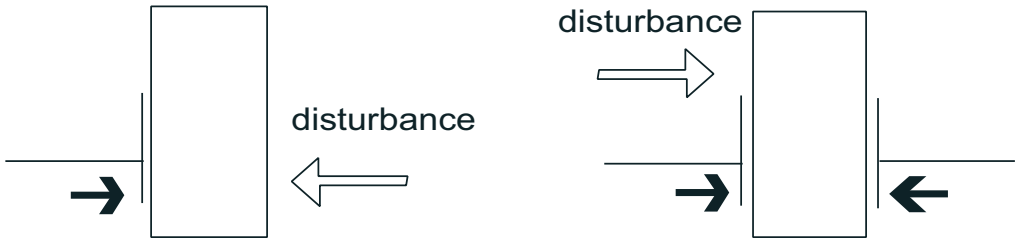

(a) Disturbance suppression using one actuator

(b) Disturbance suppression using twin actuators with antagonistic structure

Figure 2.19: Disturbance suppression characteristics of the antagonistic structure

In this weight lifting action, one noticeable this is the behavior of clenching his teeth. This 'clenching of teeth' is another appearance of impedance increase by the antagonistic structure.

There are a number of attempts to make artificial muscles using smart materials such as shape memory alloys[8]. Those kinds of materials tend to have nonlinear characteristics and are hard to control. Application of this antagonistic structure to those materials can be a solution to the difficulty in control. If those materials are installed as a pair in a symmetric way, the nonlinear characteristic such as hysteresis and friction can be cancelled out[9]. This is a kind of wisdom that human muscles teach us.

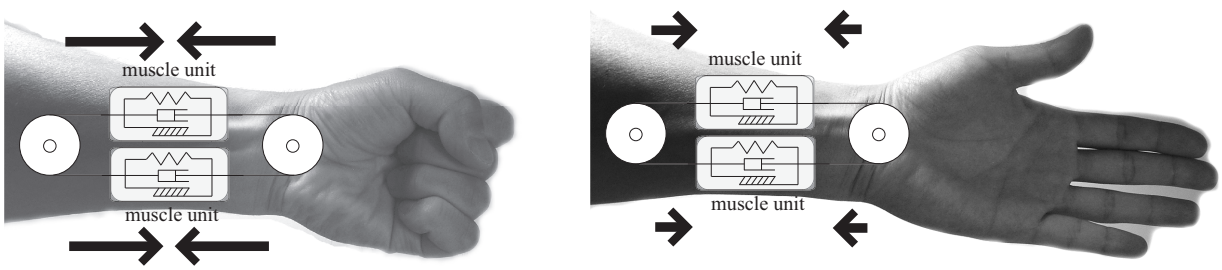

(a) Griping hand

(b) Relaxed hand

Figure 2.20: Feedforward disturbance suppression control in human muscular contol

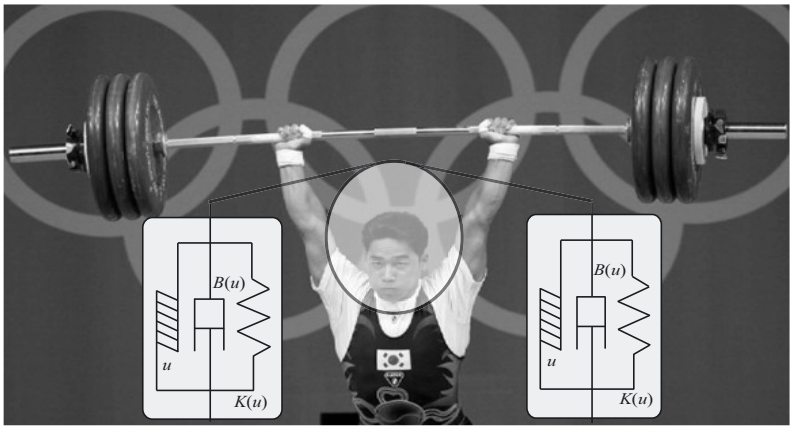

Figure 2.21: Human force control using his clenching

2.3.3 Examination of Biarticular Muscle from the Viewpoint of Control Design

In human muscles, there is one more important feature which makes it possible to control his behavior with the previously-prepared force patterns in an open-loop way. Another characteristic of the structure of muscles is the key to it.

Recent development in humanoid robots is noticeable. Though their motion seems copying human behavior, they still are limited to some certain patterns and take lots of time to make some actions. It is not only due to control problem, the actuators also have problems. For humanoid robots to move in a human-like way, their actuators should be similar with human muscles: the structure of actuators and their directions of forces.

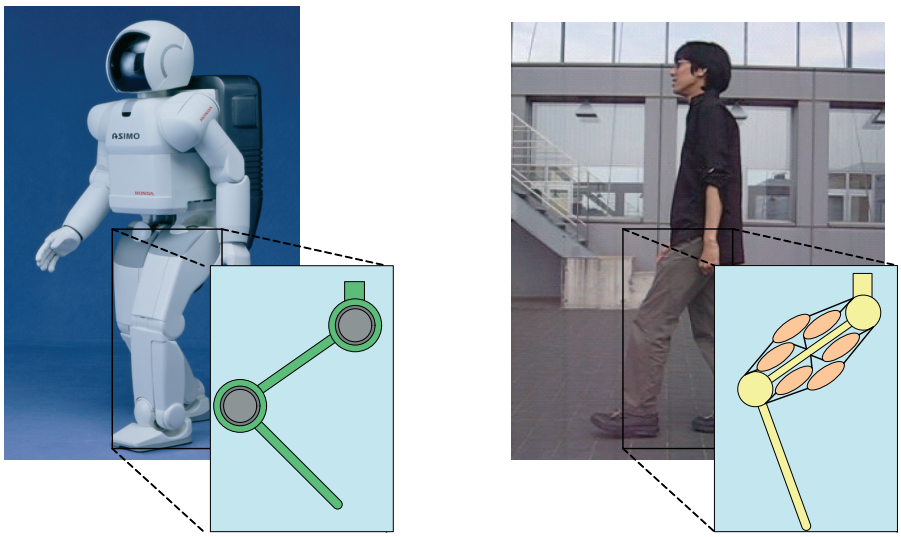

(a) Humanoid robot and its actuator (b) Human being and its muscle

Figure 2.22: Difference between actuators of robot and human

Robots use links of motors described in Figure 2.22 (a) while human uses their muscles in

Figure 2.22 (b). Comparing these two figures, we can easily see there are large differences.

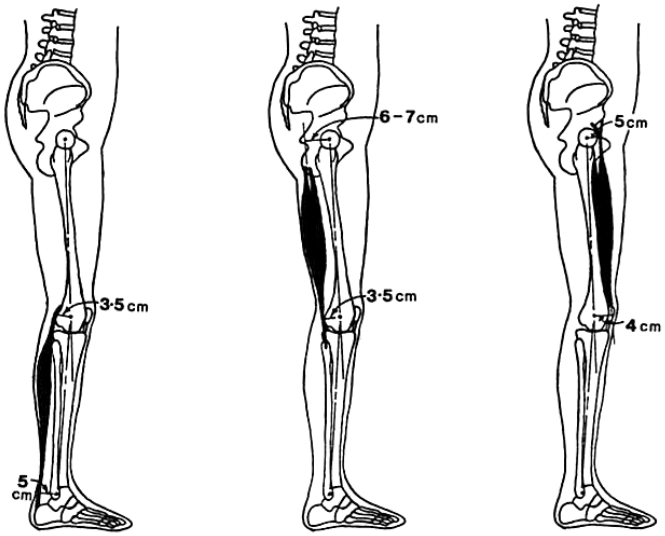

Figure 2.23: Three major biarticulate muscles of the lower limb

Human being has multi-joint muscles, some of which are described in Figure 2.23 [10]. A large number of the muscles in the human body pass over more than one joint[10]. The existence of these biarticulate muscles are quite remarkably relative to the direction of force output in the end effector, and said to be able to increase manipulability. However, the human muscles are so complicated that it is necessary to simplify it to be utilized as actuators. Figure 2.24 is the simplified model of that complicated muscles[7].

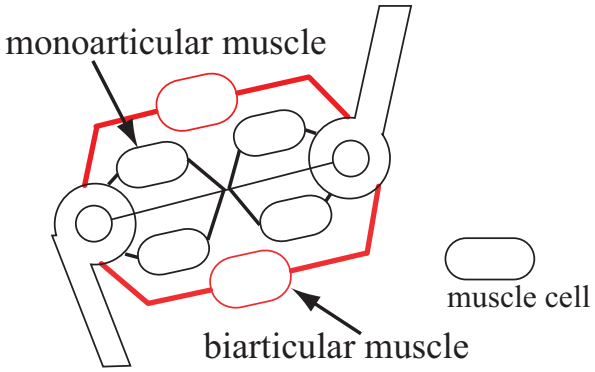

Figure 2.24: Muscle model with biarticular muscle

The two-link arm model, which is adopted in most of humanoid robots, can be represented the two pairs of monoarticular muscles in Figure 2.24. However, human has a pairs of biarticular muscles which is also described in Figure 2.24; Figure 2.23 shows three major biarticulate muscles of the lower limb. This biarticular muscle accounts for human's ability to control his behavior by feedforward torque generation, especially for the direction of output forces.

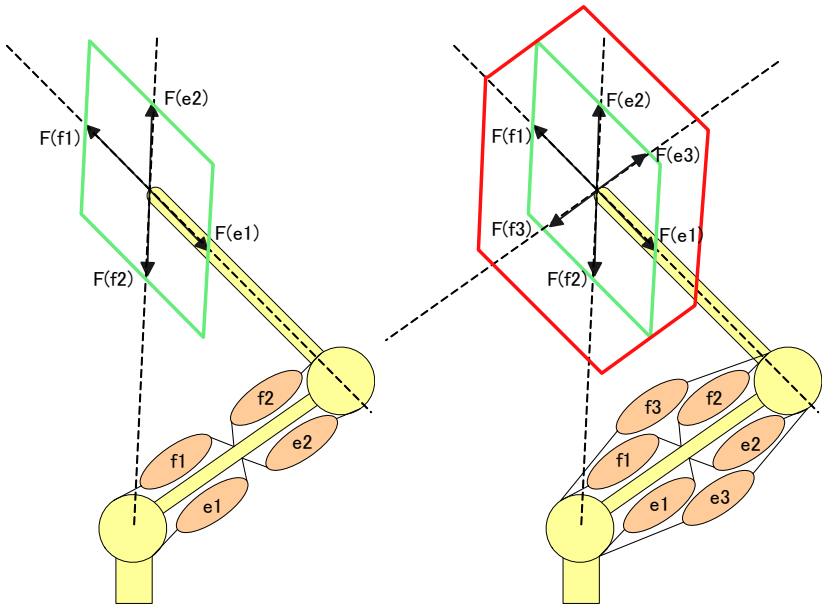

Figure 2.25: Output force distribution with and without biarticular muscle

Figure 2.25 is the output force distribution with and without biarticular muscle. We can see that the model with biarticular muscle can exert forces in all round direction regardless of its position. This distribution also means the manipulability and ability to suppress disturbances at the same time; that is, the biarticular muscles enable human the feedforward disturbance suppression, explained in the last section, in all directions, which is unable in the two-link arm model. This is the reason why the humanoid robots can not stand upright.

This biarticular muscle model still has lots of things to be researched, and with the impedance control, it may solve various problems in development of humanoid robots.

2.4 Summary

This chapter suggested fundamental ideas on the human-friendly motion control. First, this chapter revealed that all feedback control can be interpreted as impedance control and that the difference among force, velocity, and position controllers is interpreted as the difference of impedance. This interpretation provides us with more choices in the design of impedance. Furthermore, this chapter suggested some more types of impedance control: fractional order impedance control and disturbance amplification impedance control. This impedance control is examined in more details and applied to a power assistive wheelchair in Chapter 4 and 5.

This chapter also explained the feature of human muscular control in terms of motion control design and suggested its possibility for development of more advanced human-friendly motion control. The structural characteristic of human muscle such as antagonistic structure and biarticular muscle do enable impressive feedforward control feature. It allows us

robust feedforward disturbance attenuation control although one human muscle is driven by simple impedance control according to its contractile force. When this feature of impedance control in human muscular system is applied to welfare tools such as humanoid robots, it will render those tools more human-friendly.

Chapter 3

Development of Observer-based Sensor Fusion Method and its Application to Operational State Observer

3.1 Introduction

As discussed in Section 1.1.1, adaptability to various environments is important factor in the human-friendly motion control. To achieve this adaptability, an observer[17] which can estimate states of a plant by feedback can be employed. Adapting to the environment implies observation of the environment and adjusting control method according to the observation results.

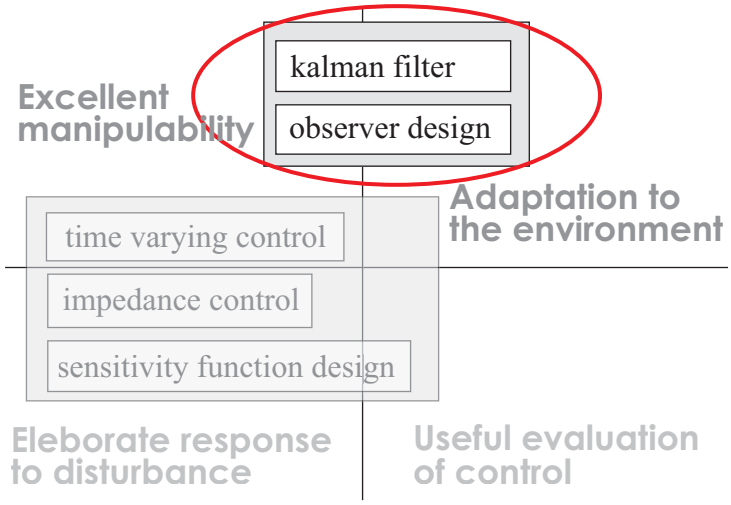

Figure 3.1: Observer can achieve the adaptability necessary for the human-friendly motion control

In this Chapter as a solution to adaptability for the human-friendly motion control problem, an observer is suggested and applied to a power-assisted wheelchair.

3.2 Definition of Operational States of a Wheelchair

3.2.1 Motions of a Wheelchair for the Advanced Control and Definition of States

Then what is the environment that a controller for a wheelchair should observe? Figure 3.2 suggests an answer to this question.

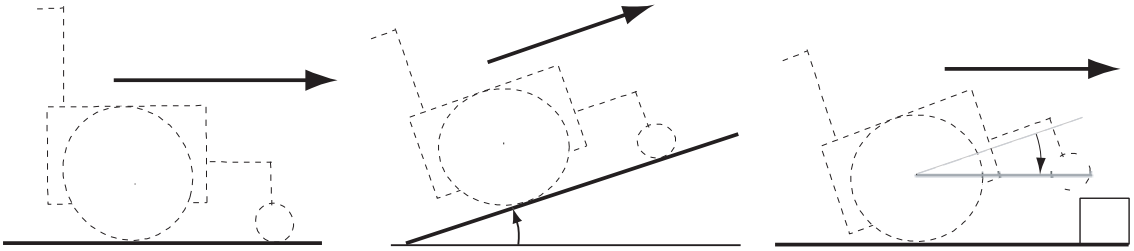

Figure 3.2: Operational states of a wheelchair

In figure 3.2, motions of a wheelchair are roughly categorized into these three phases: driving on level ground, driving on a slope, and wheelie. Here, these phases is called operational states of a wheelchair. To control a wheelchair in human-friendly way, a controller should detect in which phase the wheelchair is. This is the information an observer should observe.

The wheelchair needs different type of assisting power when it is on a slope, but conventional controllers do not consider the slope of ground. This can make dangerous situation such as overturning of the wheelchair or accelerating the speed when the wheelchair goes down a hill. To prevent these problems, assistance system should distinguish the road condition and identify the states of the wheelchair.

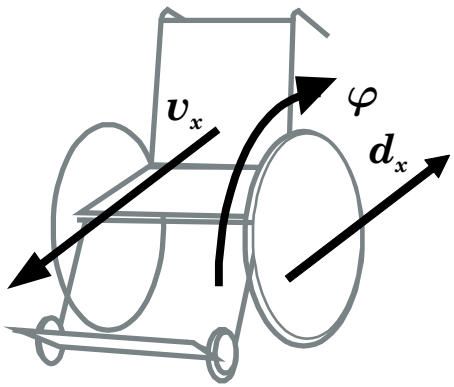

Figure 3.3: Information necessary for control of power-assisted wheelchair

In addition, there is more information we should now in controlling a wheelchair. Driving speed, v_x in the figure 3.3 and inclination angle φ in the figure 3.3 are important information

on the status of the wheelchair in each phase. d_x which is a disturbance force that disturbs wheelchair running is also an important information to detect operational states and it also can estimate the manipulation force that the user exerted and be used for force-sensor-less power assist control.

3.2.2 Derivation of a Simple Motion Equation of a Wheelchair

An observer estimates the states of a plant. It comprises a real-time simulation of the system or plant, driven by the same input as the plant, and by a correction term derived from the difference between the actual output of the plant and the predicted output derived from the observer.

$\hat{x}$ the estimated state vector of the observer is calculated through the following equation.

$$\dot{\hat{\boldsymbol{x}}} = \mathbf{A}\hat{\boldsymbol{x}} + \mathbf{B}u + \mathbf{L}\left(\boldsymbol{y} - \mathbf{C}\hat{\boldsymbol{x}}\right) \tag{3.1}$$

The first and second terms $\mathbf{A}\hat{\boldsymbol{x}} + \mathbf{B}u$ are the simulation of the system, and the last term $\mathbf{L}\left(\boldsymbol{y} - \mathbf{C}\hat{\boldsymbol{x}}\right)$ is the correction term. $\mathbf{L}$ is an observer gain or free, adjustable parameter and we can tune the observer using this $\mathbf{L}$.

In order to design an observer that can detect the operational states of a wheelchair, firstly state variables that will be observed should be defined. v_x, φ and d_x must be included in the states variables. Secondly, $\mathbf{A}, \mathbf{B}$ and $\mathbf{C}$ which describe the motion of the plant is necessary. A linearized motion equation that describes the motion of a wheelchair is necessary. To this end, motion of a wheelchair can be modeled as an inverted pendulum on a cart.

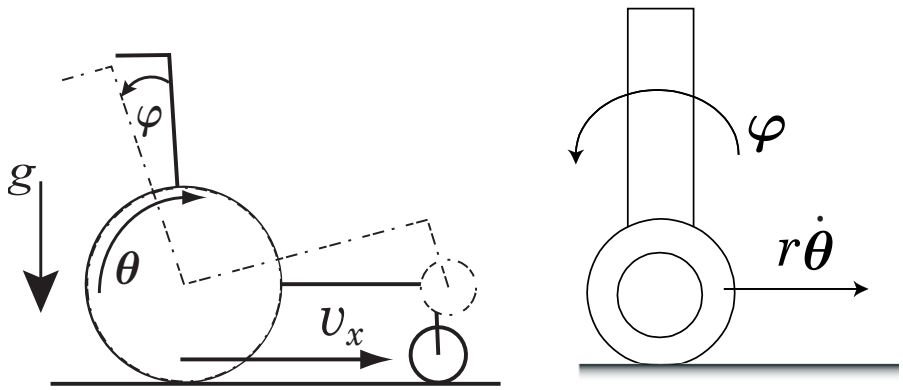

(a) states of wheelchair (b) inverted pendulum model

Figure 3.4: Analogy between a wheelchair and in inverted pendulum

Wheelchair system consists of a wheelchair and a man who rides on it. This system analogizes to a cart with an inverted pendulum[4]. Figure 3.4 shows this analogy for modeling. θ is the rotation angle of a wheel. The speed of a wheelchair is not so fast that the slip between a wheel and the ground can be ignored. From this assumption, v_x can be calculated as $r\dot{\theta}$. θ in figure 3.4 (a) corresponds with θ in (b); both means the rotation angle of a wheel. φ in the figure 3.4 means the inclination angle from the vertical axis and

it is modeled as φ in figure 3.4 (b), the pendulum angle. What should be noted is that φ is the body angle, not center-of-gravity angle from the horizon. The horizon is not the local horizon but the absolute horizon.

Based on this inverted pendulum model, motion equations of θ, φ can be described in equation (3.2), (3.3) using the Euler-Lagrange Differential Equation. Parameters used in

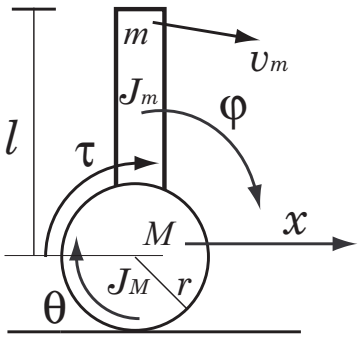

Figure 3.5: Cart with inverted pendulum model

these equations are illustrated in the figure 3.5.

$$\tau_\theta + d_\theta = \{(M+m)\, r + J_M\}\, \ddot{\theta} - mlr\ddot{\varphi}\cos\varphi + mlr\dot{\varphi}^2 \sin\varphi + B_M\dot{\theta} \tag{3.2}$$

$$\tau_\varphi = \left(J_m + ml^2\right) \ddot{\varphi} - mlr\ddot{\theta}\cos\varphi - mgl\sin\varphi + B_m\dot{\varphi} \tag{3.3}$$

τ_θ and τ_φ are input torques to θ and φ respectively. d_θ is the disturbance to θ and it is related with d_x. The relationship between d_θ and d_x is $d_x = rd_\theta$.

Generally, the inclination angle φ will not change so largely that it can be assumed to be around 0 rad. Under this assumption, some approximations in equation (3.4) can be taken. These approximations linearize the equations (3.2), (3.3) into (3.5), (3.6).

$$\cos\varphi \simeq 1, \quad \sin\varphi \simeq \varphi, \quad \dot{\varphi}^2 \ll 1 \tag{3.4}$$

$$\tau_\theta + d_\theta = \{(M+m)\, r + J_M\}\, \ddot{\theta} - mlr\ddot{\varphi} + B_M\dot{\theta} \tag{3.5}$$

$$\tau_\varphi = \left(J_m + ml^2\right) \ddot{\varphi} - mlr\ddot{\theta} - mgl\varphi + B_m\dot{\varphi} \tag{3.6}$$

However, this linearized motion equation is still quite complicated and has a problem. It can be uncertain the torque exerted by a rider works as τ_θ or as τ_φ. Usually when a rider propels his wheelchair, the torque works as τ_θ, however when a rider makes a wheelie action illustrated in figure 3.6 and goes forward slowly, the torque works as τ_θ and as τ_φ simultaneously. This means when we use the human operational torque as an input, we cannot determine whether the manipulation torque is τ_θ or τ_φ. However, considering that the operational torque usually activates τ_θ, this observer uses this torque only as τ_θ and ignores the function of the torque as τ_φ. In place of τ_φ, the proposed observer utilizes d_φ, which means input torque to φ is not given beforehand as prior information, but estimated by the observer.

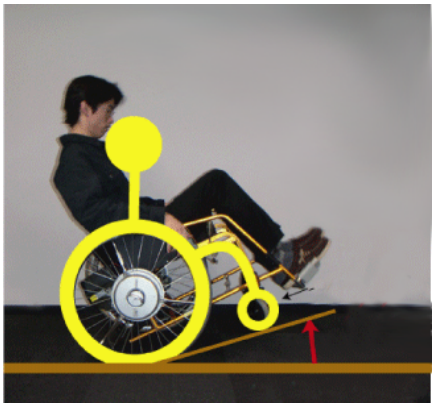

Figure 3.6: Wheelie action without going forward

Furthermore, the correlated term in the equations (3.5), (3.6) can be included in these disturbance terms. By this the equations can be simplified and robust to the modeling error.

This idea simplifies the motion equations as follows:

$$\tau_\theta + d_\theta = J_\theta \ddot{\theta} + B_\theta \dot{\theta} \tag{3.7}$$

$$d_\varphi = J_\varphi \ddot{\varphi} + B_\varphi \dot{\varphi} \tag{3.8}$$

3.3 Development of Observer Based on Kalman Filter Theory

Based on the motion equations derived above, an operational state observer is designed here. The state variables are defined as

$$x = \begin{pmatrix} \dot{\theta} & \dot{\varphi} & \theta & \varphi & d_\theta & d_\varphi \end{pmatrix}^T. \tag{3.9}$$

Note that d_φ is included as a state variable to be estimated. $\mathbf{A}$ and $\mathbf{B}$ in the equation (3.1) are given as

$$\mathbf{A} = \begin{pmatrix} -\frac{B_\theta}{J_\theta} & 0 & 0 & 0 & \frac{1}{J_\theta} & 0 \\ 0 & -\frac{B_\varphi}{J_\varphi} & 0 & 0 & 0 & \frac{1}{J_\varphi} \\ 1 & 0 & 0 & 0 & 0 & 0 \\ 0 & 1 & 0 & 0 & 0 & 0 \\ 0 & 0 & 0 & 0 & 0 & 0 \\ 0 & 0 & 0 & 0 & 0 & 0 \end{pmatrix}, \quad \mathbf{B} = \begin{pmatrix} \frac{1}{J_\theta} \\ 0 \\ 0 \\ 0 \\ 0 \\ 0 \end{pmatrix} \tag{3.10}$$

To verify this simplification, detailed version of model equation is employed. $\mathbf{A_{dt}}$ and $\mathbf{B_{dt}}$ in the following equation (3.11) are the detailed version based on the inverted pendulum

model explained in Section 3.2.2.

$$\mathbf{A_{dt}} = \frac{1}{D}\begin{pmatrix} -\left(J_m+ml^2\right)B_M & -mlrB_m & 0 & m^2gl^2r & J_m+ml^2 & mlr \\ -mlrB_M & -\{(M+m)r+J_M\}B_m & 0 & \{(M+m)r+J_M\}mgl & mlr & (M+m)r+J_M \\ 1 & 0 & 0 & 0 & 0 & 0 \\ 0 & 1 & 0 & 0 & 0 & 0 \\ 0 & 0 & 0 & 0 & 0 & 0 \\ 0 & 0 & 0 & 0 & 0 & 0 \end{pmatrix}$$

$$\mathbf{B_{dt}} = \frac{1}{D}\begin{pmatrix} J_m+ml^2 \\ mlr \\ 0 \\ 0 \\ 0 \\ 0 \end{pmatrix}$$

$$\begin{aligned} D &= \{(M+m)r+J_M\}\left(J_m+ml^2\right) - m^2l^2r^2 \\ &= (M+m)ml^2r^3 + (M+m)J_mr + J_MJ_m + ml^2J_M - m^2l^2r^2 \end{aligned} \tag{3.11}$$

3.3.1 Description of Sensor Outputs

In Section 3.2.1, three physical values v_x, φ, d_x are introduced as the important information on operationa states. Each value has been measured using various sensors. v_x or in the case of a wheelchair $\dot{\theta}$ is measured by differentiating encoder outputs. φ can be measured by integrating the output of a gyroscope. d_x, especially the torque a rider exert to propel a wheelchair is measured using a torque sensor. This measurement by each sensor has its own shortcoming when it is used alone. The proposed observer which fuses all information from all sensors can overcome these shortcomings.

Three sensors are adopted for the operational state observer: encoder, gyroscope, and accelerometer. The outputs of these sensors can be described using the state variables defined in the equation (3.9). An encoder measures the rotation angle of a wheel, θ. A gyroscope measures the rotational velocity in the pitch direction, φ. As another sensor, a two-axis accelerometer is utilized here. It measures driving acceleration and gravity. Two measurements a_x, a_y by the accelerometer are illustrated in figure 3.7.

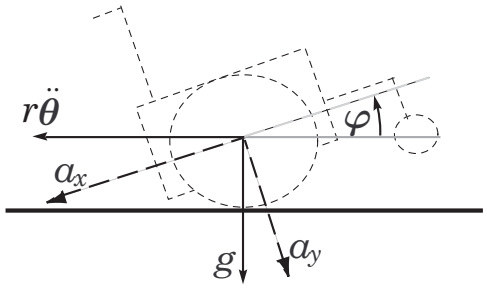

Figure 3.7: Accelerations measured by accelerometer

Consequently, the output equations of three sensors can be given as Table 3.1.

Table 3.1: Output equation of each sensor

Encoder	$y_{\text{enc}} = \theta$
Gyroscope	$y_{\text{gyro}} = \dot{\varphi}$
Accelerometer	$y_{\text{acc}_x} = r\ddot{\theta}\cos\varphi + g\sin\varphi$
	$y_{\text{acc}_y} = g\cos\varphi - R\ddot{\theta}\sin\varphi$

Output equation of the accelerometer is not linear. Between two nonlinear outputs of the accelerometer, a_x can be linearized with ease. Assuming φ is not so large, $\cos\varphi$ is approximated as 1 and $\sin\varphi$ is approximated as φ. This results in the linearization of a_x;

$$a_x = r\ddot{\theta}. \tag{3.12}$$

This linearized output can provide linear output equation for the design of the operational state observer.

The linear output equation is described as

$$\boldsymbol{y} = \begin{pmatrix} \theta \\ \dot{\varphi} \\ a_x \end{pmatrix} = \mathbf{C}\boldsymbol{x} + \mathbf{D}u. \tag{3.13}$$

$\mathbf{C}$ and $\mathbf{D}$ is given as

$$\mathbf{C} = \begin{pmatrix} 0 & 0 & 1 & 0 & 0 & 0 \\ 0 & 1 & 0 & 0 & 0 & 0 \\ -r\frac{B_\theta}{J_\theta} & 0 & 0 & g & \frac{r}{J_\theta} & 0 \end{pmatrix}, \quad \mathbf{D} = \begin{pmatrix} 0 \\ 0 \\ \frac{r}{J_\theta} \end{pmatrix} \tag{3.14}$$

$$\mathbf{C_{dt}} = \begin{pmatrix} 0 & 0 & 1 & 0 & 0 & 0 \\ 0 & 1 & 0 & 0 & 0 & 0 \\ -\frac{r}{D}\left(J_m + ml^2\right)B_M & -\frac{r}{D}mlrB_m & 0 & \frac{1}{D}m^2r^2l^2g + g & \frac{r}{D}\left(J_m + ml^2\right) & \frac{r}{D}mlr \end{pmatrix}$$

$$\mathbf{D_{dt}} = \begin{pmatrix} 0 \\ 0 \\ \frac{r}{D}\left(J_m + ml^2\right) \end{pmatrix}. \tag{3.15}$$

Here also $\mathbf{C_{dt}}$ and $\mathbf{D_{dt}}$ are the detailed version of output equation based on the equation (3.11).

3.3.2 Decision of Observer Gains Based on the Characteristics of Sensors and States

The observer has three outputs, which makes the decision of observer gain not so simple so that the kalman filter method is adopted for the calculation of the observer gain. Kalman filter determines the optimal gain according to the covariance of noises in the system.

Equation (3.16) and (3.17) describes a system with noises.

$$\begin{aligned} \dot{\boldsymbol{x}} &= \mathbf{A}\boldsymbol{x} + \mathbf{B}u + \boldsymbol{w} \\ \boldsymbol{y} &= \mathbf{C}\boldsymbol{x} + \mathbf{D}u + \boldsymbol{v} \end{aligned} \tag{3.16}$$

$$\boldsymbol{w} = \begin{pmatrix} w_{\dot{\theta}} & w_{\dot{\varphi}} & w_{\theta} & w_{\varphi} & w_{d_\theta} & w_{d_\varphi} \end{pmatrix}^T$$

$$\boldsymbol{v} = \begin{pmatrix} v_{\text{enc}} & v_{\text{gyro}} & v_{\text{acc}} \end{pmatrix}^T \tag{3.17}$$

$\boldsymbol{w}$ is system noise and $\boldsymbol{v}$ is sensor noise. The kalman filter determines the observer gain $\mathbf{L}$ based on the covariance matrix of these noises $\boldsymbol{w}, \boldsymbol{v}$. The noise covariance data for this determination of the observer gain are set as follows.

$$E\left[\boldsymbol{w}\boldsymbol{w}^T\right] = \mathbf{Q} = \text{diag}\left(Q_{\dot{\theta}}, Q_{\dot{\varphi}}, Q_{\theta}, Q_{\varphi}, Q_{d_\theta}, Q_{d_\varphi}\right) \tag{3.18}$$

$$E\left[\boldsymbol{v}\boldsymbol{v}^T\right] = \mathbf{R} = \text{diag}\left(R_{\text{gyro}}, R_{\text{enc}}, R_{\text{acc}}\right) \tag{3.19}$$

$Q_{\dot{\theta}}, Q_{\dot{\varphi}}, Q_{\theta}, Q_{\varphi}, Q_{d_\theta}, Q_{d_\varphi}$ and $R_{\text{gyro}}, R_{\text{enc}}, R_{\text{acc}}$ are the adjustable parameters in this observer. How these parameters affect the observation performance is examined by experiments in next Section.

3.4 Experimental Results

As mentioned above, three sensors adopted here have their own shortcomings when they are used alone. At first, the encoder measures the rotation angle of wheel. To obtain the velocity information which is necessary for the feedback control introduced in next Section from an encoder, the output of the encoder should be differentiated. This differentiation makes the measurement noisy and incorrect at low speed. Secondly, the gyroscope measures the rotational velocity in the pitch direction. The inclination angle can be given by integrating the output of the gyroscope. In this calculation, sensor noise in the gyroscope is also integrated and results in the drift phenomenon. Lastly, accelerometer measures the gravity and acceleration of motions, but the accelerometer is usually subject to the noise. Following experiments makes clear that sensor fusion by the proposed observer design can overcome these shortcomings and provide good measurements.

3.4.1 Verification of the Simplified Model

Figure 3.8 roughly shows the effectiveness the proposed observer. It compares the observation by the proposed observer with the conventional estimation. In the figure (a), the dotted line is the estimation by differentiation of the encoder output, and the solid line is the observation by the observer. In the figure (b), the dotted line is the estimation by integration of the gyroscope, and the solid line is the observation by the observer. The observation by the proposed observer is not so different from the conventional estimation so that we can verify the accuracy of observation. The experiments were done on level ground and on a slope. Figure 3.8 shows these two experiment results.

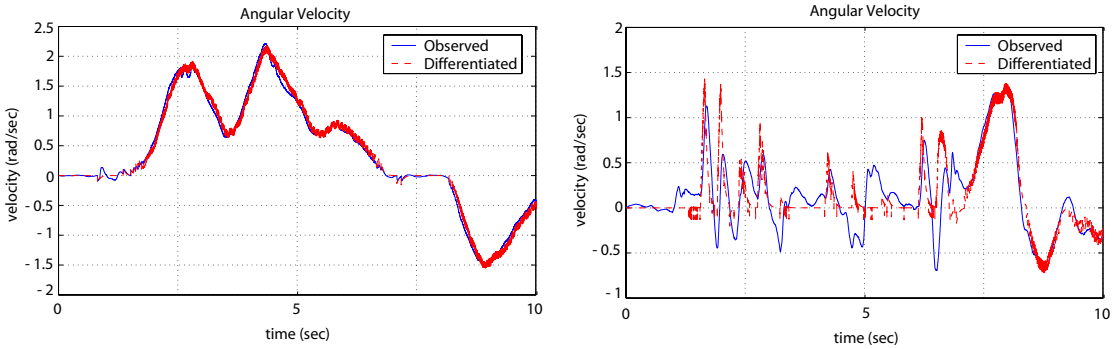

(a) estimated angular velocity $\hat{\dot{\theta}}$ (left: on level ground, right: on a slope)

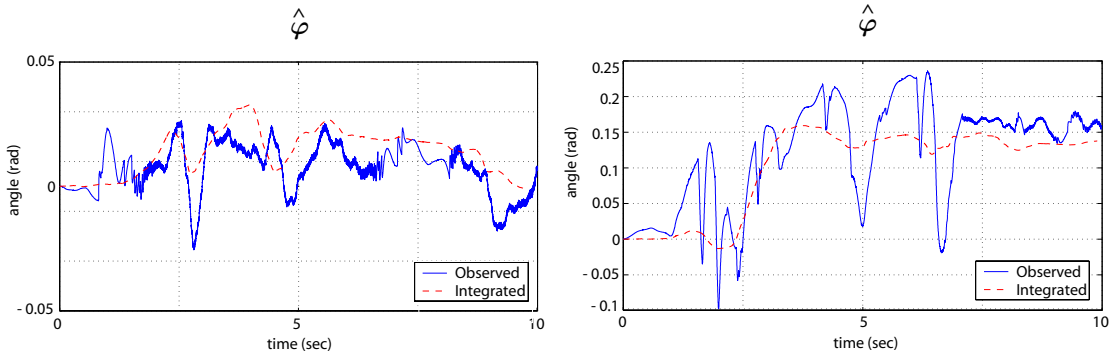

(b) estimated inclination angle $\hat{\varphi}$ (left: on level ground, right: on a slope)

Figure 3.8: Observation results using the simplified model

To verify the simplified model, the observation result based on the detailed version of the equation (3.11) is shown in Figure 3.9. This estimation uses the same measurement data as Figure 3.8: experiments on level ground and on a slope. Comparing the two observations, it is clear that observation with the simplified model has almost same estimation performance with the more detailed version. This experiment result suggests that an observer with a simple model is sufficient to get the information when the parameters - the covariance matrix in this experiment - are adjusted properly. Especially, this observation system has three sensors which can estimate the states by themselves. This abundant sensor information allows the observer to estimate accurate information with the simple model.

3.4.2 Fast and Noise-less Estimation of Velocity

Closer examination reveals the excellent performance of the proposed observer. Figure 3.10 is the velocity observation. The solid line is the estimation by the proposed observer, and the dotted line is the differentiation of the encoder output. The differentiated velocity is very noisy and delayed while the estimation of the proposed observer is fast and not noisy.

This velocity-observation performance at low velocity is important in control of a wheelchair. A wheelchair drives at slow velocities and decelerates to a stop frequently. It is an important requirement to get accurate velocity information of a wheelchair even when it runs at

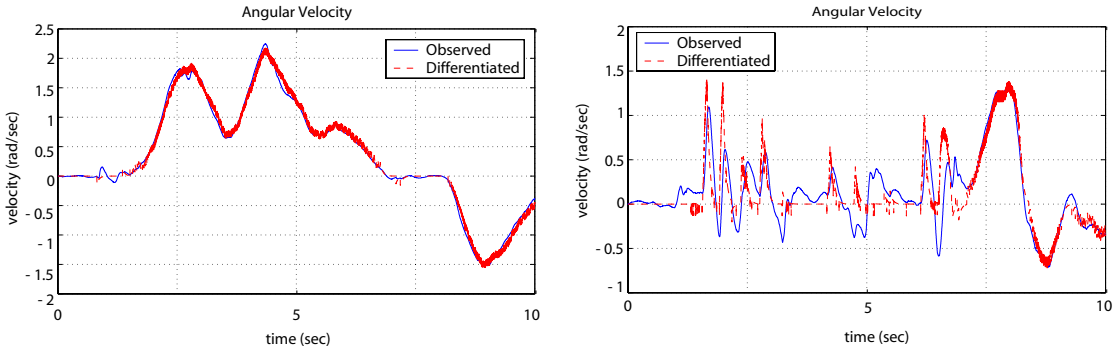

(a) estimated angular velocity $\hat{\dot{\theta}}$ (left: on level ground, right: on a slope)

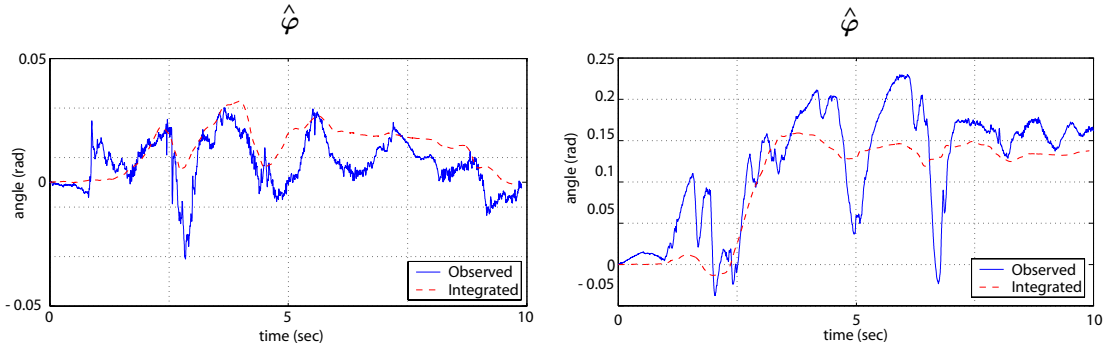

(b) estimated inclination angle $\hat{\varphi}$ (left: on level ground, right: on a slope)

Figure 3.9: Observation results using the detailed model

slow speed.

Feedback control proposed in Chapter 4 uses the velocity information of a wheelchair, and it even differentiates that velocity. If the velocity itself is noisy, the feedback control cannot provide satisfying performance to the user. As introduced in Section 1.1.1, in human-friendly control such as control of a wheelchair, these noise or vibration in signal can affect the user's feeling in a displeasing way. In this meaning, obtainment of velocity information of high quality by the proposed observer can be an important technology for human-friendly control.

3.4.3 Sensor-noise Robust Estimation of Inclination Angle

Estimation by integrating the gyroscope signals is subject to sensor noise. The proposed observer solves this problem; it can compensate for the drift using the accelerometer signals. To investigate the robustness of proposed observer, a noise is added to the gyroscope output at 10 sec. Figure 3.12 depicts the estimation of φ. Three experiments were done: on level ground, on a slope, a wheelie. The dotted line is the estimation by integrating the gyroscope signals in each experiment. After 10 second when an impulse type noise in Figure 3.11 is added, in the estimation by integration, this noise is also integrated and makes the estimation fail, and never recovers from the error. On the other hand, the proposed observer recovers from the error and converges to the right answer. All the three experiments show

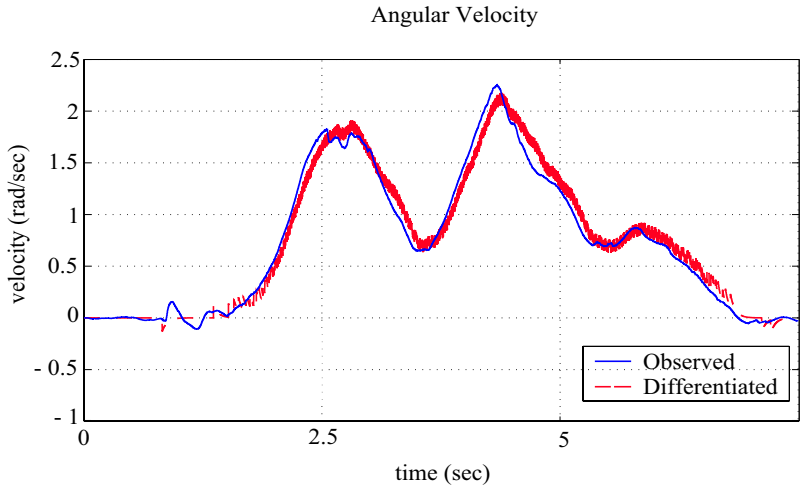

Figure 3.10: Fast and correct estimation of velocity by the proposed observer

that the robustness holds in various environments.

This robustness is due to the observer-based sensor fusion. The portion each sensor contributes to the estimation is decided by the covariance matrix which is made use in the design of the kalman filter gain. Equation (3.17) is the covariance matrix. According to this covariance matrix, the observation performance changed as Figure 3.13 shows. When the portion of the accelerometer becomes larger, the recovery from the error will be faster, however the estimation becomes subject to the noise in the accelerometer.

There is a research on the prevention of a wheelchair from tipping over[11]. It adjusts the assist ratio according to the inclination angle φ. However, only a gyroscope is used to get φ there and it could not avoid the drift phenomenon. In that case, this proposed observer can be a solution. There is another function the observer has.

3.4.4 Distinction of Operational Status

The estimated angle $\hat{\varphi}$ is not sufficient for the control of a wheelchair. In the research [11], the assisting torque will decrease when φ increases to avoid tipping over. However, increase in φ does not always mean tipping over or wheelie. It also means the angle of a slope where the wheelchair is on. The decrease in the assist ratio can help prevention of tipping over during a wheelie, but it can decrease the torque which is necessary to attenuate the gravity's effect on the wheelchair when it is on a slope. In this meaning we need to distinct whether the wheelchair is on a slope or during its wheelie.

The estimation of $\hat{d}_\theta$ can make distinction between slopes and wheelies. If the wheelchair is on a slope, the gravity act as a disturbance in the backward direction, but if the wheelchair is during a wheelie, it is not. Figure 3.14 shows the estimated $\hat{\varphi}$ and $\hat{d}_\theta$ on a slope and during a wheelie. Both $\hat{\varphi}$ have non-zero value, and we cannot tell the actual state of the wheelchair. However $\hat{d}_\theta$ are apparently different. While $\hat{d}_\theta$ has a constant value on a slope, during a wheelie, it does not. By this experiment, the effectiveness of the proposed observer

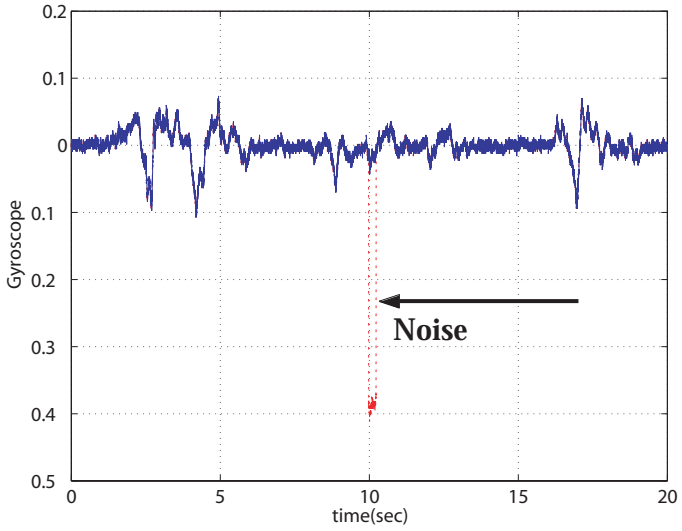

Figure 3.11: Impulsive noise added to the measurement of the gyroscope

as an operational state observer is proved.

3.5 Summary

The human motion control system consists of the nervous system and the muscle system. The human nervous system is an excellent sensory system helping human control and allowing quite complicated human motion. Human-friendly motion control also needs this kind of sensory system. For instance, robots in Figure 1.4 and other power assistive tools in Figure 1.4 employ a number of sensors to establish this sensory system, however to use as many sensors as necessary is not feasible; the proposed observer-based sensor fusion is one solution to this problem and can work as a substitute of this human nervous system. In this meaning, the proposed operational state observer is one example that can be a key technology in human-friendly motion control. The proposed observer is useful not only for a wheelchair but also for other welfare tools such as humanoid robots. The states which are monitored by the operational state observer - velocity, pitch angle, disturbance in each state - are important values in human locomotion; human also uses this information for his locomotion. In this meaning, the proposed observer can be generally used for various mobile robots or tools that assist locomotion.

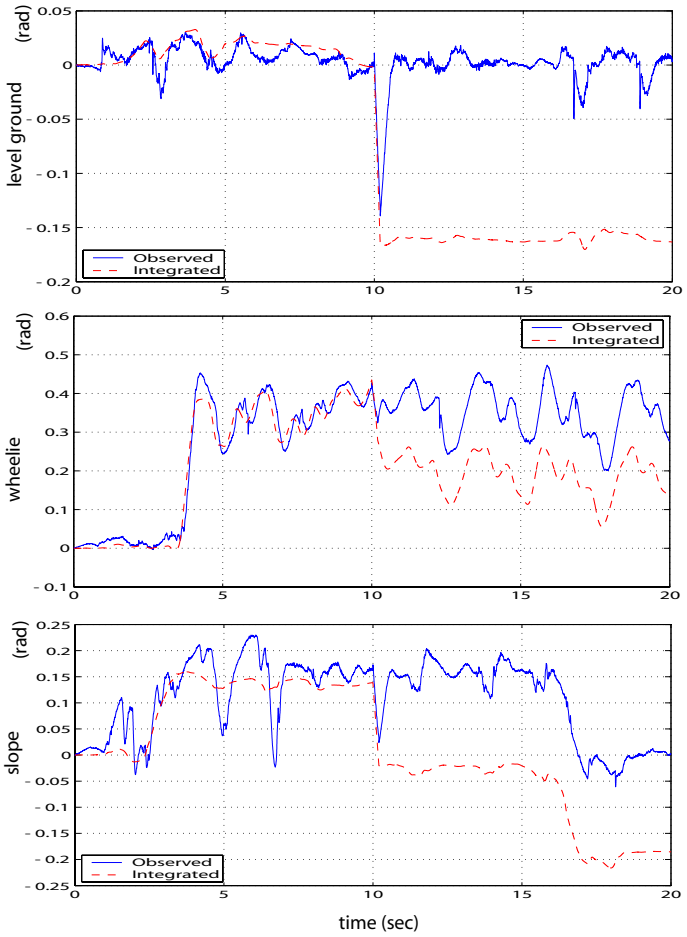

Figure 3.12: Inclination angle estimation ($\hat{\varphi}$) in various environments

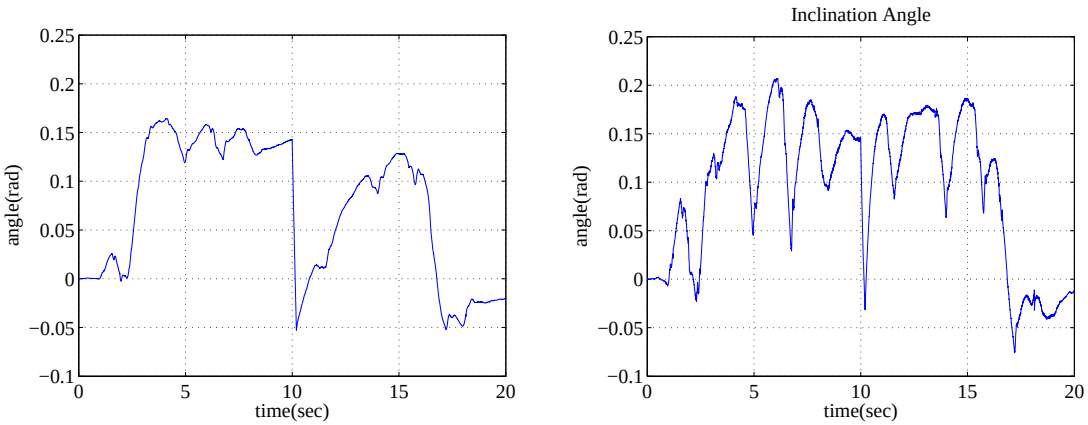

Figure 3.13: Change in the observation performance according to the change in the covariance matrix

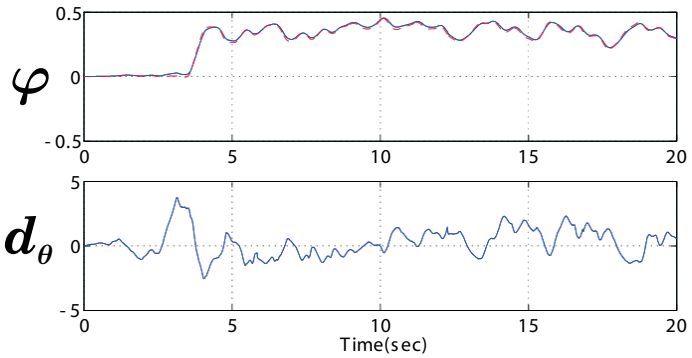

(a) $\hat{\varphi}$, $\hat{d}_\theta$ during a wheelie

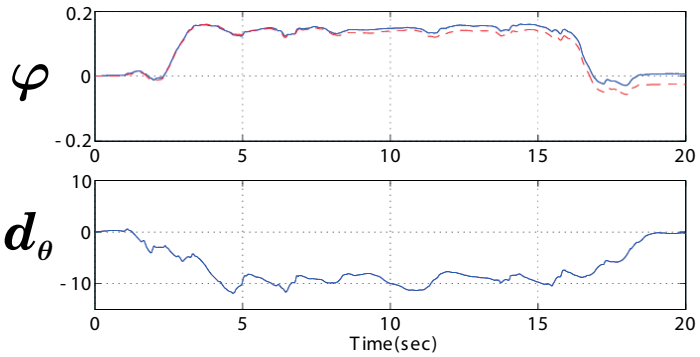

(b) $\hat{\varphi}$, $\hat{d}_\theta$ on a slope

Figure 3.14: Distinction between a wheelie action and slope using $\hat{d}_\theta$

Chapter 4

Human-friendly Design of Disturbance Attenuation Control for a Wheelchair

4.1 Introduction

This chapter deals with the feedback control design portion of human-friendly motion control. In Chapter 2, the relationship between control design and reaction force design is scrutinized, and it provides a viewpoint to design a controller in human-friendly way. This chapter applies that thought to design of feedback control of a wheelchair. As a major disturbance to a wheelchair, the gravity's effect is handled.

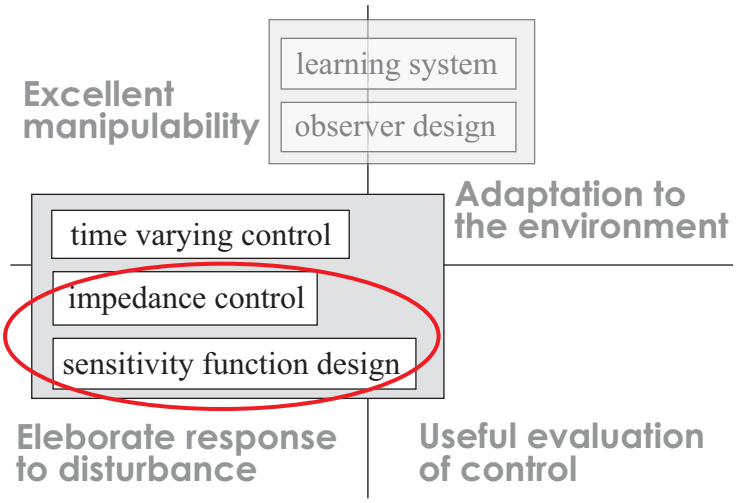

Figure 4.1: Design of a feedback controller in a human-friendly way

Necessary Assistance for a Wheelchair on a Slope

Problems in the conventional power-assist control which easily happens on a slope explained in the introduction: excessive assisting torque causing tip over and gravity inter-

ference. These are related to safety of the rider and must be coped with to make the power-assisted wheelchair in a human-friendly way.

Firstly, the magnitude of the torque necessary to drive a wheelchair forward on a slope is much larger than that for driving on level ground. Figure 4.2 shows the necessary torques for

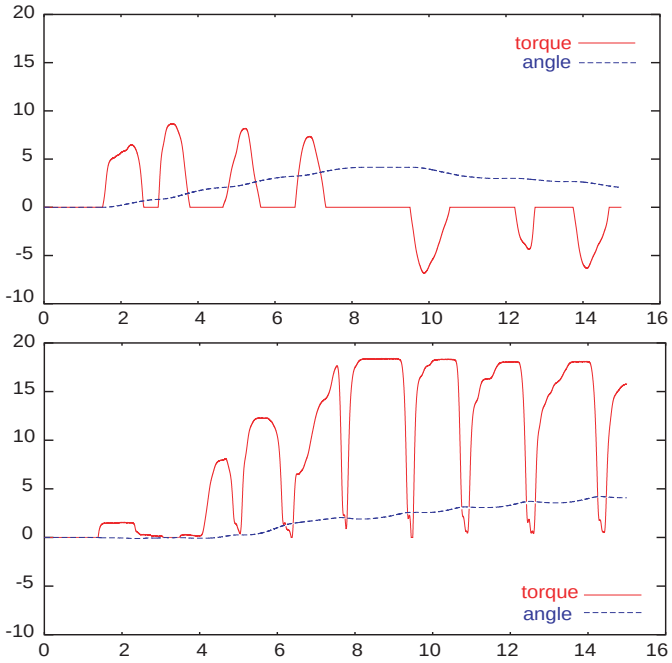

Figure 4.2: Necessary torques to drive a wheelchair (Upper: drive on level ground, Below: drive on hill)

driving on level ground and driving on a slope. On a slope, torque necessary for maintaining the height against the gravity is several times larger than the torque necessary for driving the wheelchair forward. This toque should be assisted, but it is not in the conventional power-assisting control.

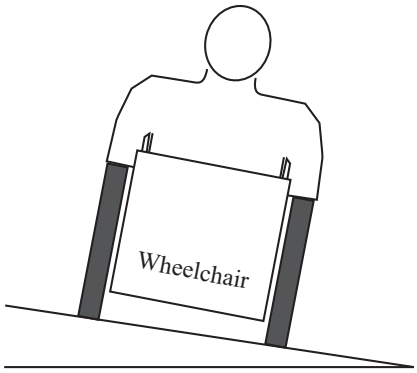

Figure 4.3: Gravity acting laterally on a wheelchair

Gravity also interferes with the moving direction of a wheelchair. On a slope described in Figure 4.3, the wheelchair will easily turn by the gravity. It is quite difficult to keep

going straight. Also, the torque necessary for keeping the direction is much larger than the torque for going forward. This lateral disturbance should be rejected too.

From these facts, we can see the disturbance rejection should be done in two dimensions. The other thing we should notice is the difference in design of disturbance-rejection control on two disturbances. Forward disturbance should be rejected in the velocity level, and lateral disturbance should be rejected in position level. This point will be explained later in this chapter.

4.2 Design of Disturbance Attenuation Control in the Forward Direction

In this section, a controller that attenuates the gravity's effect in the forward direction is developed. Basic strategy is based on the impedance control explained in Section 2.1.

4.2.1 Appropriated Impedance Design for Disturbance Attenuation in a Wheelchair

In Section 2.1, it was made clear that three kinds of the most frequently used motion control - force control, velocity control, position control - can be described in one form: impedance control. Then, what kind of impedance control among these three is most suitable for the attenuation of the gravity's effect?

Force control can provide the torque that makes a wheelchair stop on a hill without human operator's power. However, to provide the exact torque, we should have the correct model of the wheelchair. This is not acceptable, because the weight of a rider is not constant and wheelchair's motion has lots of nonlinearity such as friction so that the precise modeling of a wheelchair's motion is neither possible nor practical.

On the other hand, position control can provide the torque enough to stop the wheelchair without the model of the wheelchair, and if it has a high gain, which also can be a large stiffness, it can suppress the gravity sufficiently. However, the position control does not accord with the rider's feeling and consequently makes the rider feel unnatural. Under position control, when a disturbance is added, the wheelchair will move a certain amount by the disturbance. After the disturbance is removed, the wheelchair goes back to its original position (Figure 4.4). This is the characteristics of the position control (See Figure 2.6).

What should we note is that human is accustomed to the velocity control in the back and forth direction. Position error in this direction does not mean much to riders in a vehicle. People are not sensitive in the position in back and forth direction. On the other hand, error in velocity in this direction has significant meaning. For this reason, unintentional going back described in Figure 4.4 produces unnatural feeling for the rider, because its direction, which means a sign of velocity, is against the rider's intention. This unintentional change in velocity is unacceptable. Therefore, we can say that the position control is not suitable

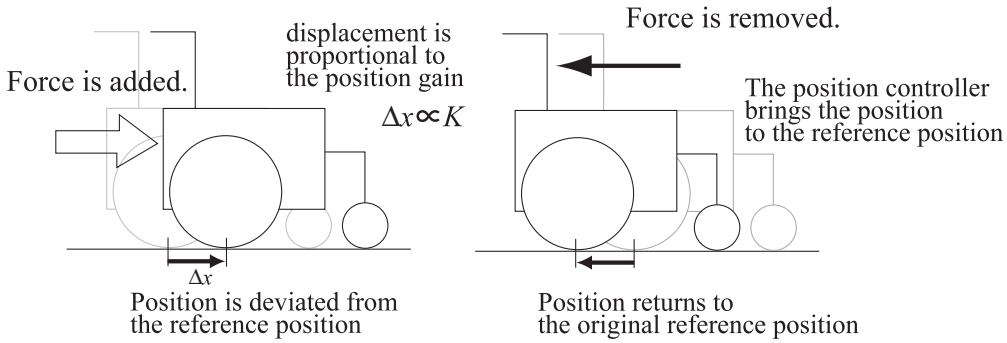

Figure 4.4: Motion of the position-controlled wheelchair

for a wheelchair control in spite of its robustness. After these considerations, we can see that the velocity control is most adequate to the gravity suppression control.

Velocity control does not need to be control to track a reference velocity. Compliance control can be modified to the velocity control. Figure 4.5 shows the structure of gravity attenuation controller proposed in this research. This is a compliance control which also is a velocity control, because it has no stiffness in the impedance.

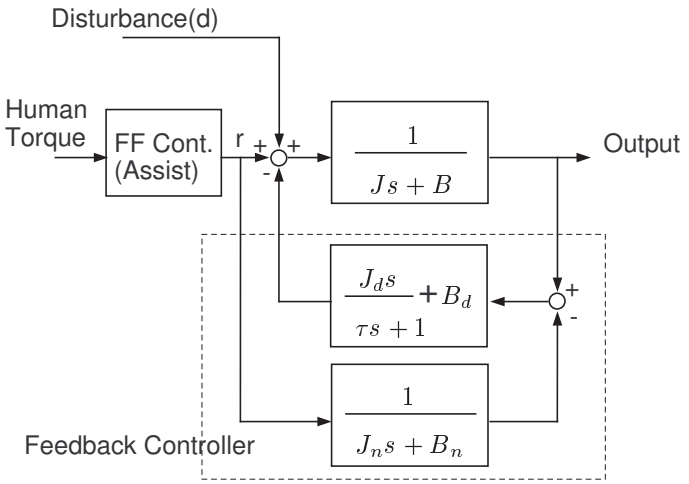

Figure 4.5: Structure of proposed disturbance attenuation controller for a wheelchair

$\frac{1}{Js+B}$ is the dynamics of the wheelchair, and "FF Cont.(Assist)" means a feedforward controller to amplify the rider's propelling torque, and it will be $\frac{\alpha}{\tau_f+1}$, where α is an assist ratio. Further discussion on this feedforward assist control will be done in next section. Controller in the dotted rectangular is the gravity attenuation controller.

Increasing the friction and inertia of the wheelchair makes the wheelchair seem heavy to gravity. The controller will produce just a certain amount of power to attenuate the effect of gravity on the wheelchair. Nevertheless, this controller has no stiffness, and consequently it does not provide actions like Figure 4.4. When a disturbance is applied, the velocity is deviated from the reference velocity; on a slope, a wheelchair will if the rider does not apply

any torque to the wheelchair The amount can be modified arbitrarily based on the inertia and friction of the wheelchair changed by the filter C. To this end, we adopt $J_d s + B_d$ as C, and it will change like follows:

$$\frac{1}{Js+B} \rightarrow \frac{1}{(J+J_d)s+(B+B_d)}. \tag{4.1}$$

4.2.2 Combination with Tip-over Protective Control

In last section, a power assistance that compensates the gravity on a hill is proposed. However, there is another problem when we control a wheelchair on a hill. The wheelchair will be tilted and its center of balance will shift to the unstable area, on a hill, that is, inadequate power assistance makes the wheelchair unstable and tip over, because assisting power will work in the same direction with gravity.

To cope with this problem, we start with the composition of power assisting torque. Now that we employed the feedback controller in last section, the power assisting torque consists of feedforward portion and feedback portion. Between these portions, the feedforward portion accounts for tip over of the wheelchair, because its magnitude and momentum is much larger than those of feedback portion.

The feedforward portion amplifies the torque applied by the rider. It consists of a first-order time delay given as

$$\alpha \frac{1}{1+\tau s} \tag{4.2}$$

where α is power-assist ratio and τ is the time constant of first order delay. τ is set small at the beginning of propelling and large at the ending:

$$\tau = \begin{cases} \tau_{fast} & \frac{d}{dt}T_{human} > 0 \\ \tau_{slow} & \frac{d}{dt}T_{human} < 0 \end{cases}, \quad (\tau_{fast} < \tau_{slow}) \tag{4.3}$$

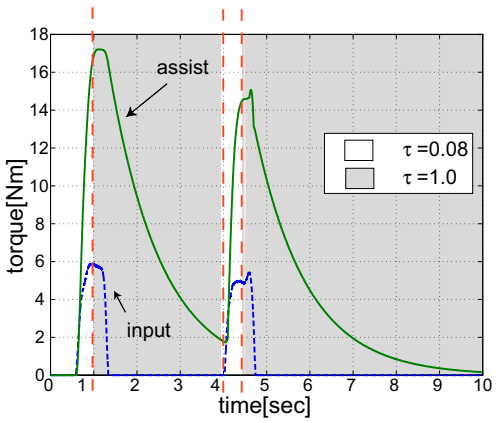

Figure 4.6: Input torque and assist torque versus time.

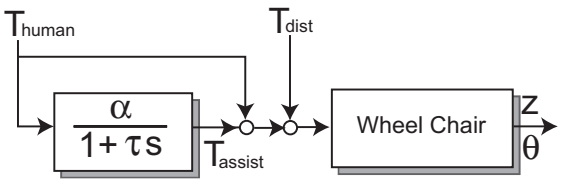

Figure 4.7: Basic power assistive controller used for tip-over protective control

Following values are adopted in Figure 4.7.

$$\tau_{fast} = 0.08[s], \quad \tau_{slow} = 1.0[s]. \tag{4.4}$$

And the behavior of this controller is shown in Fig.4.6. Fig.4.7 shows the block diagram of power-assistance controller.

Tip over of the wheelchair can be analyzed as the interaction between φ_{CG} and its angular velocity, $\dot{\varphi}_{CG}$. φ_{CG} and $\dot{\varphi}_{CG}$ are the rotational angle and its velocity of the center of gravity of the wheelchair and its pilot in the vertical direction. The relationship between these values of the center of gravity and the pitch angle of the wheelchair chassis φ which is estimated by the operational state observer proposed in Chapter 3 can be assumed as

$$\varphi_{CG} = \varphi - \varphi_0, \quad \dot{\varphi}_{CG} = \dot{\varphi}, \tag{4.5}$$

where φ_0 is the initial angle of the center of gravity when the pilot of the wheelchair does not change his center of mass during operation.

Fig.4.8 shows the phase plane of the inverted pendulum motion. We can divide the plane into three regions depending on the level of danger; A) proper safety zone where the front wheels are in touch with the ground and φ_{CG} is stabilized, B) semi-safety zone where $\varphi_{CG} < 0, \quad \dot{\varphi}_{CG} > 0$ so that the front wheels float temporarily, but they comes in touch with the ground again by the gravity, and C) dangerous zone where the front wheels float and φ_{CG} is destabilized and the wheelchair tips over.

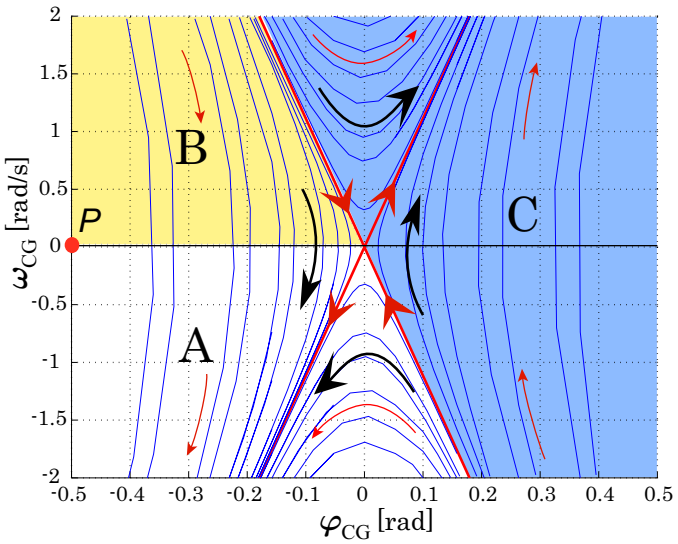

Figure 4.8: Phase plane of the angle φ_{CG}

The phase plane 4.8 describes motions by the gravity. If other torque is applied to φ_{CG} it transfers the phase to the right side and make it unstable. Taking this point into consideration, tipping over of the wheelchair can be prevented. For this problem, Hata[11] proposed assistive control which has a varying assistive function. In his research, he changed

the assist ratio which is described as α in Figure 4.7 as follows:

$$\alpha = \alpha_{\max} \exp\left(\beta \frac{\dot{\varphi}_{CG}}{\hat{\varphi}_{CG}}\right) \tag{4.6}$$

where β is the time constant which decides the decreasing speed of the assist ratio α, and $\alpha_{\max}$ is the maximum assist ratio. In [11], Hata also developed an observer that can estimate φ_{CG}, but it uses only a gyroscope as the output so that it is subject to the noise in the gyroscope. Compared with that observer, the operational state observer proposed in Section 3 can provide better estimation and consequently Hata's control can be improved. For this reason, here, the variable assist ratio α is decided using $\hat{\varphi}$ estimated by the operation state observer and the angular velocity φ of the chassis measured by a gyroscope.

$$\alpha = \alpha_{\max} \exp\left(\beta \frac{\dot{\varphi}}{\hat{\varphi} - \varphi_0}\right), \tag{4.7}$$

Another noticeable point is the independence of this tip-over protective control from the gravity-attenuation control. The control to prevent a wheelchair from tipping over is a feedforward control. On the other hand, the control that attenuates the gravity's effect on the wheelchair is a feedback control. These two controls work independently (See Figure 4.5).

Moreover, from the viewpoint of the frequency domain, they are also independent. The tip-over protective control changes the ratio α especially when the rider starts to propel. This means $\frac{d}{dt}T_{\text{human}} > 0$ and the time delay of feedforward assisting control τ_{fast} is small according to the equation (4.3). In this meaning, the feedforward tip-over protective control is related to the high bandwidth. The gravity-attenuation control feedbacks the velocity information, and it has a certain amount of time delay which is roughly equal to the time delay of the wheelchair dynamics itself, $\frac{J}{B}$. This is large enough compared with τ_{fast}, and consequently the gravity-attenuation control is mainly related to the low frequency bandwidth. These points are studied later using the experimental results.

4.2.3 Experimental Results

The effectiveness of this gravity attenuation controller is verified by experiments. Two kinds of experiments are conducted. One is done on level ground and the other is done on a hill. The results are shown in Figure 4.9. Focusing on the motor torque, we can see that on a hill, the controller produces a certain amount of motor torque while there is no human torque input, and it suppresses the falling down of the wheelchair. The amount of produced torque can be adjusted by the B_d parameter, and the parameter J_d will adjust the response time against gravity.

After 15 seconds, the rider applied the torque that runs the wheelchair backward. Even in that case, almost same torque is produced, which means the motor torque works in the opposite direction of the propulsive torque by the rider. This makes clears that the feedback control attenuates the gravity's effect regardless of the direction. To assess the effect of the

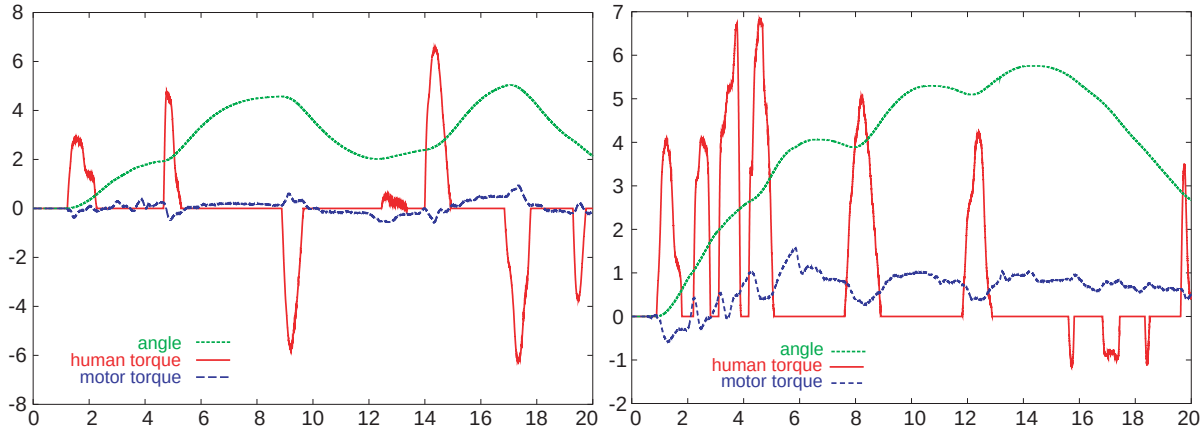

Figure 4.9: Experimental results (Left: drive on level ground, Right: drive on a hill))

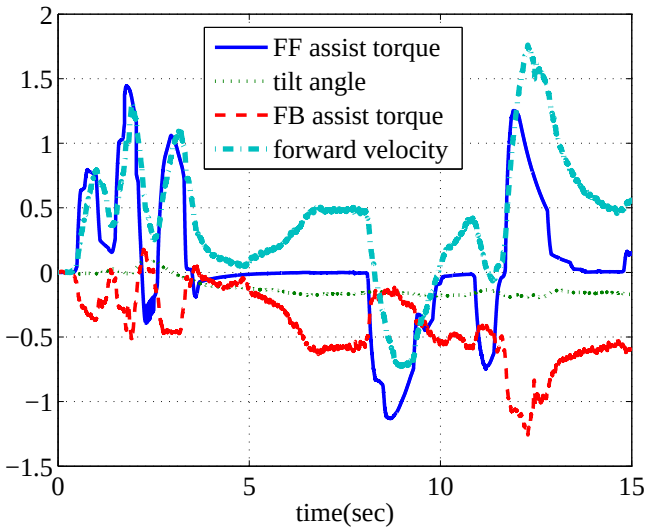

Figure 4.10: Assist torque on a downhill

controller on downward hill, another experiment is conducted on downward hill. Figure 4.10 describes the result.

Here, the tilt angle describe as dotted line in the Figure shows that from 4 second the wheelchair goes into a downhill. Then, the feedback assist torque described as the dashed line increases gradually and finally it reaches a certain value. We should notice that this controller does not remove the effect of gravity perfectly, which means that this feedback controller will not stop the wheelchair on a hill. In Figure 4.10, during the period from 7 second to 8 second, the wheelchair moves on at a constant velocity. This result is caused by the type of impedance that the feedback control adopts.

Around 12 second, the user applies his torque to move on to the forth, which means positive feedforward assist torque is applied and the wheelchair goes downward. However the feedback assist torque is still negative and it leads to slow acceleration so that it can ensure the safety of the user.

During level road operation from 0 second to 3 second, and backward propulsion on the downhill from 8 second to 10 second, the feedback assist torque is generated in the opposite direction of the feedforward torque. This is due to the difference between the nominal dynamics $\frac{1}{J_n s+B_n}$ in Figure 4.5 and the real dynamics of the wheelchair. The proposed controller produces the feedback torque according to the difference between simulated velocity and the actual velocity; that is, not only external force but also modeling error will cause the feedback assist torque. If the nominal parameters J_n and B_n are set bigger than the real values and the simulated velocity is smaller than the actual velocity, negative feedback torque is produced to track the actual velocity to the simulated velocity. This is the reason why the opposite torque to the feedforward torque is produced by the proposed feedback controller in the above experiment. Nevertheless, due to the impedance configuration in the feedback controller is not so stiff that this opposite feedback torque is not so large. This feature can be modified by adjusting the parameters J_n, B_n and the feedback impedance J_d and B_d.

Another experiment to assess the combination of the proposed feedback controller with the tip-over protective control is conducted. To investigate the effect of the tip-over protective controller on the proposed feedback control, two experiments are conducted changing the β in Equation (4.7).

At first, let us note the dotted line which means the tilt angle of the wheelchair chassis. This is estimated angle of φ in Figure 3.3 which indicates the inclination angle of the wheelchair chassis. The φ is changed by the condition of terrains on which a wheelchair traverses and also by wheelie, or lift of the front wheels. In all experiments, as the wheelchair goes up to a hill, the estimated $\hat{\varphi}$s increase and arrive at a certain constant value representing the angle of the hill. On the hill, the pilot exerts some torque to the wheels and it causes the lifting of front wheels, which is described by a peaks of $\hat{\varphi}$ in Figure 4.11.

We need to scrutinize the values of the feedback assist torque and the feedforward assist torque around these peaks of $\hat{\varphi}$ to reveal the performance of the combination. Let us take a close look around those peaks in the upper figure. First, human torque is exerted, and when $\hat{\varphi}$ is about to rise, the assist ratio decreases leading to the decrease in the feedforward assist torque. During this period, the feedback controller offers negative torque due to the modeling error in $\frac{1}{J_n s+B_n}$. After the decrease in the feedforward torque, the feedback torque returns to the constant value to compensate the gravity force. Figure 4.11 (b) is the result of the experiment with $\beta = 1$. With this control parameter, the decrease in the feedforward is insufficient, and consequently the peak of $\hat{\varphi}$ is higher that that of (a), which means the protection of tip is insufficient and results in tipping over. As discussed before, since the feedback controller provides a certain mount of torque to compensate the gravity 's force, β in the tip-over protective control should be smaller than that of without the feedback control.

This behavior of assist torque satisfies two requirements for power assist control on sloping surfaces: prevention of tipping over and compensation of the gravity. Figure 4.12 depicts the same experimental result with Figure 4.11 (a) but with the combined torque of the feedback and feedforward control.

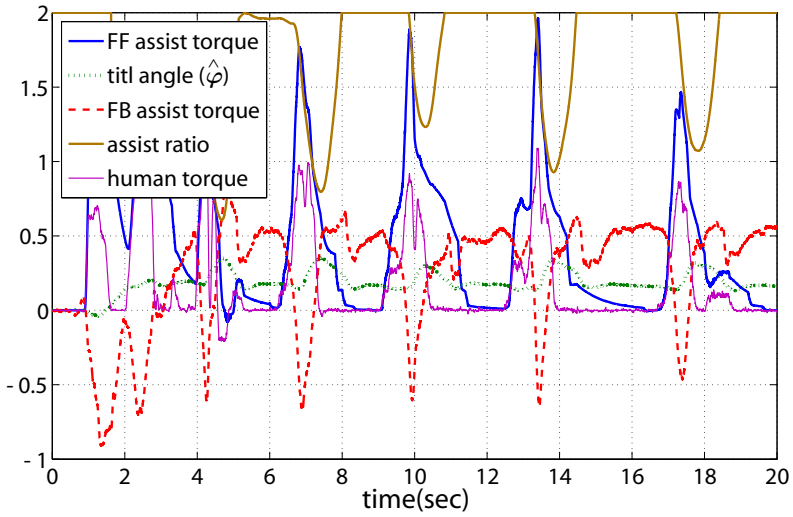

(a) $\beta = 3$

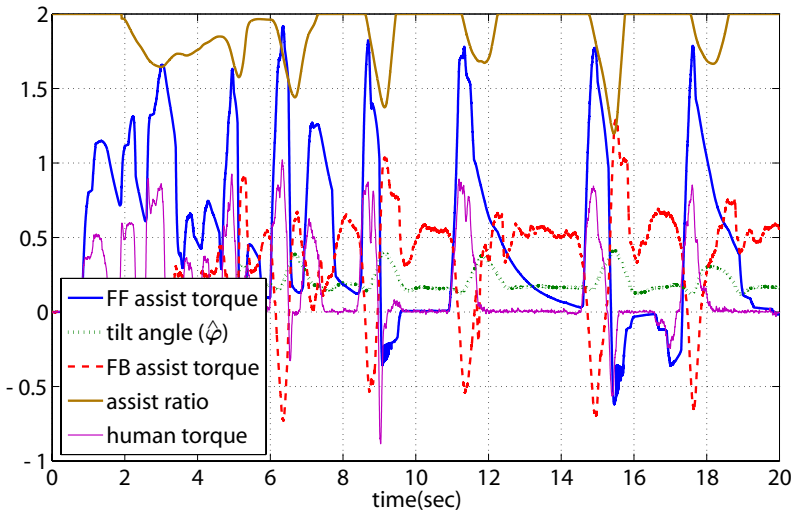

(b) $\beta = 1$

Figure 4.11: Experiment of tip-over protective control with disturbance attenuation control

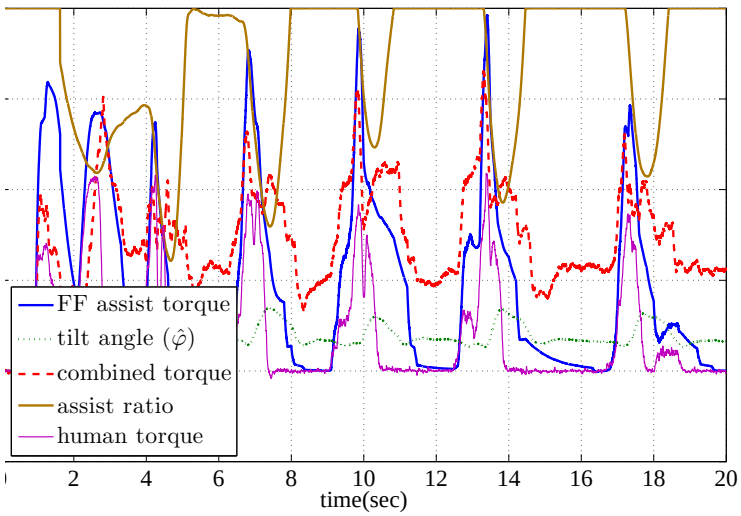

Figure 4.12: Combined assist torque during wheelies

One noteworthy point is the behavior of this combined torque after the feedforward torque is reduced by the decrease in the assist ratio. During some period after the decrease, the combined torque tends to keep a larger value than the value of the feedback torque provided while there is no human input. This additional torque is due to the feedback assist torque (see the same part of Figure 4.11) and helps reducing the dropping speed of the front wheels. This prevention of rapid shift in the center of gravity is another feature of the proposed disturbance attenuation control.

4.3 Lateral Disturbance Rejection Control

As is explained in the introduction, when a wheelchair crosses a slope as described in Figure 4.3, it is difficult to keep the direction; because the gravity works as a disturbance that changes the moving direction. This section focuses on this problem.

4.3.1 Lateral Dynamics of a Wheelchair

First, the lateral disturbance that causes changes of the moving direction should be defined mathematically so that we can control it. Figure 4.13 shows the definition; the lateral disturbance is defined as the difference between the external disturbances on the left and right wheels. Disturbance, here, means the other external torque than the motor produces.

This definition of lateral disturbance may seem too simple to explain the lateral motion in detail. The lateral dynamics of a four-wheel vehicle such as a car is, in general, described in a more complicated way [15]. It deals with the yaw-moment, side forces, cornering forces and other physical elements in lateral motion of a car. Figure 4.14 shows that physical

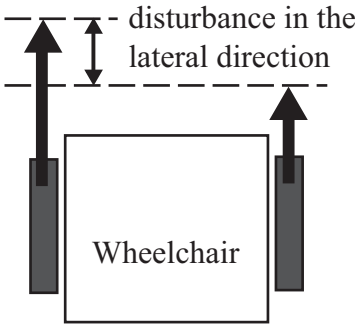

Figure 4.13: Definition of lateral disturbance

values.

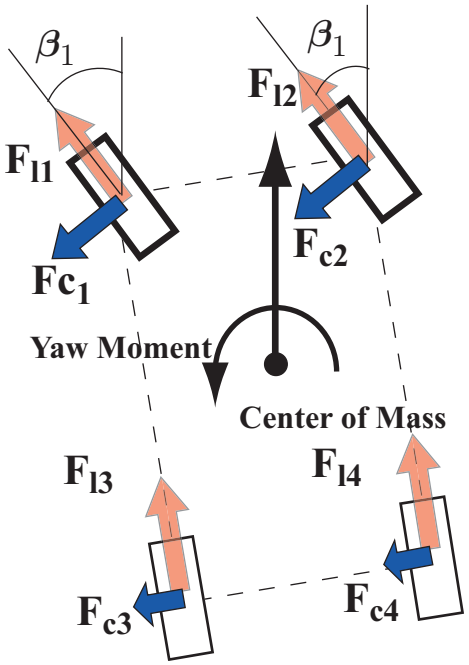

Figure 4.14: Lateral dyanamics of a four-wheel car

In the two-dimensional motion of a four-wheel car, the front wheels of a car is restricted by steering and it produces cornering forces which are described by F_{c1} to F_{c4} in Figure 4.14. These forces are induced by the side-slip angle which means the angle between the moving direction and a tire, and they are the main input forces to the lateral motion of a car. Moreover, since a car has four wheels and four cornering forces, yaw moment is generated by the relationship between them. The lateral dynamics of a car is modeled in this way.

However, the lateral dynamics of a wheelchair is simpler than that of a car. The front wheels of a wheelchair are casters and not restricted. Thus, the front wheels produce neglectable amount of cornering forces. The side-slip angle is not so large that we can neglect the cornering forces of rear wheel too. Apart from it, the length of a wheelchair

is much shorter than that of a car. Consequently, we can assume that the difference between driving forces applied two rear wheels is the only input in the lateral dynamics of a wheelchair. This assumption justifies the definition of lateral disturbance in Figure 4.13.

Figure 4.15: Casters as front wheels of a wheelchair

Using this definition, controllers which control this lateral disturbance can be designed.

4.3.2 Important Feature in the Lateral Control of a Wheelchair

Last Section proposed a controller that suppress disturbance in the back and forth direction. In human-friendly motion control, the lateral direction needs different strategy in disturbance suppression control. Human beings in a vehicle are accustomed to velocity control in the forward direction and position control to the lateral direction (see Figure 4.16). This is made clear when we investigate to which kind of steady-state people are most sensitive.

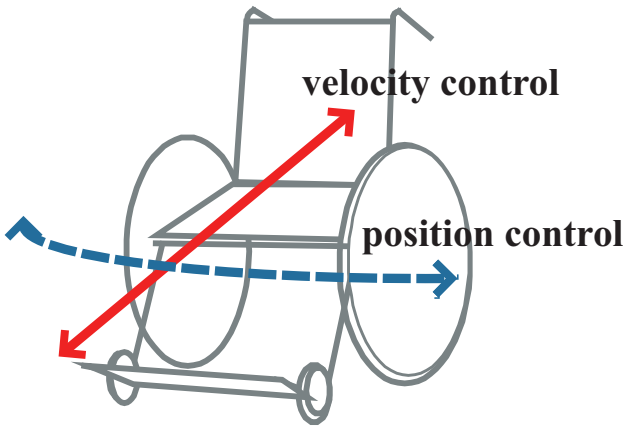

Figure 4.16: Necessary control in each direction

In the forward direction, people do not care about position errors. The precise position of a vehicle does not mean much to riders. However, an error in velocity can make rider feel unnatural. It is true that a driver in a car conducts velocity control in the forward direction using an accelerator. On the other hand, in the lateral direction, he does position control by steering because errors in lateral position results in the wrong direction.

This is the point we should take into consideration when we design lateral control for a wheelchair. Based on this idea, two controllers will be suggested.

4.3.3 Two Types of Lateral Disturbance Rejection Control

Figure 4.17 and 4.18 are the proposed controllers.

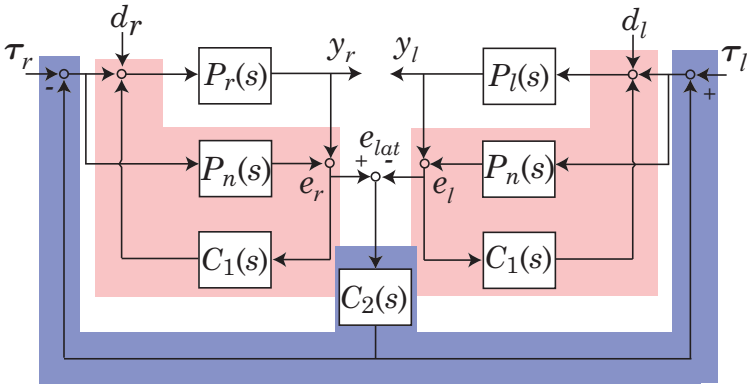

Figure 4.17: Structure of a lateral disturbance rejection controller - force control type

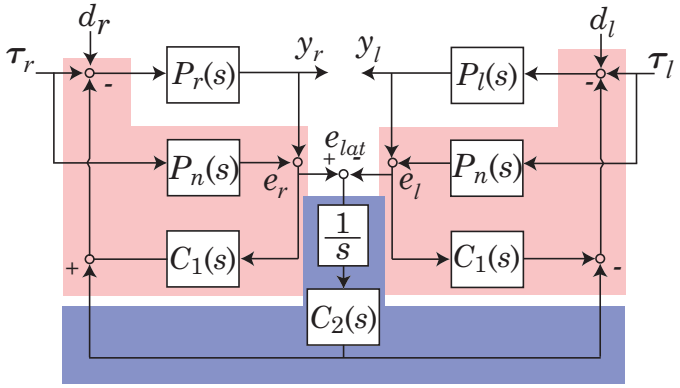

Figure 4.18: Structure of a lateral disturbance rejection controller - position control type

As discussed in the last section, small difference between the angles of two wheels makes a turn in the wheelchair. Two types of lateral controls described in Figure 4.17 and 4.18 are designed to remove this difference. One is force type that removes the lateral disturbance force; the other is the position type which makes high stiffness against the lateral disturbance force. Figure 4.17 is the force type control because it can deal with the disturbance force according to the design of C_2 filter. Figure 4.18 is the position type control because it feedbacks the position error. A more detailed explanation will be given later on the features of these two control designs.

What is noticeable is that in these Figures, the forward disturbance attenuation controllers are included too. Controllers in the red colored rectangles are the forward disturbance attenuation controllers, and controllers in the blue colored rectangles are the lateral disturbance rejection controllers. These two kinds of controllers constitute two dimensional disturbance suppression control of a wheelchair. A power assistive wheelchair has two motors in both wheels so that it can achieve this two dimensional control.

Firstly, $C_2(s)$ for the force type control in Figure 4.17 is designed. Let the lateral disturbance be defined d_{lat} like equation (4.8). d_r and d_l is the disturbance acting on the right wheel and the left wheel respectively.

$$d_{lat} = d_r - d_l \tag{4.8}$$

The purpose of this lateral assistance control is make the effect by this d_{lat} on $e_r - e_l$as small as possible. Let's define this $e_r - e_l$ as e_{lat}. Considering the transfer function from d_{lat} to e_{lat}, the controller $C_2(s)$ can be designed.

The transfer function in Figure 4.17 is

$$T_{lat1}(s) = \frac{e_r - e_l}{d_{lat}} = \frac{P}{1 + PC_1} - \frac{2PC_2P}{1 + PC_1}, \tag{4.9}$$

where $P_r = P_l = P_n$ is assumed.

To make this transfer function insensitive $C_2(s)$ is designed like equation (4.10).

$$C_2(s) = \frac{1}{2}\frac{P_n^{-1}(s)}{\tau s + 1} \tag{4.10}$$

This makes the transfer function $T_{lat1}(s)$ 0 ideally.

This $C_2(s)$ has a inverse dynamics of a wheelchair, and thus it estimates and control the lateral disturbance force under ideal conditions; this is why it can be classified as force control. In the meaning that it estimates the disturbance, this control can be a disturbance observer in the lateral control which has been researched in [20], [14].

$C_2(s)$ in Figure 4.18 is designed like below. The transfer function is different in Figure 4.18.

$$T_{lat2}(s) = \frac{e_r - e_l}{d_{lat}} = \frac{P}{1 + P(C_1 + 2\frac{C_2}{s})} \tag{4.11}$$

To achieve position type control, $C_2(s)$ should provide some stiffness against the lateral disturbances.

$$C_2(s) = \frac{1}{2}\left(K_D s + K_P\right) \tag{4.12}$$

This $C_2(s)$ makes the transfer function

$$T_{lat2}(s) = \frac{1}{(J + J_d)s^2 + (B + B_d + K_D)s + K_P}. \tag{4.13}$$

Here, K_P works as the stiffness against the lateral disturbances which is a key parameter determining how much the controller suppress lateral disturbance. In spite of this existence of stiffness K_P, a constant lateral disturbance can cause a constant position error e_{lat}. If

we want to reject that error, an integrator $\frac{K_I}{s}$ should be added in $C_2(s)$, but it may bring about some troublesome problems such as wind-up to which the integration is subject.

For suppression of the forward gravity, $C_1(s)$ employs the controller described in Figure 4.5 and just increases the inertia and damping against the forward gravity. But the $C_2(s)$ allows us a strict disturbance rejection control in the lateral direction. This is the control strategy for the two dimensional disturbance attenuation control of the wheelchair.

4.3.4 Experimental verification of proposed method

For the lateral disturbance rejection control verification, the following two strategies are the experiment was done in this way:

- Forward disturbance rejection control is designed strong, which means J_d and B_d in Figure 4.5 is small.

In contrast, lateral disturbance control is designed strong enough to suppress the gravity's effect. This design will make distinction between two controllers' performance, and by this, the effectiveness of the lateral disturbance suppression control can be verified.

- Torque exerted by the user is not assisted so that the torque will work as disturbance.

This means that we use human torques as lateral disturbances. Those disturbance torques can be measured and help us see how our proposed controller works. Figure 4.19 to 4.21 are the results. The lateral controller of the force type in Figure 4.18 is experimented.

Figure 4.19 shows the exerted torques as disturbance, and this disturbance is calculated by subtracting two exerted human input torques. The blue dotted torque is applied to a wheelchair without the lateral control, and the red line is to a wheelchair with the lateral control. At the beginning (to 5 second in the w/o control case, and to 7 second in the w/ control case), the right and left torques are exerted in the same direction so that the lateral disturbance, or the difference between the left and the right input torque is not so large. After that period, the torque is applied in the opposite directions, and it produces quite large lateral disturbance.

Figure 4.20 is the output of this applied torque, and shows the differences between the right and left wheel angles. Without the lateral control, the difference becomes large, and this will make the wheelchair turn against the user's will. While, with the control the difference does not become so large that the lateral disturbance does not interfere with the moving direction.

Independence between the forward control and the lateral control is also verified with experiments. In the following experiment, J_d, B_d in Figure 4.5 is designed small to decrease the performance of the forward disturbance attenuation control.

Figure 4.21, 4.22 shows that the proposed lateral control rejects only the lateral disturbance. Figure 4.21 is the measured disturbance, and it shows the disturbances on two wheels respectively. Until 7 second, both right and left disturbances are working in the same direction, which drives the wheelchair straight. Angles described in Figure 4.22 shows

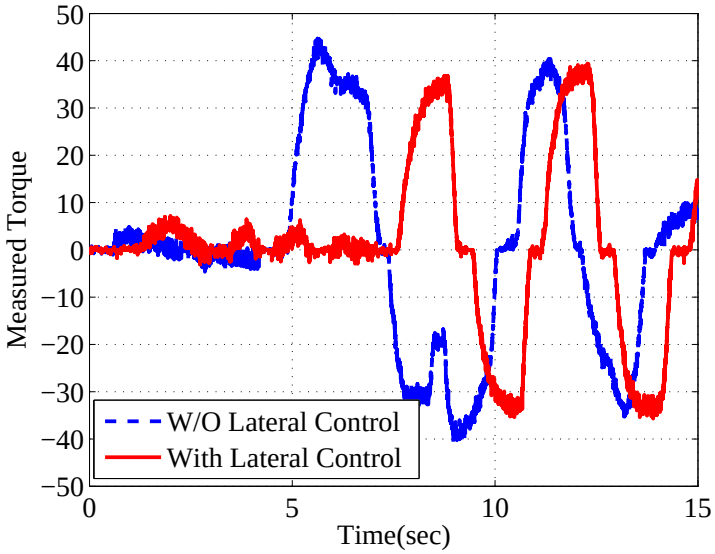

Figure 4.19: Exerted lateral disturbances

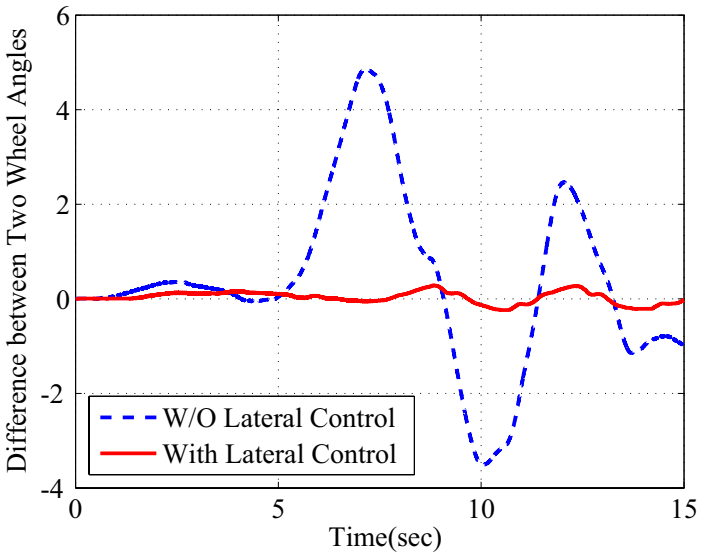

Figure 4.20: Differences between the right and left wheel angles

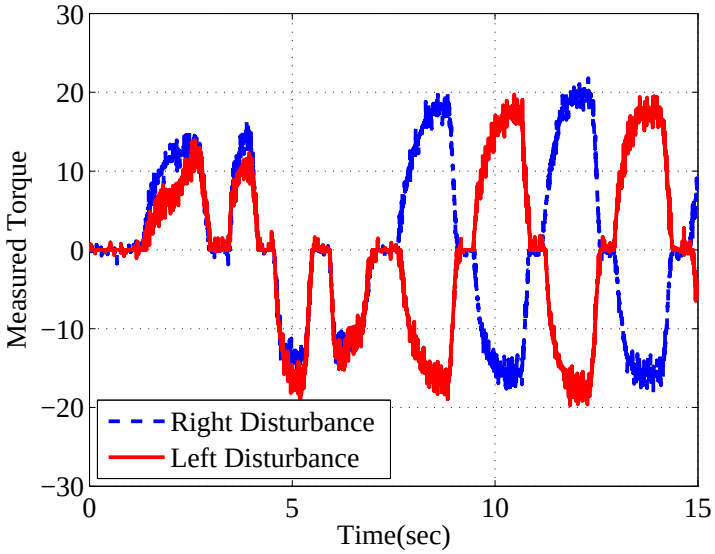

Figure 4.21: Disturbances in the same and opposite directions

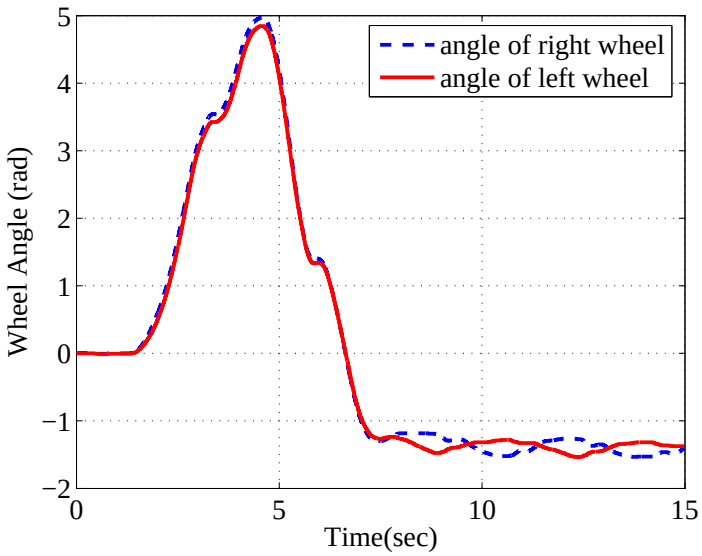

Figure 4.22: Independence of the control on the direction: wheel angles

that the wheelchair goes forward until 7 second and the disturbance is not removed. From 7 second, the torque works in the opposite direction. Although the magnitude of the torque is much larger, the angle driven by that torque is quite small and the right and left disturbances are eliminated. This makes clear that the proposed controller rejects disturbances when they are applied in the opposite direction, which means that proposed controller rejects only the lateral disturbance.

4.4 Summary

4.4.1 Three Dimensional Control for a Wheelchair

Disturbance attenuation control in two directions was proposed in this chapter. Apart from it, in the forward direction, tip-over protective control can also be added to this two-dimensional control. All these controllers can work independently, and it achieves the three dimensional control of a wheelchair: disturbance rejection control for the forward and the lateral direction, tip-over protective control for the pitch direction.

Disturbance rejection controls in two directions can work independently because the number of actuators is two and provide enough degree of freedom. It fully uses the degree of freedom of two motors in both wheels. For the forward direction, forward disturbance rejection control and tip-over protective control use the same actuator, nevertheless their frequency bandwidth are different. As a result, they can be implemented at the same time and conduct their own control without interruption.

Furthermore, these control designs are done in the human-friendly way.

4.4.2 Appropriate Disturbance Attenuation for Human User

Human-friendly design of disturbance rejection control is introduced and explained. The most important point in this human-friendly design is the consideration of the impedance concept. In contrast to the conventional industrial control applications that are designed with the aim to eliminate external disturbances and track to the reference values, in welfare tools such as power assistive tools, the performance of disturbance attenuation control should be evaluated in other way. It should consider the influence of the controller on the feeling and safety of the users. In this meaning, the impedance of a feedback control that decides how to react against disturbance is one of the most important factors of making the system human friendly because the impedance also affects the user's feeling and safety.

Impedance control has employed $\frac{1}{Ms^2+Ds+K}$ as the standard impedance. However, because impedance control is a general form of various kinds of feedback control as discussed in Chapter 2, it can have a range of impedance option. The impedance should be designed more carefully according to the cases. For instance, the proposed two-dimensional control; for the forward direction, a velocity type impedance was adopted and for the lateral direction, a position type impedance was adopted.

There are problems suggested here but unsolved; how should we design proper impedance

for welfare tools or what kind of impedance is the most suitable for each power assistive application. These can be listed as future works, and furthermore the fractional impedance or human muscle model suggested in Chapter 2 can be key technologies in this advanced impedance design.

Chapter 5

Development of External Force Amplification Control as a Sensor-free Power-assist Control

5.1 Introduction

Human-friendly motion control for power assist devices also needs external force amplification. The situation where the power assist devices are used explains this necessity; these tools are located near people so that the user himself may be a disturbance from the viewpoint of assisting motor. Consequently a controller needs to support or amplify this external force caused by the user.

This circumstance of usage calls for the following specifications.

Assist human force without any force sensor Power assist devices should assist exerted human force without a force sensor.

Guarantee users' safety Power assist devices should be more sensitive to the user's force than to a reference force.

These specifications will be satisfied by the external force amplification control proposed in this chapter.

Figure 5.1 describes the general block diagram of the usual power assist devices. They have force or torque sensors to measure the force exerted by a user, and then the controller produces necessary force reference according to the measured forces (amplified by K times in Figure 5.1). However, due to the force sensor, power assist control comes to cost too much and the way it supports the user is restricted.

The external force amplification control, as it is a controller that makes a plant sensitive or light to a external force using position feedback, can achieve power assist control without any force sensor. This is one feature of the external force amplification control.

Secondly, from a safety perspective, this external force amplification control is important. The strict disturbance (that is another name of external force) rejection which has been employed in the industrial applications is likely to endanger the user. Motor systems used near people should react more sensitively to human force. There was an accident that

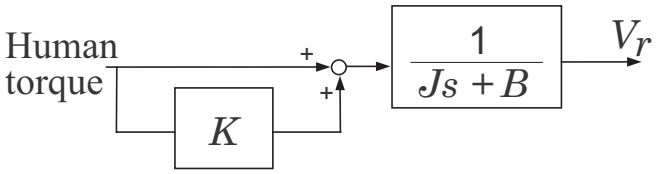

Figure 5.1: Conventional power assist system

indicates a motor system controlled without this consideration did harm. An automatic revolving door in Tokyo crushed a child to death on March 2004. If that door would have acted more sensitively to the force of the boy, he could have been saved. This is another necessity of the external force amplification control.

Figure 5.2: Revolving door accident leading to a death of a boy (Tokyo)

These two points are scrutinized; the achievement of force-sensor-less power assist control is designed for a wheelchair and verified by experiments, and the increase in the safety of users is simulated considering the two degree-of-freedom characteristics of the proposed controller.

5.2 Development of Power Assist Control by Impedance Design

5.2.1 Relationship between Impedance Design and Power Assist Control

Figure 5.3 is the most general block diagram of power assist control in more detail.

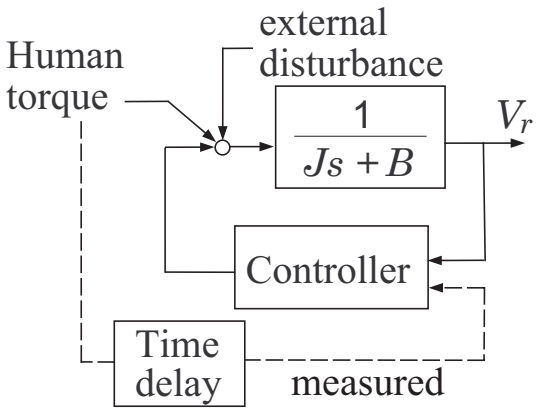

Figure 5.3: Characteristics of human torque as reference input

In this power assist control, human force is measured to be assisted by a motor, and the force sensor is a straightforward solution to obtain force information. However, from Figure 5.3, we can figure out that human force acts as disturbance to the controller because any input to the plant that is not from the motor is recognized as disturbance in feedback control. The impedance to the disturbance is decided according to the feedback controller design. This viewpoint is what this dissertation has suggested, and it is also a key to achieve the force-sensor-less power assist control.

This equivalence of human force and disturbance allows us two approaches to design this force-sensor-less power assist control: impedance control[19] approach and disturbance observer approach.

Figure 5.4 depicts the impedance control using velocity feedback.

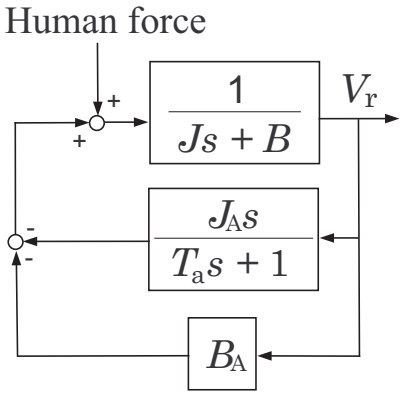

Figure 5.4: Compliance control for flexible disturbance attenuation

Note that this control is basically same with the disturbance attenuation control adopted in Section 4. This feedback control makes the dynamics from human force to the velocity of a plant as following;

$$T_{c1}(s) = \frac{1}{(J + J_A)s + (B + B_A)} \tag{5.1}$$

In this dynamics, the new inertia $J + J_A$ and the new damping $B + B_A$ (or the time constant $\frac{J+J_A}{B+B_A}$, and the DC gain $\frac{1}{B+B_A}$) are two important physical parameters. By changing J_A and B_A, we can change these two parameters.

To sensitize a motor to disturbance or amplification of external force means to make this inertia and damping small. To this end, J_A and B_A should be negative, and consequently it will be positive feedback. This is likely to make the system unstable. For this reason, using this structure directly may not be appropriate for power assist control. This structure is only suitable for disturbance attenuation. (Chapter 4 adopts this controller in the two degree-of-freedom form to attenuate the disturbance.) Nevertheless, the idea that to render the impedance of a system smaller so as to assist human force is still effective.

In next section, a novel control strategy for external force amplification based on the above idea; that is, to render the impedance for power assist control, and to use the disturbance observer.

5.2.2 Impedance Design Using the Disturbance Observer

There are some researches that use the disturbance observer to measure human force [20], [16]. These researches suggested force-sensor-less power assist controls for wheelchairs. It should be noted that these researches focus on retrieving the precise magnitude of human force from observed disturbance, because they aimed to use the estimated human force as a force or acceleration reference.

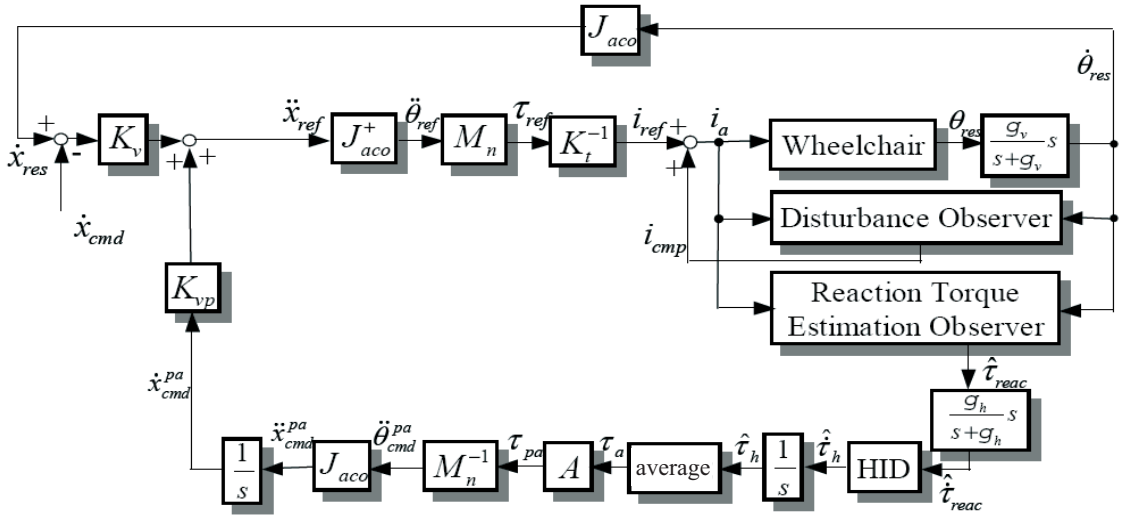

Figure 5.5: Power assist control proposed in [16]

Figure 5.5 is the controller adopted in [16]. It uses the reaction torque observer which is depicted in Figure 5.6. It estimates human force input τ_h using the disturbance observer and previously-measured other disturbance force τ_{init} such as friction. The research [20]

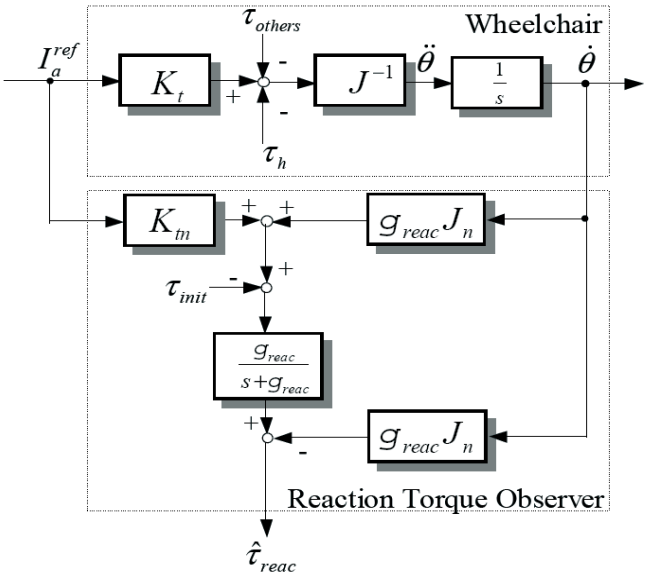

Figure 5.6: Reaction torque observer

also uses this reaction torque observer. This estimation relies on the precise model of the plant (here, a wheelchair) and the precise value of τ_{init}. The reaction torque observer can estimate only if $\tau_{init} = \tau_{other}$, but the elements that constitute other disturbances τ_{other} is varying easily. This causes problems in real applications.

The other necessary consideration is about how to use this estimated human force information. [16] and [20] used the estimated value as a command reference. This works very well when the models are correct, however, when there are modeling errors, this kind of usage may be too sensitive to those errors and even difficult to analyze the stability characteristics if the controller adopts a nonlinear filter [16].

Here, in order to realize power assist control, another usage of the disturbance observer based on the impedance concept is proposed. As discussed in the last section, decreasing inertia is related to increasing sensitivity and it results in as power assistance. Hori[18] suggested inertia control which can simulate the inertia value of motor using disturbance observer. This inertia control only adjusts inertia value in low frequency band. Adding damping factor into this control enables us to have enough parameters for impedance design.

Figure 5.7 is the proposed controller which includes the damping factor (B_M).

$\frac{1}{Js+B}$ is the dynamics of a plant. Here, the simple dynamics of a wheelchair is employed. The rectangle blocked by the dotted line is the disturbance observer which observes disturbance including human force. $\frac{1}{J_M s+B_M}$ is the target impedance, a key factor in this control design. These disturbance observer and target impedance makes the target velocity v_{imp}. As a result, the velocity of the plant will track this velocity v_{imp} with the gain A.

In this control, it is not necessary for the real velocity to track v_{imp}. Although $\frac{1}{J_M s+B_M}$ is called as the target impedance, the resultant impedance does not need to be $\frac{1}{J_M s+B_M}$, which means the gain A does not need to be high for tracking performance. The achieved

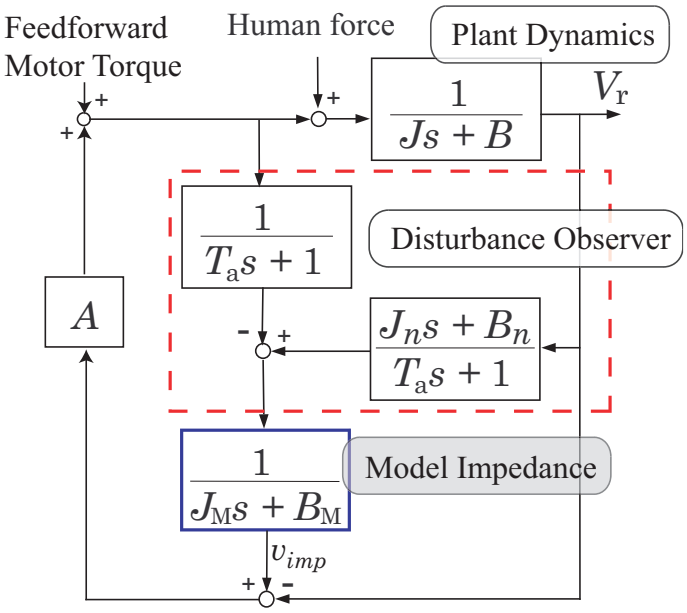

Figure 5.7: Block diagram of proposed control design

impedance shoule be considered including all parameters. With this control system, the impedance which is defined as the transfer function from human force to velocity will be given as Equation (5.2).

$$T(s) = \frac{1}{Js + B + A}\left(\frac{J_M s + B_M + A}{J_M s + B_M}\right) \tag{5.2}$$

It is true that if A is high enough, the resultant impedance will be the target impedance $\frac{1}{J_M s+B_M}$. However, since A is a good parameter that decides the impedance in Equation (5.2), it should be decided according to designer's intention in terms of impedance not velocity tracking gain. How to decide these parameters or the relationship between these parameters and control performance is explained in section 5.4.2.

5.3 Analysis of the Proposed Assistance Control Using Simulations and Experiments

5.3.1 Application to a One-link Robot System

In order to verify the proposed power assist control method, we apply the proposed controller to a robot which has one arm. The experimental setup is described in Figure 5.8.

The robot has one arm and an operator add his force to the arm. By investigating velocities driven by the human force, we can examine the performance of the proposed control method. Figure 5.9 shows the results.

Two experiments were practiced; one without proposed controller, the other with the controller. In both experiments no torque reference is supplied, and the arm is driven only

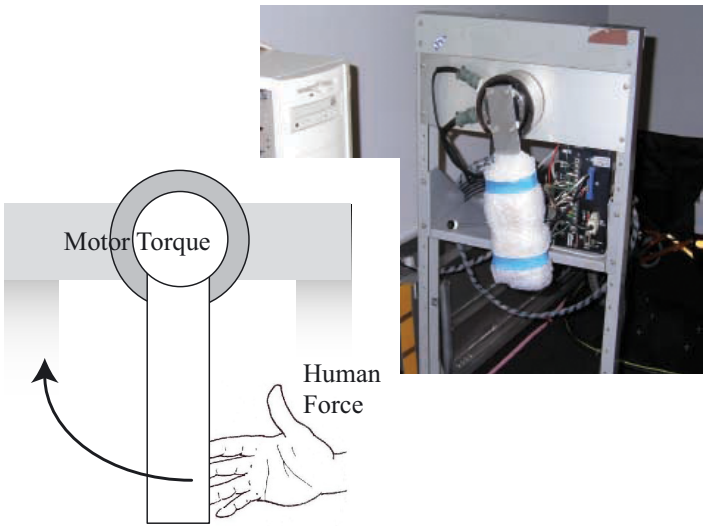

Figure 5.8: Experimental setup

Table 5.1: Parameter values (normalized to motor voltage)

J	0.024	B	0.1	J_M	0.005	B_M	0.001	A	1

by the external human force. Figure (a) shows observed disturbances in both experiments, and the disturbances include human force. We can see the ranges of both force are not so different each other.

Figure (b) shows the velocities of the robot arm. In spite of the similar ranges of input forces, the ranges of velocities are different each other. Velocity with proposed control is almost two times bigger than the one without control.

Figure (c) shows tracking characteristic of the controller. From this result also suggests appropriate J_M, B_M and A is able to achieve desired disturbance reaction design.

5.3.2 Analysis of Two Degree-of-freedom Characteristics

This proposed control algorithm can also be a solution to the revolving door problem. This section formulates the problem from the viewpoint of control design, and explians how the proposed control design can be a solution to the problem.

Figure 5.10 depicts two operational situations of a revolving door. Figure 5.10 (a) shows general operation where the door is revolving at a constant speed. This operation needs a constant torque reference for a motor, and the magnitude of the torque can calculated based on the dynamics of the door. Let us model the dynamics as

$$\omega_{door} = \frac{1}{J_{door}s + B_{door}} \left(\tau_{ref} + \tau_{ext}\right), \tag{5.3}$$

where ω_{door} is the rotational velocity of the door, and τ_{ref} is the torque by a driving motor. If the driving torque τ_{ref} is $B_{door}\omega_{ref}$, and there is no external torque, the door will revolve

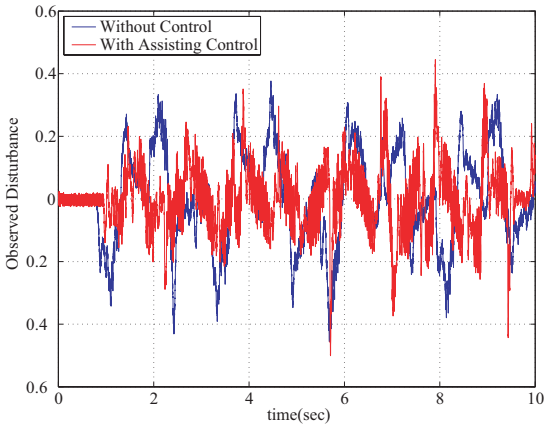

(a) observed disturbance (including human force)

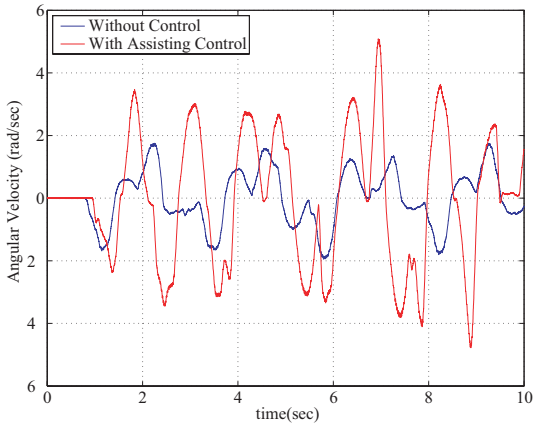

(b) velocities of the robot arm (with and without control)

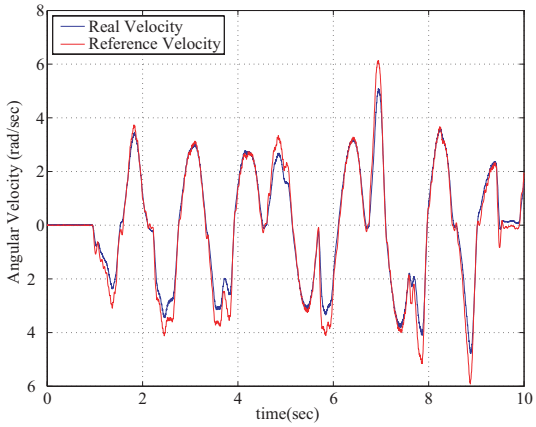

(c) velocity tracking

Figure 5.9: Experimental results

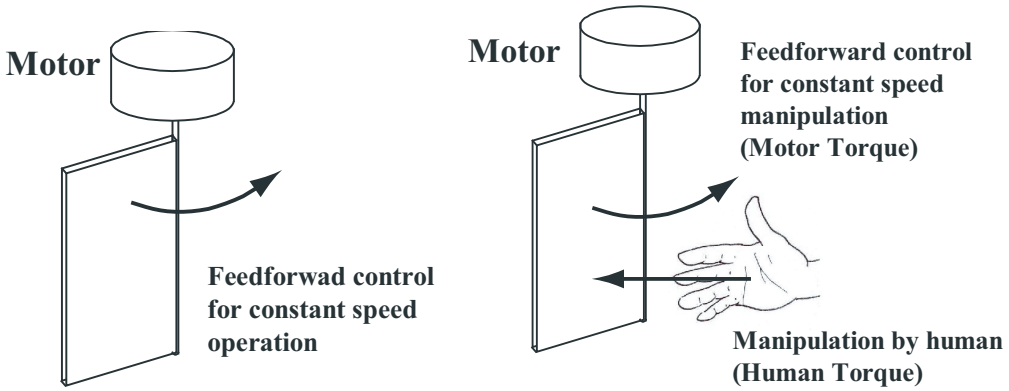

(a) General operation (b) Force is applied by a human

Figure 5.10: Operational situations of a revolving door

at the constant velocity ω_{ref}.

τ_{ext} is other external torque to the door, and human force applied to the door is regard as this τ_{ext}. Figure 5.10 (b) describes the situation where a human applies his torque as a external force to the door. In this operation, a human should exert the same torque as the motor to stop the door.

This is the problem. If the door is big and B_{door} is large, τ_{ref} to revolve the door needs to be large. Under this circumstance, when the door is too big or the person is too weak, the motor's torque defeats human torque, and endangers him because a person who wants to stop the door by his force, should provide the same large force to stop the door.

What difference the proposed controller can produce if it is applied to this system? The dynamics with the proposed controller will be

$$\omega_{door} = \frac{A}{J_{door}s + B_{door} + A}\tau_{ref} + \frac{1}{J_{door}s + B + A}\left(\frac{J_M s + B_M + A}{J_M s + B_M}\right)\tau_{ext}. \tag{5.4}$$

In order to make clear the difference, the force to stop the revolving door will be compared. Without the proposed external force amplification control, the necessary force was

$$\tau_{ext} = -\tau_{ref} = -B_{door}\omega_{ref}. \tag{5.5}$$

On the other hand, with the proposed control the relationship comes to be 5.6.

$$\tau_{ext} = -\frac{AB_M}{B_M + A}\tau_{ref} = -\frac{AB_M}{B_M + A}B_{door}\omega_{ref}. \tag{5.6}$$

This equation means that the feedforward motor torque τ_{ref} will be confronted by the human force with a ratio of $-\frac{AB_M}{B_M+A}$. It is interesting that the ratio can be arbitrarily decided regardless of the physical values of the plant such as J_{door}, B_{door}. Usually, the ratio is set smaller than 1, which is explained in Section 5.4.2.

This is the two degree-of-freedom characteristic of the proposed controller. The dynamics by a feedforward motor torque and by external torque are determined separately. In general operation, a motor provides a certain amount of torque to revolve the door at a certain

velocity, and this is a feedforward control. However, when external force is applied, the system moves more sensitively to the external force by the proposed feedback control. Thus, in spite of a large magnitude of the feedforward reference torque, a human can stop the door with smaller force.

A simulation is conducted using the parameters in Table 5.1 to ascertain this fact. Figure 5.11 shows the result.

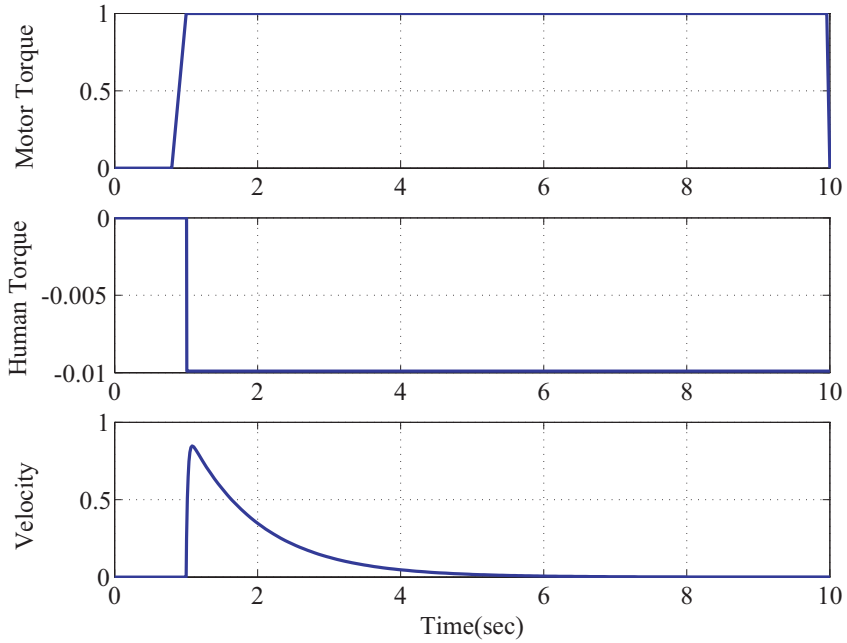

Figure 5.11: Simulation considering revolving door application

Parameters in Table 5.1 are chosen to the simulation. The upper figure is the feedforward reference torque τ_{ref}, the middle figure is human force τ_{ext}, and the lower figure describes the velocity of a plant ω_{door}. After the feedforward reference torque is produced at 1 second, the human force is applied, then the velocity comes to zero gradually. Notice that the human force necessary to stop the plant is almost $\frac{1}{100}$ (precisely $\frac{0.01}{1+0.01}$ with the parameters in Table 5.1) times the force τ_{ref}. The possibility of the proposed controller as a solution to the revolving door accident is verified by this simulation.

5.4 Application to a Wheelchair as Force-sensor-less Power Assist Control

5.4.1 Problems in the Conventional Pushrim Activated Power Assist Wheelchair

In this section, the proposed external force amplification control is applied to a wheelchair. Recent power assist wheelchairs are mostly pushrim-activated wheelchairs [2]. The wheelchair

used for experiments in this research is the JW-II by YAMAHA, which is also pushrim-activated type. Figure 5.12 shows overall view of the wheelchair and the location of a torsion sensor attached between the pushrim and the tire. These kinds of force sensors only measure forces that are applied to limited parts of the wheelchair. In these cases, only the torque applied to the pushrim is measured. For this reason, a human helper who assists a person on a wheelchair by pushing the wheelchair does not benefit from power assist control. If a sensor is installed in the handle for a helper, a rider will not benefit. In this way, the force sensors restrict the way that power assist control works. Moreover, the sensors are expensive and become one reason that makes the power assist wheelchairs cost that much.

Consequently, the power assist wheelchair can be said one of the most suitable application of the proposed external force amplification control since the force-sensor-less power assist control can cope with these two problems.

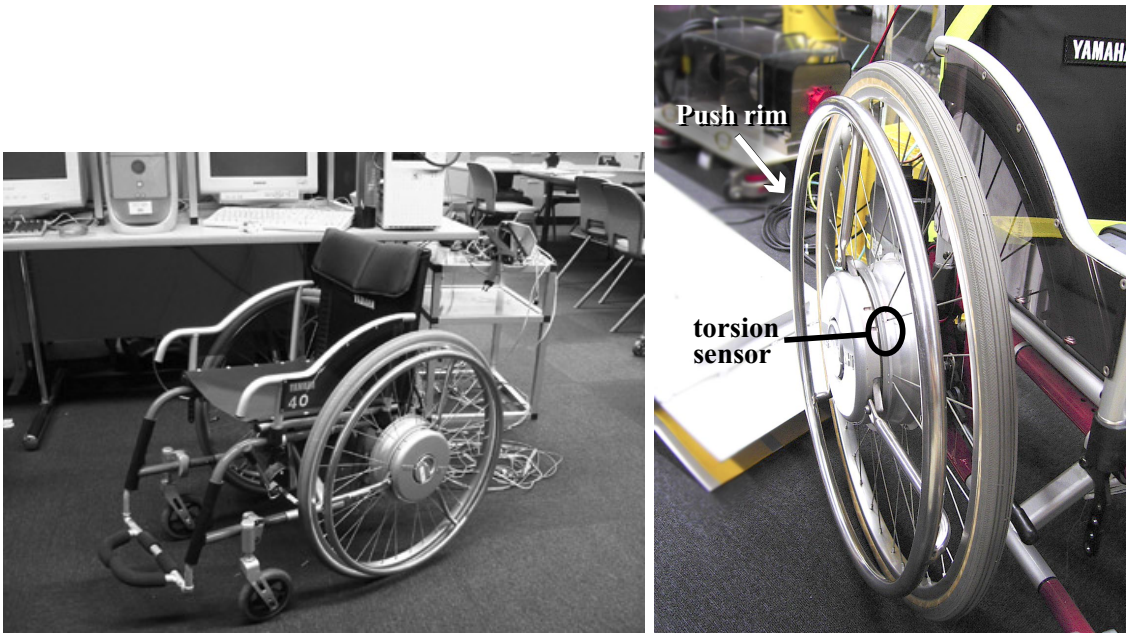

Figure 5.12: Experimental equipment

Figure 5.13 is the control strategy for the realization of a power assist wheelchair with the force-sensor-less power assist technique. First, the proposed external force amplification control is the core technology in achieving this wheelchair. Apart from it, we need to know how to tune the parameters in the controller and how the model uncertainty affects the performance of the system. Moreover, the influence of the gravity to the system should be considered because the gravity also will be amplified in this system.

These three issues are addressed in the following sections.

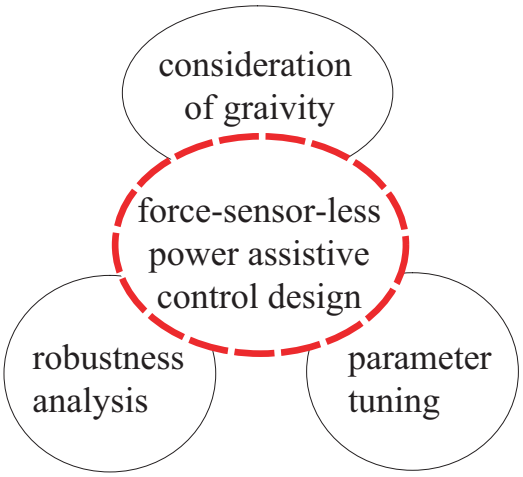

Figure 5.13: Strategy for a sensor-free power-assist wheelchair

5.4.2 Numerical Consideration of Control Parameters

The control parameters adopted in Section 5.2.2 are left unexplained. In this section, relationship between the parameters and control performance is clarified in this section. For the application to the power assist wheelchairs, the explanation of the parameters can be done with a step torque input because human torque applied to a wheelchair can be modeled as a step or impulse signal (Figure 5.14 is a torque pattern in usual operation). Moreover, we need some simplicity for the mathematical analysis of parameters. For these reasons, the analysis from now is done with a step torque input.

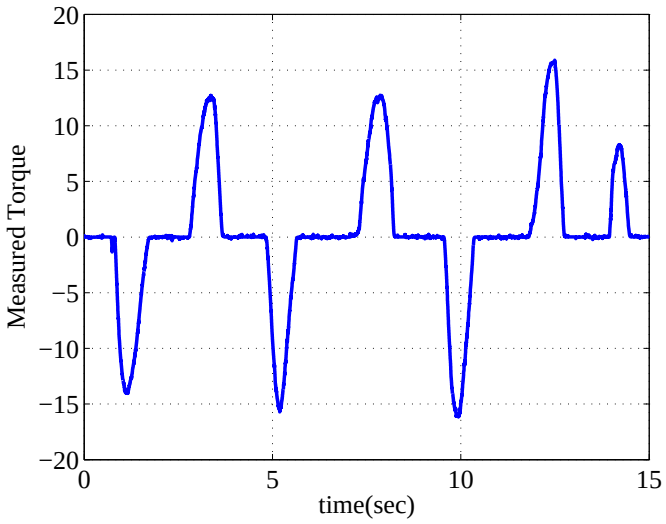

Figure 5.14: Usual torque pattern by a user

Dynamics from human force to velocity of a wheelchair without the proposed control can

be simplified as

$$P(s) = \frac{1}{Js + B} = \frac{1}{\tau_b s + 1} \tag{5.7}$$

For simplicity, DC gain, which is $\frac{1}{B}$, is normalized as 1 here. The only parameter of the wheelchair, then will be τ_b which corresponds to $\frac{J}{B}$.

With the proposed control, this dynamics is converted to Equation (5.8).

$$P_{c2}(s) = \frac{1}{Js + B + A}\left(\frac{J_M s + B_M + A}{J_M s + B_M}\right) = K' \frac{1}{\tau_{b'} s + 1} \frac{\tau_h s + 1}{\tau_l s + 1}, \tag{5.8}$$

where some new parameters are adopted for analysis. The relationship between the parameters are: $K' = \frac{B_M + A}{(B+A)B_M}$, $\tau_{b'} = \frac{J}{B+A}$, $\tau_l = \frac{J_M}{B_M}$, and $\tau_h = \frac{J_M}{B_M + A}$. These new three parameters can be modified by changing the control parameters J_M, B_M, A. Using the new parameters, analysis of control performance can be conducted in time domain. Three key indexes of the performance are the time constant, the DC gain, and the peak value of jerk.

Time constants and DC gain

The DC gain is represented by K', and it means the same as the assistance-ratio in the conventional power assist control (α in Figure 1.7). Also in the proposed control method, this value is interpreted as the gain in the low frequency band. In the high frequency band, the gain will be changed.

In Equation (5.2), $\tau_{b'} = \frac{J}{B+A}$,$\tau_l = \frac{J_M}{B_M}$ are two time constants. To investigate the role of these two time constants, step torque is used as an input to $P_{c2}(s)$. Then, the velocity of the wheelchair will be

$$v_r(t) = 1 - \frac{\tau_{b'} - \tau_h}{\tau_{b'} - \tau_l} e^{-\frac{1}{\tau_{b'}} t} + \frac{\tau_l - \tau_h}{\tau_{b'} - \tau_l} e^{-\frac{1}{\tau_l} t}, \tag{5.9}$$

where τ_h is set smaller then $\tau_{b'}, \tau_l$.

If $\tau_{b'} > \tau_l$ then, $e^{-\frac{1}{\tau_l} t} > e^{-\frac{1}{\tau_{b'}} t}$ and the coefficients will be $\tau_{b'} - \tau_h > \tau_l - \tau_h$. As time goes on, the relationship between the coefficients $\tau_{b'} - \tau_h$ and $\tau_l - \tau_h$ plays more important role than that of $e^{-\frac{1}{\tau_l} t}$ and $e^{-\frac{1}{\tau_{b'}} t}$ does, which means the first term has a larger effect on this velocity. But there also can be a period where the effect by $e^{-\frac{1}{\tau_l} t} > e^{-\frac{1}{\tau_{b'}} t}$ is larger than the effect by the coefficients; the second term has a larger effect on this velocity.

As discussed in the last section, when a person is riding a wheelchair, he controls the velocity. At the accelerating phase, he adds torque until the velocity reaches a certain level. We call this certain velocity level as 'satisfying velocity', and the time to reach 'satisfying velocity' as 'velocity climbing time'. In Figure 5.15 (a), the two velocity patterns are depicted, and the satisfying velocity and climbing time are described. Decrease in this climbing time is related to the power assistance. To decrease the velocity climbing time, DC gain K' should be high or time constants $\tau_{b'}, \tau_l$ should be small.

At the deceleration phase, the velocity damping time (described in Figure 5.15 (b)) plays an important role in power assistance. It is related to $\tau_{b'}, \tau_l$. To increase the velocity damping time those time constants should be long.

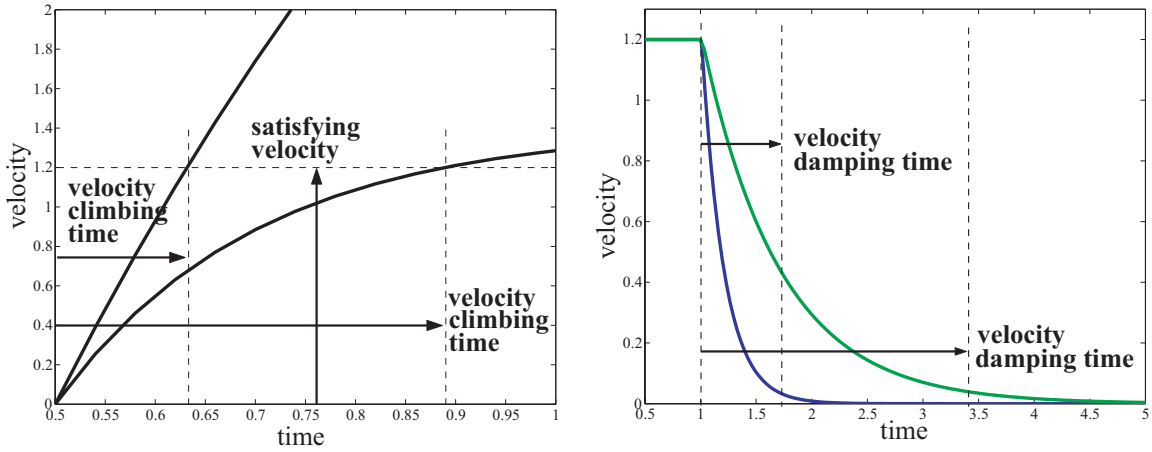

(a) when accelerating

(b) when decelerating

Figure 5.15: Important parameters in velocity

These analysis advises that the decision of J_M, B_M and A can be done taking the velocity climbing time and the velocity damping time into consideration.

Jerk-peak attenuation

Jerk is occasionally used as an index of how smooth or how comfortable the system is [21], [22]. For this reason, here, the jerk of the controlled wheelchair is considered as an index of power assist control performance. First, if a step torque is used as an input to the wheelchair expressed by Equation (5.7), the jerk will be

$$\frac{1}{\tau_b}\delta(t) - \frac{1}{\tau_b^2}e^{-\frac{1}{\tau_b}t}. \tag{5.10}$$

The first term $\frac{1}{\tau_{b'}}\delta(t)$ is mainly concerned with the peak value of jerk. If this term is too big, the human will feel unsafe.

If a controller amplifies the applied force up to K times, jerk will be increased by K times, too. This is not good for comfort of a wheelchair user.

In the case of the proposed power assist control, jerk will be

$$K'\left(\frac{\tau_h}{\tau_{b'}\tau_l}\delta(t) + \frac{\tau_h - \tau_{b'}}{\tau_{b'}^2(\tau_{b'} - \tau_l)}e^{-\frac{t}{\tau_{b'}}} + \frac{\tau_h - \tau_l}{\tau_l^2(\tau_l - \tau_{b'})}e^{-\frac{t}{\tau_l}}\right). \tag{5.11}$$

Also the first term is the jerk-peak term, and it has K' and $\frac{\tau_h}{\tau_l}$. K' is the DC gain and is related to the assistance, and as explained above it is necessary to keep this K' as high as for good assistance performance. On the other hand, this will result in the increase of jerk, so that we should reduce the jerk-peak by setting $\frac{\tau_h}{\tau_l} < 1$; that is, the jerk-peak can be reduced without any loss in the DC gain.

The criterion $\frac{\tau_h}{\tau_l} < 1$ means that the gain at high frequency must be lowered to reduce the jerk-peak. In the low frequency, high assistance-ratio is adequate for good assistance

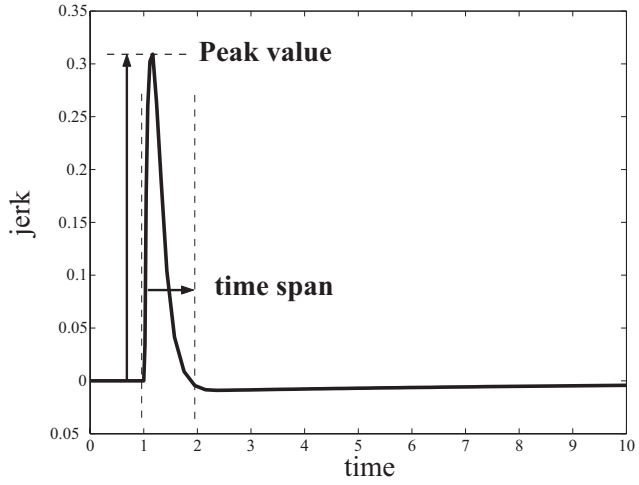

Figure 5.16: Important parameters in jerk

performance, and in the high frequency, low assistance-ratio is adequate for the attenuation of the jerk-peak.

Figure 5.16 shows a jerk pattern with low-pass filtered step torque as input. Two factors in this figure are important for power assistive control design. First is the peak value of jerk, and second is the time span while jerk has a nonzero value.

The peak value is related to how a person feels while accelerating, and the time span is related with the velocity climbing time. A small peak value is good for the comfort of a rider, but a too small peak makes the velocity climbing time longer and worsens power assistance. But if we have sufficient time span by setting adequate time constants $\tau_{b'}, \tau_l$, the power assistance will be improved.

5.4.3 Analysis of the Effect of Modeling Error

We adopt the disturbance observer to estimate human torque using the physical model of the wheelchair and the user on it. Errors in this model will affect the performance of this controller. In this section, how the error in the model will affect the controller is analyzed. To make the analysis simple, two parametric errors $\Delta J, \Delta B$ are considered. The analysis is done from two points of view: the stability and the performance.

Stability Analysis

The parametric errors are defined as:

$$\Delta J = J_n - J, \Delta B = B_n - B, P_n(s) = \frac{1}{J_n s + B_n} \tag{5.12}$$

$$\Delta(s) = \frac{\Delta J s + \Delta B}{J s + B}, P(s) = P_n(s)(1 + \Delta(s)), \tag{5.13}$$

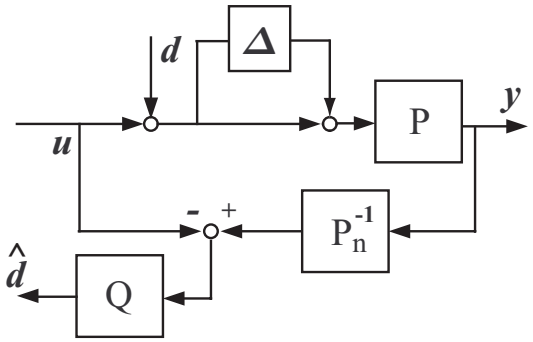

Figure 5.17: Disturbance observer with modelling error

where J_n, B_n are the inertia and damping values used for the disturbance observer design, and J, B are the real values of inertia and damping.

If there are the errors $\Delta J, \Delta B$, the closed-loop transfer function will change from the equation (5.2) to

$$\hat{d} = d + (\Delta J s + \Delta B) y \tag{5.14}$$

$$T(s) = \frac{J_M s + B_M + A}{(Js + B + A)(J_M s + B_M) - A\Delta J s - A\Delta B}. \tag{5.15}$$

This equation indicates that a positive ΔJ or ΔB can make the system unstable. This explains that the proposed controller can be unstable with the real inertia and damping are less than the nominal value and suggests that the nominal value should not be so large. The error in the inertia (ΔJ) is related to the first-order term of the system dynamics, and can make the motion oscillatory. This ΔJ is caused by change of user's weight. The error in the damping (ΔB) is related to the constant term so this error will change the power-assist ratio in the low frequency band, and this ΔB is caused by running resistances and other reasons.

Analysis on Assistance Performance

The analysis above can be applied to the performance evaluation. The errors ΔJ and ΔB affect the assistance performance respectively. ΔJ changes the transient response of the assistance since it is related to the first order term. The response time and oscillation can be changed according to the ΔJ. ΔB has influence on the low frequency bandwidth. This changes the ratio between the peak values of assisting motor torque and the torque exerted by the user. The lasting time of assisting power in one stroke will be influenced by ΔB.

This analysis is demonstrated by some simulations. Figure 5.18 shows the results. In these simulations, the real inertia J is set as 0.024, and the real damping B as 0.1. The nominal value of the inertia, J_n is changed from 0.01 to 0.05, and the nominal B_n is changed from 0.01 to 0.13. It is found that the stability is weakened when the nominal values are larger than the real values and the assistance performance becomes worse when the nominal values are less. Large ΔJ makes the response rapid and oscillatory, and small ΔJ makes

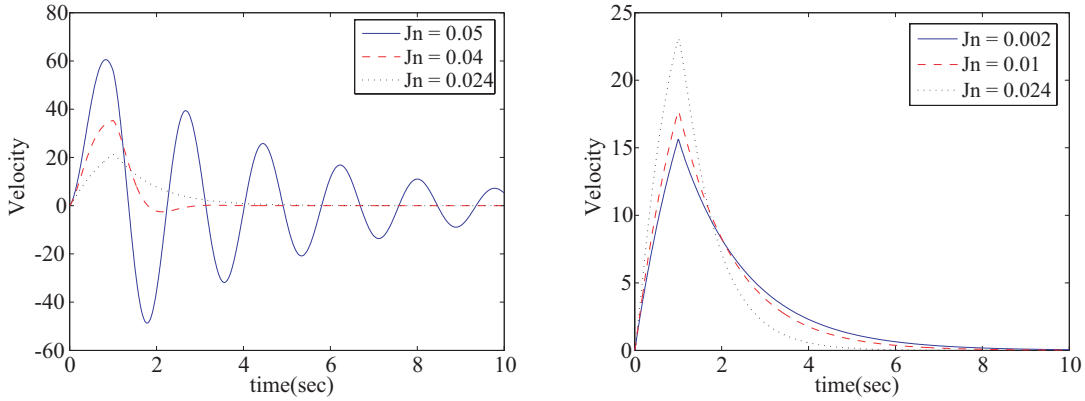

(a) $J_n > J$ (b) $J_n < J$

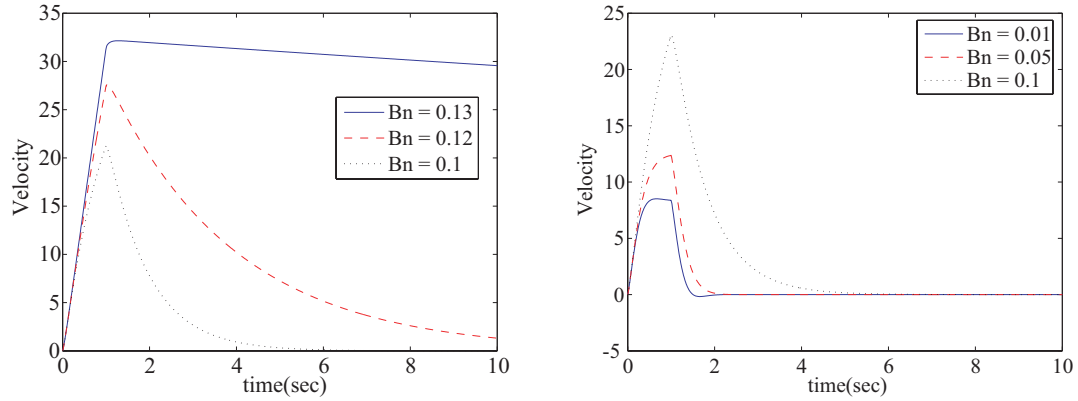

(c) $B_n > B$ (d) $B_n < B$

Figure 5.18: Simulation results with modeling error

the response slow. On the other hand, large ΔB tends to make offset in the observed disturbance and make the whole system unstable, and small ΔB decreases the assisting torque.

The nominal values of J_n, B_n in the proposed controller (Figure 5.7) is decided considering the above analysis.

5.4.4 Suppression of the Gravity

Another problem caused estimation of human force using the disturbance observer is the distinction between human force and the gravity. As the disturbance observer uses only the velocity of the wheelchair and the input motor torque, it is basically impossible to distinguish precise human torque from other disturbance. Among disturbances that affect the operation of a wheelchair, the gravity is the most dominant element.

The effect of the gravity on the proposed controller can be attenuated using the operational state observer proposed in Section 3.

Mostly, the gravity interferes with the operation of the wheelchair on a sloping surface.

On a slope, the gravity's effect can be formulated as

$$f_g \propto g \sin \varphi, \tag{5.16}$$

where g is the gravity acceleration, and φ is the angle of the slope. In the system controlled by the proposed controller, this f_g works as the τ_{ext} in Equation (5.4), which means this gravity's force will be also assisted by control. However, we can estimate φ using the operational state observer, if we use this angle in the proposed controller, the gravity's effect will be decreased.

Figure 5.19 shows a way to use this estimated φ for the gravity compensation in the external force amplification control. As the gravity's effect is proportional to the angle φ,

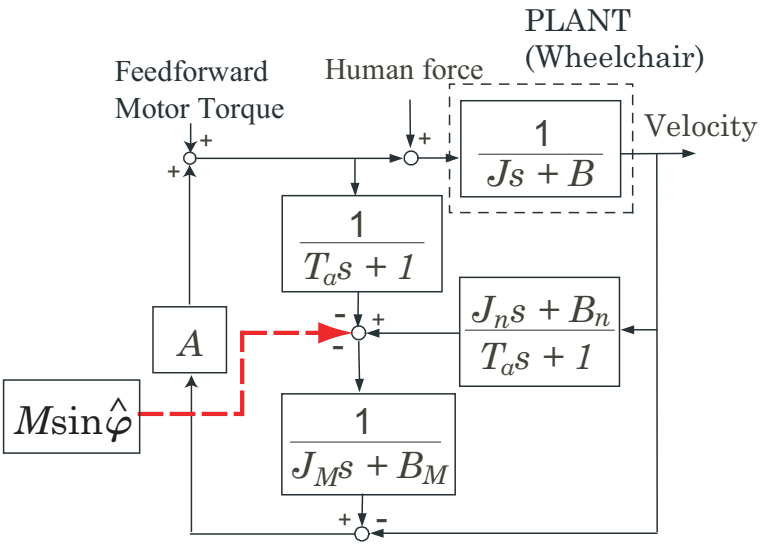

Figure 5.19: Gravity suppression in external force amplification control

precise human torque can be calculated from τ_{exp} by

$$\hat{\tau}_{human} = \hat{\tau}_{exp} - M \sin \hat{\varphi}. \tag{5.17}$$

Using this $\hat{\tau}_{human}$ instead of $\hat{\tau}_{exp}$, the proposed force-sensor-less power assist control can remove the gravity's effect, and provide satisfactory assistance even on a slope.

5.4.5 Experimental Results

Based on the above investigation, the proposed external force amplification controller is applied to a wheelchair. First, a rider has propelled rims of wheels with and without the control. The results are described in Figure 5.20

Figure 5.20 (a) is the observed disturbances including human force, 5.20 (b) is the velocities of a wheel, and 5.20 (c) shows tracking characteristic of the controller. These results explain almost same things with the robot experiments. The ranges of the observed disturbances are similar in both cases, while the ranges of velocities are different each other.

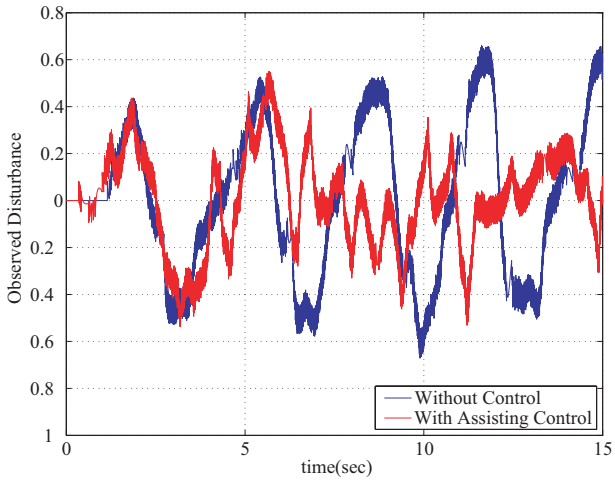

(a) observed disturbance (including human force)

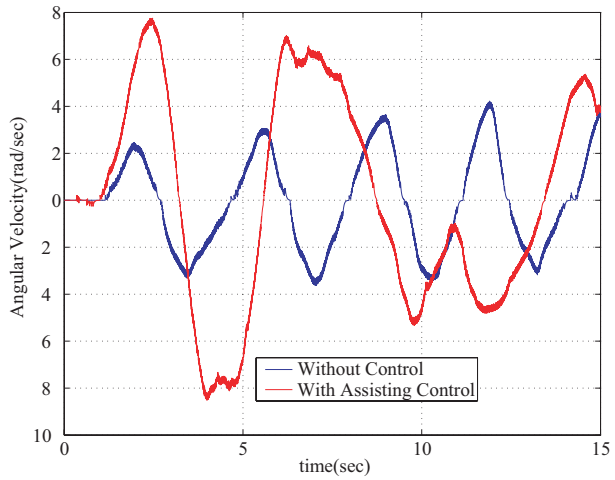

(b) velocities of a wheel (with and without control)

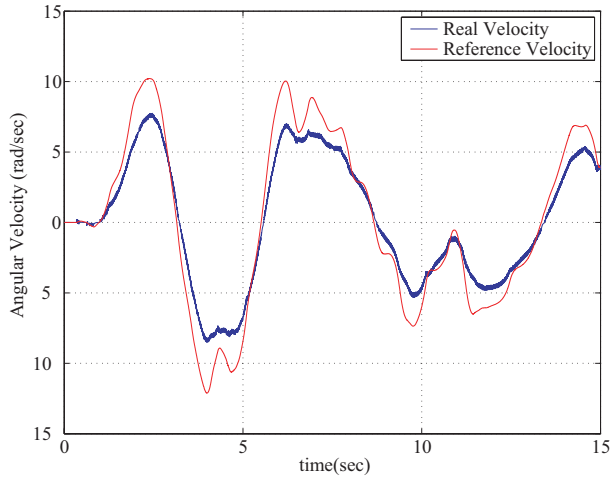

(c) velocity tracking

Figure 5.20: Experimental results

Velocity with proposed control is bigger than the one without control, especially in the first stroke.

One of most important point in this control design is that, even though the observed force is not so precise or smooth enough, the model impedance for velocity reference will work as a filter that smoothes the observed force to provide stable and smooth assistance. The physical velocity will track the reference velocity generated by the model with some accuracy that can be modified using the gain A in figure 5.7, and this is another filtering for smoothing and stabilization.

5.5 Summary

This chapter also insists that the adjustment of the plant's impedance to disturbances using feedback control can a key design to achieve human-friendly motion control. The external force amplification control proposed in this chapter is another example suggesting that rendering the impedance small can work as force-sensor-less power assist control.

For human-friendly motion, motor systems should be sensitive to disturbance when a person works as disturbance. To achieve this sensitivity, this chapter proposed a control design that will sensitize the plant to the disturbance. The proposed external force amplification control can be said as a hybrid type of compliance control type and disturbance observer type, for force-sensor-less power assist control. Although it employs the disturbance observer, it does not use the estimated disturbance as a torque input. The controller uses it to achieve a impedance that will make the plant sensitive to the disturbance. The design does not focus on how to obtain the precise human torque, but on what impedance the controller can achieve. This is the major design feature of the proposed controller.

In order to apply the proposed control to a wheelchair, three points were investigated: numerical consideration of control parameters for a power-assisted wheelchair, analysis of the effect of modeling error, and how to reduce the gravity's effect on sloping environments. The idea explained in section 5.4.2, 5.4.3 is to be demonstrated by experiments, yet the conducted experiments indicates that the proposed controller can achieve power assist control of a wheelchair without a force sensor.

Chapter 6

One-hand Propulsion Control as a Time-varying Impedance Control

There are some researches on variable impedance. For instances, [23] and [24] reveal that variable impedance can realize more natural and safe motion of artificial actuators. This chapter applies that variable impedance concept to a wheelchair. This application is possible because all proposed controllers for a wheelchair are designed based on the impedance concept.

The controller that is proposed in this chapter will help people to propel a wheelchair with only one hand. This operation is achieved by changing impedance.

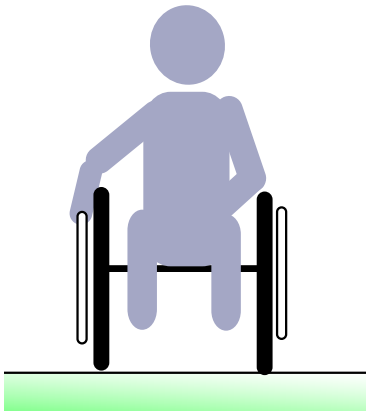

Figure 6.1: Wheelchair propulsion with only one hand

There are may attempts to make a wheelchair controllable by one hand[25]. This chapter aims to achieve one-hand propulsion only by a control algorithm without any additional devices. For the realization of one-hand propulsion, the controller should cope with two problems:

1. How to obtain necessary lateral information on the user's intention from human torque on one rim

2. How to design a controller that can change the direction based on the obtained lateral information.

Other researches adopt some novel devices for the former problem. Those approaches can work well and be best solution to the problem. However, the method which will be proposed in this chapter relies only on the human force on one rim even for the lateral information. Although this method may seem extraordinary in terms of practical usage, the algorithm will be suggested as one example of variable impedance control that sensitively varies according to changes in human torque.

At first, the design of the controller is addressed.

6.1 Design of a Time-varying Controller for One-hand Propulsion

6.1.1 Control Strategy to Propel a Wheelchair Straight with One Hand

In order to keep a wheelchair straight in the face of unbalanced human torque, the following two functions are necessary:

1. To provide the same assist torque based on the measured human torque on one rim
2. To remove the effect of lateral disturbances.

The former is easily realized by using the measured torque applied on one side. The latter is what this paper addressed in Chapter 4.3. A controller described in the figure 6.2 has the blocks that achieve these two functions.

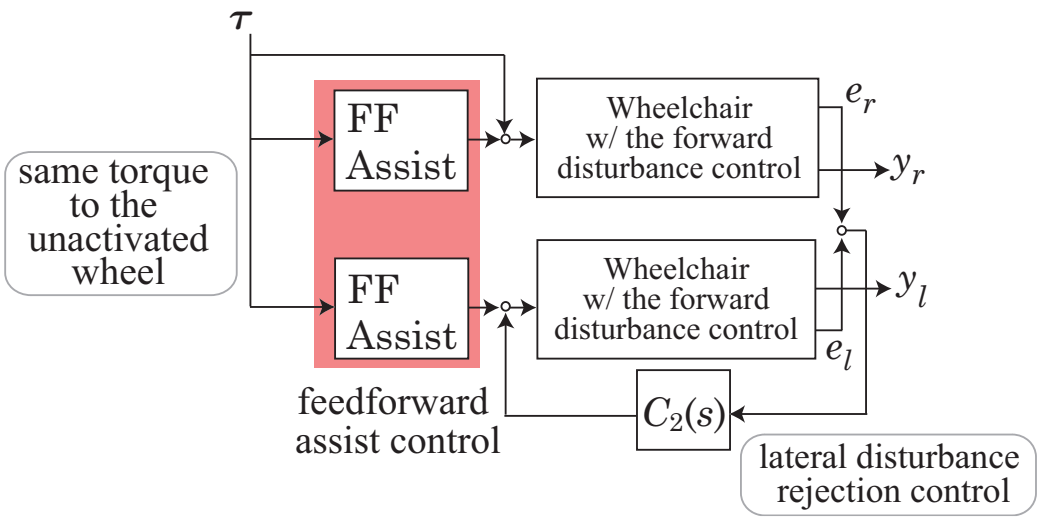

Figure 6.2: Controller for going forward with torque on one wheel

6.1.2 Introduction of a Varying Synchronizing Coefficient

A parameter that will decide the heading angle of the wheelchair is introduced here. This parameter allows us to control the rotational motion of the wheelchair easily. Figure 6.3 is the one-hand propulsion control architecture this paper proposes.

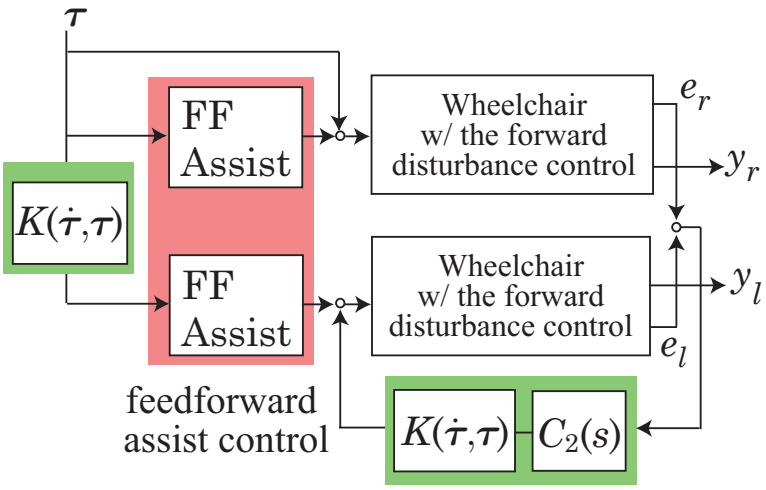

Figure 6.3: Controller with the synchronization function $K(\dot{\tau}, \tau)$

This system has K as the parameter that determines the heading angle. This parameter K can be defined as a synchronizing coefficient, and a function of the human torque input τ is adopted for this K here. At first, let us consider the case when $K(\dot{\tau}, \tau)$ is 1. Then the same torque is given to the feedforward assist controller, which will provide the wheelchair with the same assist torque. $C_2(s)$, here, is the controller which was proposed in section 4.3, and will remove any lateral disturbances. Consequently, if $K(\dot{\tau}, \tau)$ is 1, the controller allows the wheelchair to go straight with human torque on one side.

On the other hand, if $K(\dot{\tau}, \tau)$ is zero, the controller will not work in this way. With zero $K(\dot{\tau}, \tau)$, all the controls that keeps the wheelchair straight will go away, and it will lead to make the wheelchair turn. In this way, decision of this K between 0 and 1 will decide the heading angle of a wheelchair and achieve the one-hand propulsion.

Then, how should we decide this K? There can be various ways to decide this K, such as using special devices. In this paper, we adopt the function of $\dot{\tau}$ and τ as this K.

6.2 Projection of Human Intention to a Control Parameter

6.2.1 Measurement and Analysis of Human Torque

The proposed controller uses only human torque on one rim as the input to the wheelchair. Due to this strategy, it is necessary to derive additional information from the torque input.

To this end, human torque is measured, and the observation of that torque will help us in patternizing the human torque. Figure 6.4 is the measured human torque described in the phase plane. The x-axis is the magnitude of the torque and the y-axis is that of the differentiated torque.

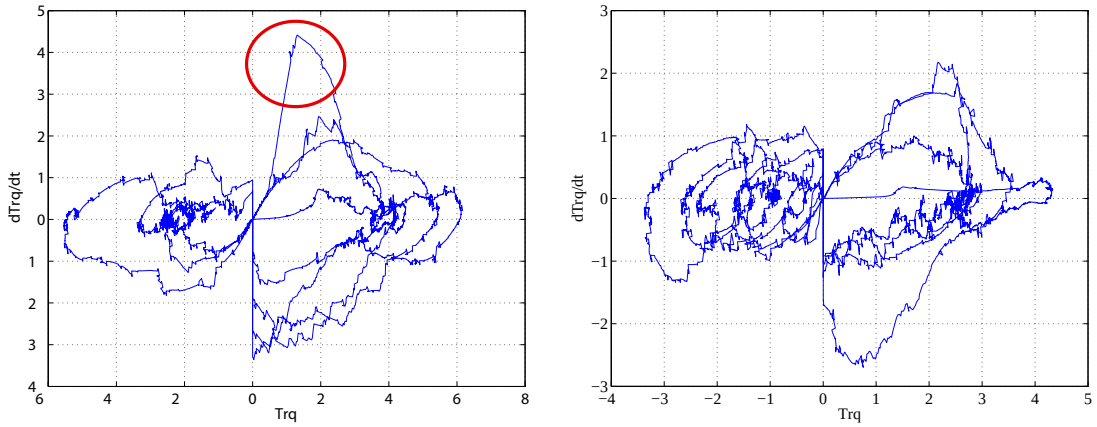

Figure 6.4: Examples of torque pattern

This phase plane reflects the possibility of the differentiated torque as an additional input. The left figure has a circled peak which does not appear in the right figure. This peak in the y direction does not have long-term influence in the back and forth driving, and can be regarded as a redundant action. This redundant signal is suitable as the input to the lateral direction because of its little influence on the forward driving. Using this additional signal, human can transmit his will to the controller.

6.2.2 Projection to a Synchronization Coefficient

To use the differentiated torque as the input for the lateral direction, the torque plane is divided into two segments: straight-going mode region and turning mode region. Figure 6.5 shows this division.

The location of human torque in the phase plane decides whether the wheelchair will goes straight or turn: If the differentiated torque is in the straight-going segment, the controller will drive both wheels at the same speed, and if it is in the turning mode, the controller will assist only one wheel.

Note that this division is not two-valued logic, but gradual. Otherwise, the user can feel that his operation is not continuous and awkward. The two segments are connected in a fuzzy way. The sigmoid function is employed to realize fuzzy division.

The sigmoid function is applied to $K(\dot{\tau}, \tau)$ described in Equation(6.1).

$$K(\dot{\tau}, \tau) = \mathrm{sgn}(\tau) \frac{1}{1 + e^{-\beta_o(\dot{\tau} - \dot{\tau}_0)}} \tag{6.1}$$

τ_0 represents the threshold from where the two modes are divided, and β_o determines the width in which K changes in the fuzzy way. With this $K(\dot{\tau}, \tau)$, experiments are done.

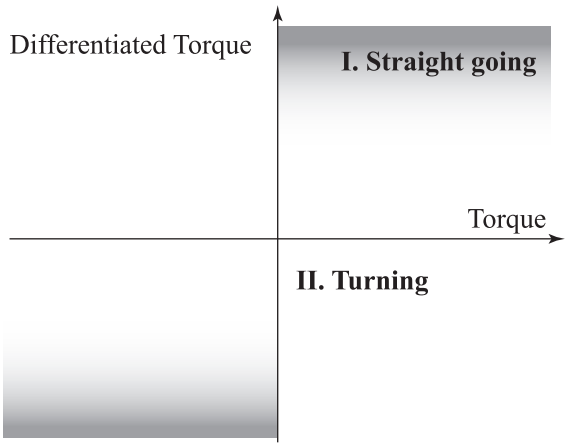

Figure 6.5: Division of the torque phase plane for one-hand propulsion

6.3 Experimental Results

An experiment is conducted to verify the function of K as the key control parameter to determine the synchronization of two wheels.

6.3.1 Verification of the Synchronization Coefficient K

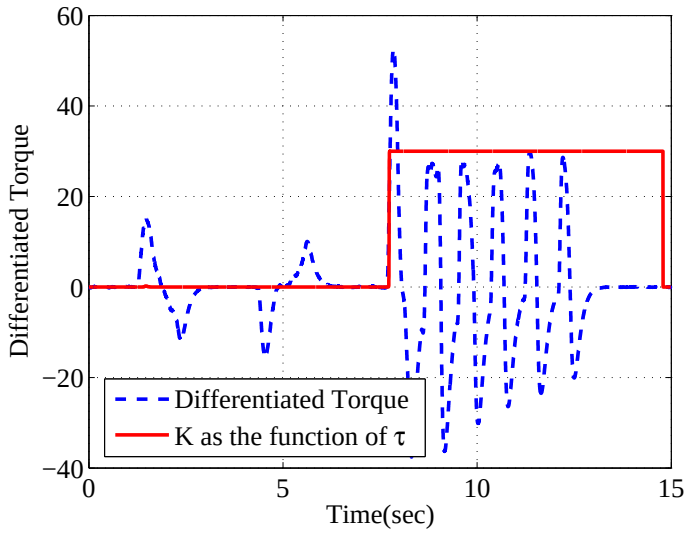

Figure 6.6: $\dot{\tau}$ and $30K(\dot{\tau}, \tau)$

Figure 6.6 and 6.7 are the experimental results. In this experiment, β_o and τ_0 in Equation (6.1) are chosen as 1.0 and 20. Furthermore, a limitation is applied to K so that K will not be bigger than 1. Once K becomes 1, the value will be held on until the velocity of the wheelchair and the torque τ become 0, which represents that the wheelchair stops. Figure 6.6 shows the experimental result of $\dot{\tau}$ and K as the function of $\dot{\tau}$ and τ. For convenience,

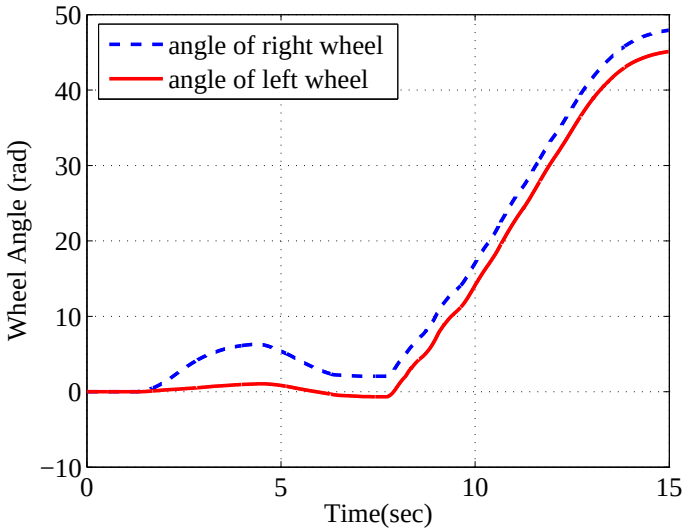

Figure 6.7: Wheel angles as the result of one-hand propulsion control

the described value of K is 30 times the real value. K is changed according to $\dot{\tau}$. In Figure 6.6, around 8 second, K becomes 1 and the value is held to about 15 second. K is decided as desired.

Figure 6.7 is the angles of the right and left wheels. Until 8 second, only the right wheel moves and it makes the wheelchair turn. After 8 second, the wheelchair goes into the straight-going mode for K becomes 30, and the right and left wheels turn at the same velocity. This is a simple experiment, but it indicates the proposed controller works as desired, and the user can change the direction of the wheelchair by adjusting his torque.

6.3.2 On-road Experiment

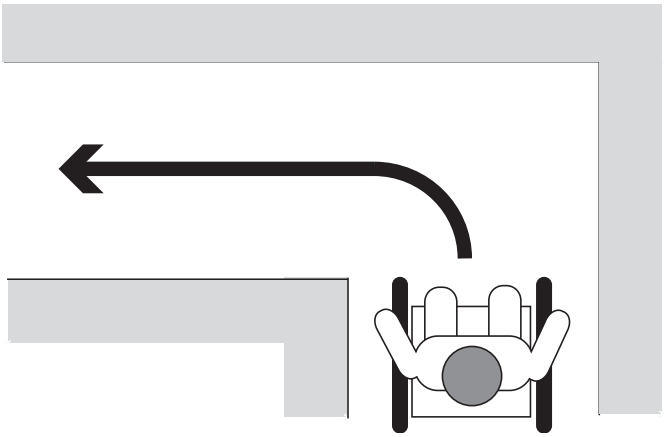

Figure 6.8: Illustration of conducted on-road experiment

Figure 6.8 is the illustration of the experiment conducted on a road. The mission given to

assess the effects of the proposed controller is that a rider go through the course in Figure 6.8 using one hand. To do this, the rider firstly should turn his wheelchair to 90 degrees, and then he should propel the wheelchair in a straight line. All these operation should be done with one hand.

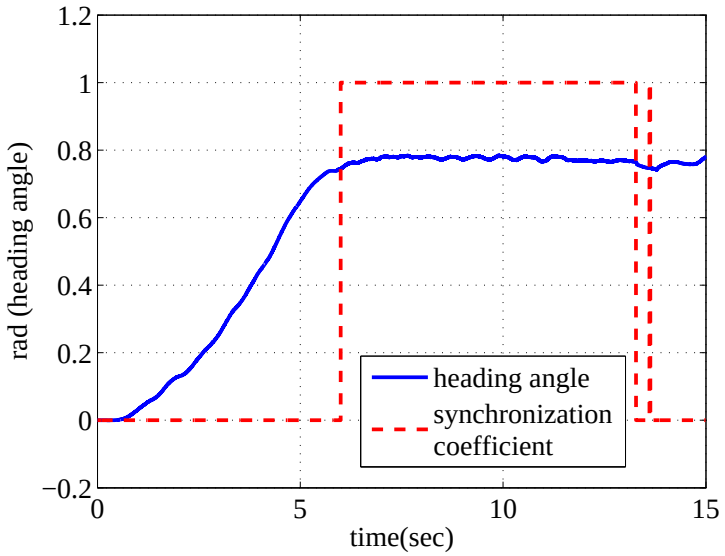

Figure 6.9: Changes in heading angle as the result of proposed control

Figure 6.9 is the experimental result. The solid line is the heading angle of the wheelchair in radian, and the dotted line indicates the value of K. From 0 second to around 6 second, the heading angle changes from 0 to around 0.7, which means the wheelchair is turning during this period. From 7 second, the wheelchair goes into straight-going mode, which can be accounted for by the value of K, the synchronization coefficient.

This result suggests that with the proposed control can successfully achieve one-hand propulsion without any other devices.

6.4 Summary

The most noticeable feature in the proposed control is the suggestion of a time-varying control parameter that reflects human intention. Occasionally, to meet some requirements from users, a controller needs to be time varying, and it is also one of the necessary feature for human-friendly motion control (Figure 6.10).

This scheme proposed in this chapter is to project human intention on the directions on a control parameter that adjusts the synchronization ratio of two wheels. The design of this projection is an important factor in human-friendly motion control. This chapter provided a fuzzy projection from human intention to the synchronization coefficient as an example of this projection. Although the differentiated torque was employed to transmit human intention, it would be alright to use other devices to obtain it. Nevertheless, this

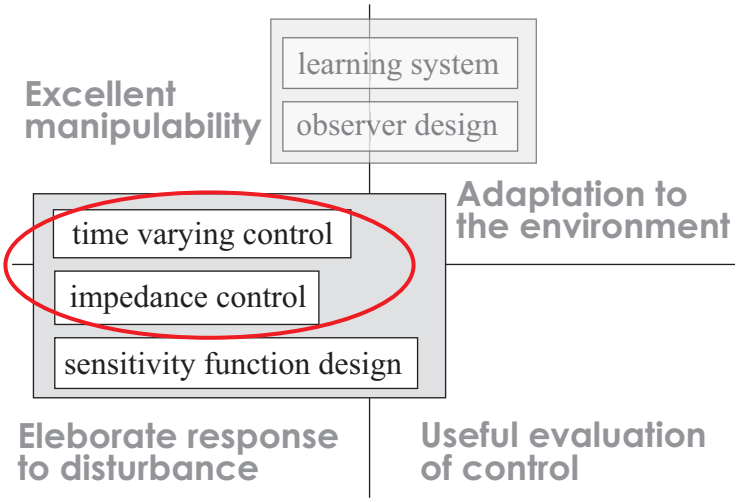

Figure 6.10: Significance of the proposed controller in human-friendly motion control

projection in control design is important in those cases as well.

Chapter 7

Conclusions

In this dissertation, several approaches to establish human-friendly motion control are suggested. The requirements listed in Chapter 1 has been addressed in this dissertation, and they are applied to a wheelchair.

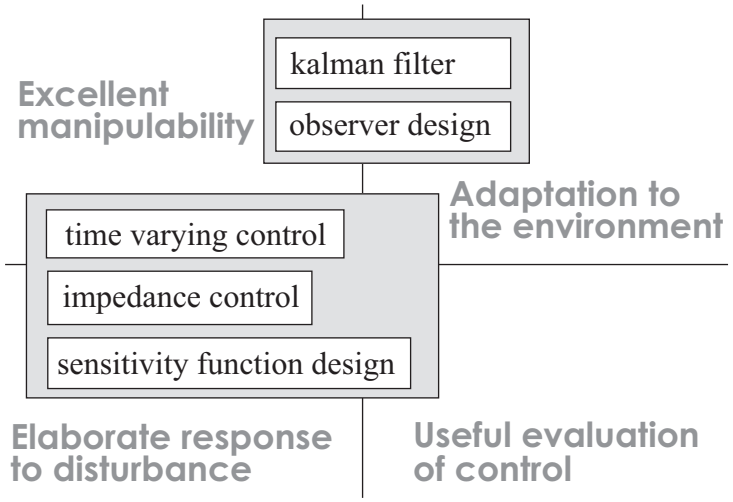

Figure 7.1: Proposed solutions in this dissertation for the Human-friendly Motion Control

Figure 7.1 is the strategies suggested in this dissertation. These solutions are categorized as two theories: observer design and feedback control design. To render a controller human-friendly implies to mimic motion control of human movement. Human neuromuscular system which activates human motion has a nervous system and a muscular system, and the suggested solutions have the same structure; state observers for nervous system, and feedback controllers for muscular system.

Observer design investigated in Chapter 3 can be interpreted as a kind of sensor fusion methods. To establish an effective nervous system in artificial tools, various sensors become necessary and sensor fusion algorithms also. What this dissertation insists is a state observer design is a good algorithm for that sensor fusion algorithm. The other point this dissertation insists is the generality of the proposed operational state observer; it is useful not only for a wheelchair but also for other welfare devices such as humanoid robots. The states monitored by the operational state observer - velocity, pitch angle, disturbance in each

state - are important in other welfare tools because they are related to human locomotion. Additionally sensors used for the operational state observer also have similar functions with sensing organs of human. These considerations prove the importance of the proposed operational state observer.

Impedance control in Chapter 2 is the main issue scrutinized in this dissertation. The most important feature of human-friendly feedback control design is located in the change of the viewpoint for the design of a controller. In conventional industrial control applications, the controllers are designed to eliminate external disturbances, and tracking to the reference values is the definition of control performance. However, it is different in human-friendly motion control design; parameters and structure of a feedback controller should be interpreted as impedance of the system and be designed considering influence on the feeling and safety of the users.

This impedance based interpretation can be applied to various kinds of feedback control as a general form of feedback controllers and provides a new design insight of it. For instance, in Chapter 4, two feedback controllers are designed based on this impedance concept in an attempt to suppress the disturbances on a wheelchair. The controllers are designed in terms of what type of impedance is the most suitable for each control purpose and prove the effect of the impedance concept in human-friendly motion control design. Moreover, this new insight allows us a quite novel feedback control such as a fractional order impedance control and helps us understanding the function of human muscle; Chapter 2 introduced also these new approaches.

Apart from this disturbance attenuation application, impedance control allows us disturbance amplification control which is essential in human-friendly motion control. This control design and application were studied in Chapter 5. The proposed control design enables a motor to assist human force without a force sensor and also ensures the user's safety. In contrast to other researches on the development of this force-sensor-less power assist control which focus on the precise monitoring of human force, the proposed control achieves power assist function based on impedance design, which is the main idea throughout this dissertation.

The control algorithms proposed from Chapter 2 to 5 are time-invariant methods. For human-friendly motion control, however, time-varying control is also necessary; one example of the time-varying impedance controls in human muscle control is explained in Section 2.3. Chapter 6 suggests a time-varying control for a power assist wheelchair. The idea of projection from the user's intention to time-varying control parameter is important in this control design. This concept of projection is significant for the design of time-varying human-friendly motion control. In Chapter 6 a synchronizing coefficient was used as a time-varying factor, which was a simple example of this projection-based time-varying impedance control. For more advanced control, some more complicated impedance can be utilized.

The power assist wheelchair was the only one application in this dissertation; however, this dissertation investigated a general design method of human-friendly motion control in terms of impedance design. Each of the proposed control has potential to be applied to the other conventional welfare devices and improve their functions.

AppendixA

Realization of Fractional Order Differentiation

To implement fractional order control suggested in Chapter 2, fractional derivatives should be realized in the controller. To this end, here, basic understanding on fractional derivatives is explained: mathematical definition of fractional derivatives and its realization method.

A.1 Mathematical Definition

The mathematical definition of fractional derivatives and integrals has been the subject of several different approaches[26]. By Riemann-Liouville definition which is the most frequently encountered definition, the fractional order integrals are defined as

$$ {}_{t_0}D_t^{-\alpha} = \frac{1}{\Gamma(\alpha)} \int_{t_0}^{t} (t-\xi)^{\alpha-1} f(\xi) d(\xi) \tag{A.1} $$

where

$$ \Gamma(x) = \int_0^{\infty} y^{x-1} e^{-y} dy \tag{A.2} $$

is the Gamma function, t_0 and t are limits and α is the order of the operation.

Using this definition of integrals, the definition of fractional order derivatives can be given as

$$ {}_{t_0}D_t^{-\alpha} f(t) = \frac{d^{\gamma}}{dt^{\gamma}} \left[{}_{t_0}D_t^{-(\gamma-\alpha)} \right], \tag{A.3} $$

where γ is an integer that satisfies $\gamma - 1 < \alpha < \gamma$.

The other approach is Grunwald-Letnikov definition:

$$ {}_{t_0}D_t^{-\alpha} = \lim_{\substack{h \to 0 \\ nh = t - t_0}} h^{-\alpha} \sum_{r=0}^{n}{}' (-1)^{\alpha} f(t - rh) \tag{A.4} $$

where the binomial coefficients are

$$ \begin{pmatrix} \alpha \\ 0 \end{pmatrix} = 1, \quad \begin{pmatrix} \alpha \\ r \end{pmatrix} = \frac{\alpha(\alpha-1)\cdots(\alpha-r+1)}{r!}. \tag{A.5} $$

The Laplace transform of Riemann-Liouville fractional order derivative with order $\alpha > 0$ is calculated as

$$ L\left\{ {}_{t_0}D_t^{-\alpha} f(t) \right\} = s^{\alpha} F(s) - \sum_{n-1}^{j=0}{}' s^j \left[{}_{t_0}D_t^{-\alpha-j-1} f(0) \right], \tag{A.6} $$

where $(n-1) \leq \alpha < n$. If

$$ {}_{t_0}D_t^{-\alpha-j-1} f(0) = 0, j = 0, 1, 2, \ldots, n-1 \tag{A.7} $$

then

$$ L\left\{ {}_{t_0}D_t^{-\alpha} f(0) \right\} = s^{\alpha} F(s) \tag{A.8} $$

This is the definition of s^{α} that is necessary for the realization of impedance control.

A.2 Frequency-band Approximation

It is reported that the fractional order system has an infinite system and it is impossible to perfectly calculate fractional derivatives in real application. For the feasible realization of fractional order system, there are a variety of approximation methods such as Short Memory Principle[28], Tustin Taylor Expansion and Sampling Time Scaling [27]. In addition to these direct discretizations of fractional derivatives, there is frequency-band approximation method which is reported as most useful realization. This section explains this frequency-band approximation method using a broken-line approximation method.

The broken-line approximation method uses fractional order system's frequency responses since it can be exactly known. However, the order of the approximation should be infinite so as to approximate the responses in whole frequency range. This infinite order approximation is not practicable so that this approximation limits the frequency bandwidth where frequency-band fractional order I^{α} will be realized.

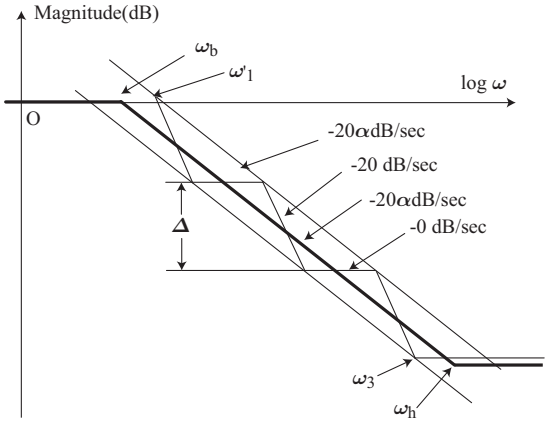

Figure A.1: An example of broken-line approximation (N = 3)

Figure A.1 illustrates how the broken-line approximation methods realizes the frequency response of a fractional order system with a limited frequency bandwidth. This approximation is formulated as Equation (A.9).

$$ \left(\frac{\frac{s}{\omega_h} + 1}{\frac{s}{\omega_b} + 1} \right)^{\alpha} \simeq \prod_{i=0}^{N-1} \frac{\frac{s}{\omega_h'} + 1}{\frac{s}{\omega_b'} + 1} \tag{A.9} $$

Based on Figure A.1, two factors ζ and η are introduced to calculate ω_i and ω'_i:

$$\zeta = \frac{\omega_i}{\omega'_i}, \eta = \frac{\omega'_{i+1}}{\omega_i}, \tag{A.10}$$

which means ζ and η describes the width of one broken-line on the log scale.

This derives Equation (A.12), and therefore the first point ω_0 and the last point ω'_{N-1} can be given as Equation(A.11).

$$\omega_0 = \eta^{\frac{1}{2}}\omega_b, \omega'_{N-1} = \eta^{-\frac{1}{2}}\omega_h \tag{A.11}$$

$$\zeta\eta = \left(\frac{\omega_h}{\omega_b}\right)^{\frac{1}{N}} \tag{A.12}$$

The freqeuncy of each point can be calculated as

$$w_i = (\zeta\eta)^i\omega_0, \omega'_i = \zeta(\zeta\eta^i\omega_0. \tag{A.13}$$

The frequency-band fractional order controller has -20αdB/dec gain slope, while the integer order factors $\frac{1}{\left(\frac{s}{\omega'_i}+1\right)}$ have -20dB/dec. For the same magnitude change Δ:

$$-20\alpha = \frac{\Delta}{\log\zeta + \log\eta}, -20 = \frac{\Delta}{\log\zeta} \tag{A.14}$$

Thus

$$(\zeta\eta)^\alpha = \zeta \tag{A.15}$$

Therefore ζ and η can be expressed respectively by

$$\zeta = \left(\frac{\omega_h}{\omega_b}\right)^{\frac{\alpha}{N}}, \eta = \left(\frac{\omega_h}{\omega_b}\right)^{\frac{1-\alpha}{N}} \tag{A.16}$$

Finally

$$\omega_i = \left(\frac{\omega_h}{\omega_b}\right)^{\frac{i+\frac{1}{2}-\frac{\alpha}{2}}{N}} \omega_b, \omega'_i = \left(\frac{\omega_h}{\omega_b}\right)^{\frac{i+\frac{1}{2}+\frac{\alpha}{2}}{N}} \omega_b \tag{A.17}$$

Figure A.2 shows the bode diagrams of ideal frequency-band case ($\alpha = 0.4, \omega_b = 200\text{H}z, \omega_h = 10000\text{H}z$) and its 1st-order, 2nd-order and 3rd-order approximations by broken-line approximation method. Even the case with $N = 2$ can give a satisfactory accuracy in frequency domain.

As explained before, this broken-line approximation limits the bandwidth where s^α is realized. This results in the limitation of feasible fractional impedance described in Figure 2.16. In spite of this limitation, fractional impedance realized by this approximation is still useful since the frequency range of human sensory system is also restricted to a certain frequency range. This point is to be experimented.

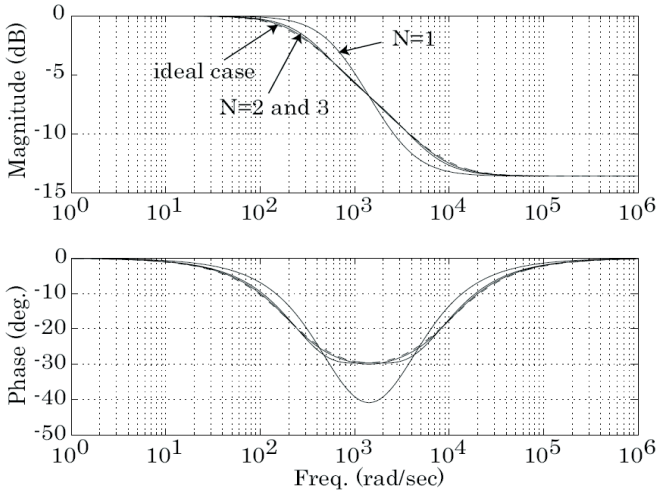

Figure A.2: Bode plots of ideal case, 1st, 2nd and 3rd-order approximations

AppendixB

Novel Design of an Instantaneous Speed Observer

For the proposed controllers applied to power assist wheelchair, precise velocity information is the most important output. Velocity information estimated by the proposed operational state observer has been used in this dissertation. The observer can correctly estimate the velocity of wheelchair at low speed. However, it uses three sensors so that it may increase the production cost of the power assist wheelchair.

Generally, encoders are used to obtain velocity information; motor speed information is calculated from the increased pulse number of an encoder in a sampling period, but in cases where the rotary encoder has low resolution or the velocity becomes low, velocity calculation with the differentiation of the encoder output becomes noisy and incorrect.

The wheelchair which is the main application in this dissertation usually runs at low speed and frequently it stops. If a feedback controller for a wheelchair uses the differentiated encoder output as velocity in this operational condition, the performance will deteriorate due to its noise. For this velocity estimation problem, the instantaneous speed observer [29] has been suggested. Here, a novel design of this speed observer is proposed to improve the estimation performance at low speed.

B.1 Development of Nove Speed Observer

Figure B.1 shows the structure of instantaneous speed observer [29],[30]. The structure of this speed observer is same as that of general observers, but it can not obtain output information of the plant at each sampling period, because of the low resolution of the encoder. Precise value is obtained in a few samples, which means the sampling time of observer-state update by output error is several times as long as control sampling time. This is the characteristic of the instantaneous speed observer.

Conventional instantaneous speed observers feedback the output error information only one time after it gets a new encoder pulse. This feedback strategy has some problems. As is described in Figure B.2, observation error does not decrease while the observer can not get any new pulse from the encoder, which makes the observation imprecise and even unstable.

To make this observer stable, variable gain decision strategy is employed in [30]. However,

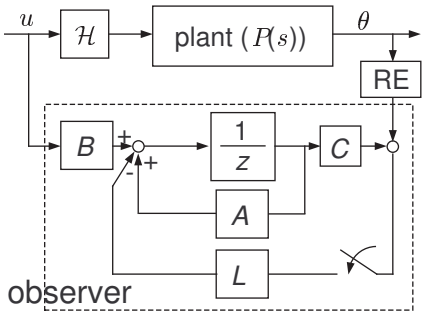

Figure B.1: Structure of the instantaneous speed observer

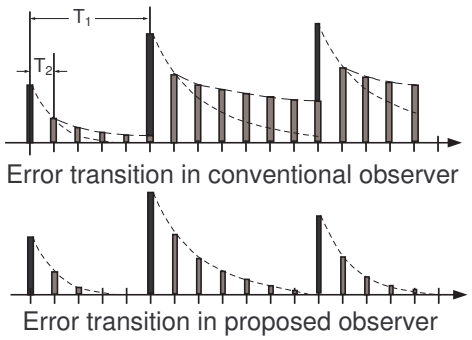

Figure B.2: Error transitions in two observers

it still uses the observation error only once after the encoder reads the pulse.

Output error information should be fedback more frequently to achieve stable and fast observation, even while the encoder does not give out new pulse information. The transition of observation error can be calculated based on the observer dynamics. By feedback of calculated output error, fast and stable instantaneous speed observer can be realized.

The instantaneous speed observer is described as

$$\begin{aligned} \hat{x}[n] &= \mathbf{A}_d \hat{x}[n-1] + \mathbf{B}_d u[n-1] + \mathbf{L}\left(y[n] - \hat{y}[n]\right) \\ \hat{y}[n] &= \mathbf{C}_d \left(\mathbf{A}_d \hat{x}[n-1] + \mathbf{B}_d u[n-1]\right) + \mathbf{D}_d u[n] \end{aligned} \tag{B.1}$$

$$\hat{x}[n] = \begin{pmatrix} \hat{\omega}[n] \\ \hat{\theta}[n] \\ \hat{d}[n] \end{pmatrix}, \mathbf{A}_d = \exp \begin{pmatrix} -\frac{B}{J}T_2 & 0 & \frac{T_2}{J} \\ T & 0 & 0 \\ 0 & 0 & 0 \end{pmatrix}, B_d = \begin{pmatrix} \frac{T_2}{J} \\ 0 \\ 0 \end{pmatrix}, \mathbf{C}_d = \begin{pmatrix} 0 & 1 & 0 \end{pmatrix} \tag{B.2}$$

where ω is angular velocity, θ is rotated angle of a wheel, d is input disturbance, and T_2 is sampling time. $\mathbf{A}_d, \mathbf{B}_d, \mathbf{C}_d$ correspond to $\mathbf{A}, \mathbf{B}, \mathbf{C}$, and $\mathbf{D}_d$ is 0 here.

The term $\mathbf{L}\left(y[n] - \hat{y}[n]\right)$ is the feedback of observation error. However, the measurement of output $y[n]$ is not available at each sampling time if the encoder has low resolution. To use that quantized and inaccurate $(y[n] - \hat{y}[n])$ for feedback will make the observation inaccurate and even unstable.

For this reason, conventional instantaneous observer does not feedback output error while there is no new pulse reading from the encoder. It switches its feedback phase like below.

$$\begin{cases} \hat{x}[n] = \mathbf{A}_d\hat{x}[n-1] + \mathbf{B}_d u[n-1] + \mathbf{L}\left(y[n] - \hat{y}[n]\right) \\ \cdots \text{when there is new pulse reading from the encoder} \\ \hat{x}[n+k] = \mathbf{A}_d\hat{x}[n+k-1] + \mathbf{B}_d u[n+k-1] \\ \qquad\qquad\qquad\qquad\qquad\qquad \cdots \text{otherwise.} \end{cases} \tag{B.3}$$

B.2 Performance Verification by Simulation

Transition of observation error will be affected by this feedback switching. Let us assume that there is no new pulse reading for K sampling times. The encoder reads a new pulse when $t = nT_2$, and there has been no new pulse reading until $t = (n+K)T_2$. Then the observation error at $t = (n+K)T_2$ can be expressed as follows.

$$e[n+K] = \mathbf{A}^{K-1}(\mathbf{I} - \mathbf{L}\mathbf{C}_d)\mathbf{A}_d e[n] = \mathbf{G}_1(K)e[n] \tag{B.4}$$

The eigenvalues of $(\mathbf{I}-\mathbf{L}\mathbf{C}_d)\mathbf{A}_d^K$ express convergence speed of observation. If the observer can feedback observation error at every sample, this error transition will be,

$$e[n+K] = \left((\mathbf{I} - \mathbf{L}\mathbf{C}_d)\mathbf{A}_d\right)^K e[n] = \mathbf{G}_2(K)e[n]. \tag{B.5}$$

Figure B.3 shows the transitions of eigenvalues of these two matrices $(\mathbf{G}_1, \mathbf{G}_2)$ according to K. We can find out from this figure that convergence speed of conventional observer $(\mathbf{G}_1(K))$ is slower. The gain tends to be high for this reason.

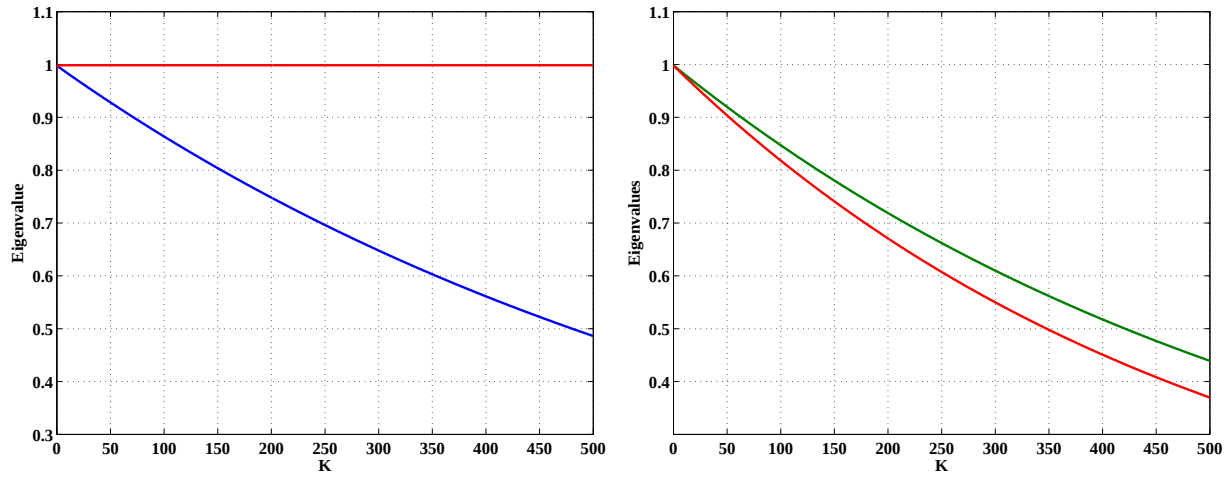

Figure B.3: Eigenvalue transitions of two matrices (left: $\mathbf{G}_1(K)$, right: $\mathbf{G}_2(K)$)

Our proposal for this problem is using simulated output error $\varepsilon_y[n]$ instead of the real output error $(y[n] - \hat{y}[n])$ while accurate output measurement $y[n]$ is not available. Compared with the conventional observer, the proposed observer feedbacks observation error at each sampling time. This will result in fast observation.

There will be no drastic changes in the target system while the encoder can not get new pulse, which means it is reasonable to model observation error as a step during that period.

It is necessary to distinguish two variables to explain this in more detail.

$\varepsilon_y[n]$: observation error estimation to be feedback

ε_{yn} : the real output error $y[n] - \hat{y}[n]$

$\varepsilon_y[n]$ will be same as $\varepsilon_{yn} = (y[n] - \hat{y}[n])$ only

1. when the encoder reads a new pulse.
2. when observation error $(y[n] - \hat{y}[n])$ is bigger than the resolution.

This is the condition for the update of $\varepsilon_y[n]$.

Except these two cases, $\varepsilon_y[n+k]$ will be calculated value based on the last output error ε_{yn}.

$$\varepsilon_y[n+k] = \mathbf{C}_d\mathbf{A}_d\left(\left(\mathbf{I} - \mathbf{L}\mathbf{C}_d\right)\mathbf{A}_d\right)^{k-1}\mathbf{E}_1\varepsilon_{yn} \tag{B.6}$$

Here we introduced the matrix $\mathbf{E}_1$

$$\mathbf{C}_d\mathbf{E}_1 = \mathbf{I}_m = 1, \quad \mathbf{E}_1 = \begin{pmatrix} 0 \\ 1 \\ 0 \end{pmatrix} \tag{B.7}$$

Using this predicted observation error, the proposed observer is designed as Figure B.4. This observer employs a latch instead of a switch which is adopted in the conventional observer.

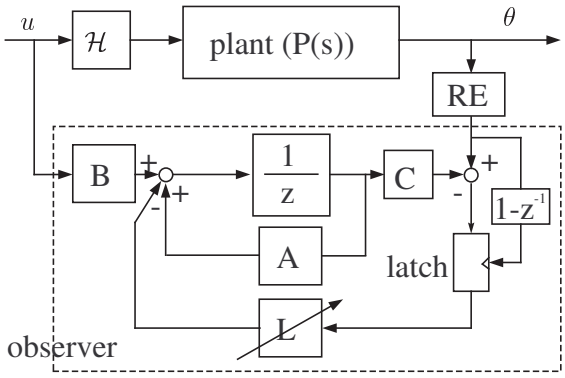

Figure B.4: Structure of the proposed instantaneous speed observer

A brief description of proposed observer is as follows,

$$\begin{cases} \hat{x}[n] = \mathbf{A}_d\hat{x}[n-1] + \mathbf{B}_d u[n-1] + \mathbf{L}\left(y[n] - \hat{y}[n]\right) \\ \quad \cdots \text{when the update condition of } \varepsilon_y[n] \text{ is satisfied} \\ \hat{x}[n+k] = \mathbf{A}_d\hat{x}[n+k-1] + \mathbf{B}_d u[n+k-1] + \mathbf{L}\varepsilon_y[n+k] \\ \qquad\qquad\qquad\qquad\qquad\qquad \cdots \text{otherwise.} \end{cases} \tag{B.8}$$

Error transition by this observer is given as

$$e[n+K+1] = \mathbf{G}_3(K+1)e[n] = \left(\mathbf{A}_d\mathbf{G}_3(K) - \mathbf{L}\mathbf{C}_d\mathbf{A}_d\left((\mathbf{I}-\mathbf{L}\mathbf{C}_d)\mathbf{A}_d\right)^K\mathbf{E}_1\mathbf{C}_d\right)e[n] \tag{B.9}$$

$\mathbf{G}_3(K+1)$ will change according to the equation (B.10)

$$\mathbf{G}_3(K+1) = \mathbf{A}_d\mathbf{G}_3(K) - \mathbf{L}\mathbf{C}_d\mathbf{A}_d\left(\left(\mathbf{I}-\mathbf{L}\mathbf{C}_d\right)\mathbf{A}_d\right)^K\mathbf{E}_1\mathbf{C}_d \tag{B.10}$$

To calculate the matrix $\mathbf{G}_3(K+1)$, we introduce a matrix $\mathbf{E}_2$:

$$\mathbf{E}_2 = \mathbf{I} - \mathbf{E}_1\mathbf{C}_d = \begin{pmatrix} 1 & 0 & 0 \\ 0 & 0 & 0 \\ 0 & 0 & 1 \end{pmatrix} \tag{B.11}$$

Multiplying on the left by this $\mathbf{E}_2$, the first and third columns of $\mathbf{G}_3$ can be calculated as follows,

$$\mathbf{G}_3(K+1)\mathbf{E}_2 = \mathbf{A}_d\mathbf{T}_{pr}(K)\mathbf{E}_2 = \mathbf{A}_d^K\mathbf{T}_{pr}(1)\mathbf{E}_2 = \mathbf{A}_d^K\left(\left(\mathbf{I}-\mathbf{L}\mathbf{C}_d\right)\mathbf{A}_d\right)\mathbf{E}_2 \tag{B.12}$$

In the same way, multiplying on the left by $\mathbf{E}_1$, the second column of $\mathbf{G}_3$ can be calculated as follows,

$$\begin{aligned}\mathbf{G}_3(K+1)\mathbf{E}_1 &= \mathbf{A}_d\mathbf{G}_3(K)\mathbf{E}_1 - \mathbf{L}\mathbf{C}_d\mathbf{A}_d\left(\left(\mathbf{I}-\mathbf{L}\mathbf{C}_d\right)\mathbf{A}_d\right)^K\mathbf{E}_1 \\ &= \left(\left(\mathbf{I}-\mathbf{L}\mathbf{C}_d\right)\mathbf{A}_d\right)^K\mathbf{G}_3(1)\mathbf{E}_1 = \left(\left(\mathbf{I}-\mathbf{L}\mathbf{C}_d\right)\mathbf{A}_d\right)^{K+1}\mathbf{E}_1\end{aligned} \tag{B.13}$$

Then, we can find out that $\mathbf{G}_3$ has the first and third columns of $\mathbf{G}_1$ in Equation (B.4) and the second column of $\mathbf{G}_2$ in equation (B.5).

$$\mathbf{G}_3(K+1) = \mathbf{G}_3(K+1)\mathbf{E}_1 + \mathbf{G}_3(K+1)\mathbf{E}_2 = \mathbf{A}_d^K\left(\left(\mathbf{I}-\mathbf{L}\mathbf{C}_d\right)\mathbf{A}_d\right)\mathbf{E}_2 + \left(\left(\mathbf{I}-\mathbf{L}\mathbf{C}_d\right)\mathbf{A}_d\right)^{K+1}\mathbf{E}_1 \tag{B.14}$$

Figure B.5 shows the transition of eigenvalues of $\mathbf{G}_3$ according to K. It shows smaller eigenvalues compared with $\mathbf{G}_1$ in Figure B.3. These smaller eigenvalues of $\mathbf{G}_3$ will result in the fast observation speed.

Fast convergence speed of the proposed observer is verified by a computer simulation. Figure B.6 shows observations of velocity and disturbance by a conventional observer and proposed observer. We can make sure that frequent output error feedback results in fast and good estimation.

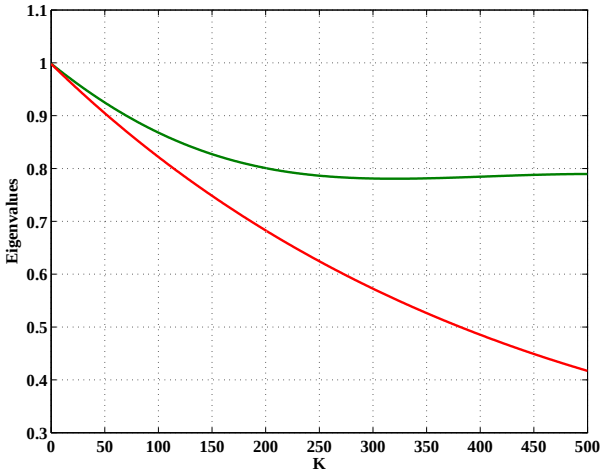

Figure B.5: Eigenvalue transitions of $\mathbf{G}_3$

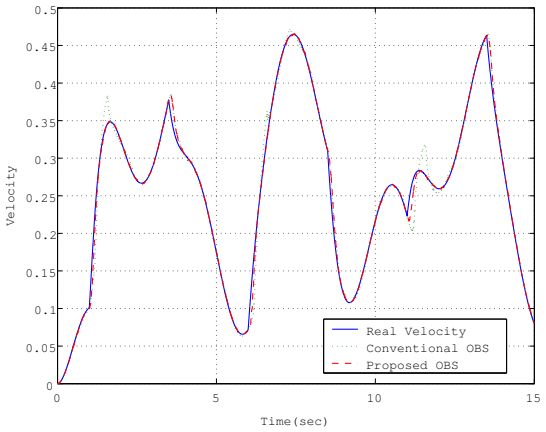

1) Velocity observations

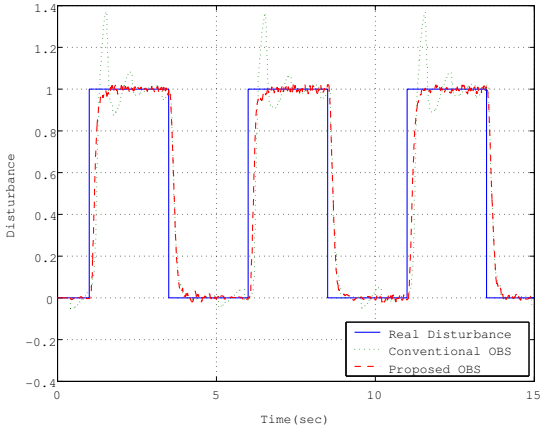

2) Disturbance observations

Figure B.6: Differences in convergence speed

Biblography

[1] Ohnishi Kouhe, etc. "Motion Control for Advanced Mechatronics", *IEEE/ASME Trans. on Mechatronics*, pp.56-67, Vol.1, No.1, March 1996.

[2] Dan Ding and Rory A. Copper: "Electric-Powered Wheelchairs", *IEEE Control Systems Magazine*, Vol. 25, No. 2, pp. 22- 34, 2005

[3] http://www.independencenow.com/

[4] Yoshihiko Takahashi, Tsuyoshi Takagaki, Jun Kishi, and Yohei Ishii: "Back and forward moving scheme of front wheel raising for inverse pendulum control wheelchair robot", *the 2001 IEEE Int. Conf. on Robotics and Automation*,pp. 3189-3194, Korea, May 21-26, 2001.

[5] Dowben, R.M.: "Contractility with Special Reference to Skeletal Muscle", in Mountcastle V (ed): *Medical Physiology*. St. Louis, CV Mosby, 1980, pp 95-96.

[6] K.Ito and T.Tsuji: "The Bilinear Characteristics of Muscle-Skeletomotor System and the Application to Prosthesis Control" , *Trans. IEE of Japan*, 105-C, 10, 201-208, 1985. (in Japanese)

[7] M.Kumamoto, T. Oshima, T. Yamamoto: "Control Properties Induced by the Existence of Antagonistic Pairs of Bi-articular Muscles - Mechanical Engineering Model Analyses", *Human Movement Science*, 13. pp.611-634, 1994.

[8] http://darbelofflab.mit.edu/Robotics/MASA/MASA.htm

[9] N. Hayashida, et al., "A Friction Compnesation in Twin Drive System" *6th INternational Workshop on Advanced Motion Control* pp. 187-192, 2000.

[10] David A. Winter: *Biomechanics and Motor Control of Human Movement*, John Wiley & Sons, Inc, 2005

[11] Naoki Hata, Yoichi Hori: "Backward Tumbling Control for Power Assisted Wheel-chair based on Phase Plane Analysis", *Medicine and Biology*, 2003.9, Mexico

[12] Takaji Umeno, Yoichi Hori: "Robust Speed Control of DC Servomotors using Modern Two-Degrees-of-Freedom Controller Design", *IEEE Trans. on Industrial Electronics*, Vol.38, No.5, pp.363-368, 1991

[13] Kenji Tamaki, Kiyoshi Ohishi, Kouhei Ohnishi and Hunio Miyachi: "Two-Degrees-of-Freedom Control of DC Servo Motor by Means of Passive Adaptive Control", *Transactions of the Society of Instrument and Control Engineers* Vol.22, No.11, pp.1175 1182, 1986. (in Japanese)

[14] Takeaki Sugimoto, Hirokazu Seki, Susumu Tadakuma: "Rectilinear Driving Improvement of Power Assisted Wheelchair Based on Disturbance Estimation of Right and Left Wheels", *Japan Industry Applications Society Conference 2004*, Y-35, 2004.

[15] Masato Abe: *Vehicle Dynamics and Control 2nd Revised Version*, Sankai-dou, 2003.(in Japanese)

[16] Yukiko Kaida, Toshiyuki Murakami: "An Approach to Detection of Human Input Torque and Its Application to Power Assist Motion in Electric Wheelchair" *Japan Industry Applications Society Conference 2004*, Vol II, pp.419-424, 2004. (in Japanese)

[17] B. Gopinath: "On the control of linear multiple input-output systems", *the Bell Technical Journal*, Vol. 50, No. 3, pp. 1063-1081, March, 1971.

[18] Y.Hori: "Design of Inertia Imulator using Disturbance Torque Observer", *Japan Industry Applications Society 1987*, pp.91-94, 1987. (in Japanese)

[19] H.Kazerooni, T.B.Sherindan, P.K. Houpt: "Robust Compliant Motion for Manipulators, PART I,II", *IEEE Journal of Robotics and Automation*, Vol.2, No.2, pp.83-105, 1986.

[20] Seiichiro Katsura, Kouhei Ohnishi: "Advanced Motion Control for Wheelchair Based on Environment Quarrier", *Trans. IEE of Japan*, Vol. 125-D, No. 7, pp. 698-704, 2005.

[21] Y. Mizoshita, S. Hasegawa, and K. Takaishi: "VIbration Minimized Access Control For Disk Drives", *IEEE Trans. on Magnetics*, Vol. 31, No. 3, pp.1793-1798, 1996.

[22] Tai Chien Hwa, Shin-ichiro Sakai, and Yoichi Hori: "Proposal of a Novel Method of Motion COntrol of Electric Vehicles Utilizing Speed Trajectory Shaping" *Japane Industry Applications Society Conference 2002*, Vol3. pp.1289-1292, 2002. (in Japanese)

[23] Joaquin A. Blaya and Hugh Herr: "Adaptive Control of a Variable-Impedance Ankle-Foot Orthosis to Assist Drop-Foot Gait", *IEEE Trans. on Neural Systems and Rehabilitation Engineering*, Vol. 12, No. 1, 2004.

[24] Dubey, R.V., Tan Fung Chan, Everett, S.E., "Variable damping impedance control of a bilateral telerobotic system ", *IEEE Control System Magazine*, pp.37-45, Vol.17, No.1, 1997.

[25] T. Yasuda, T. Sano, and K. Tanaka: "A manipulation mechanism with a ring for one hand use wheelchair", *Welfare Engineering Symposium 2004*, pp.31-34, 2004. (in Japanese)

[26] K. B. Oldham and J. Spanier: *The Fractional Clculus*, Academic Press, New York and London, 1974

[27] C. Ma : *Fractional Order Control and Its Applications in Motion Control*, Ph.D. dissertation, University of Tokyo, 2004.

[28] I. Podlubny: "Fractional Differential Equations", *Mathematics in Science and Enginerring* Vol. 198, New York and Tokyo, Academic Press. 1999.

[29] Yoichi Hori : "Robust and Adaptive Control of a Servomotor Using Low Precision Shaft Encoder", *IEEE IECON'93*, 1993.

[30] L. Kovudhikulrungsri, T. Koseki : "Improvement of Speed Estimation of an Induction Motor with a Low-Resolution Sensor for Pure Electric Braking System" *ICEE 2001*, pp. 43-47.

List of Publications

Journals

1. 呉 世訓, 堀 洋一, 「軸ねじれ振動抑制を考えたTCSC制御器設」計, 電気学会産業応用部門誌, Vol.120-D, No.8/9, pp.980-986, 2000.8

2. 呉 世訓, 堀 洋一, 「軸ねじれ振動抑制を考えたTCSC制御器設計」, 総合試験所年報, Vol.58, pp.253-258, 2000.1

3. Nobutaka Bando, Sehoon Oh and Yoichi Hori: "Disturbance Rejection Control based on Adaptive Identification of Transfer Characteristics from Acceleration Sensor for Hard Disk Drives System", 電気学会論文誌D部門, Vol. 123, No. 12, 2003.

4. 呉 世訓, 堀 洋一:「環境適用を目指した車椅子の運転状況オブザーバの設計と応用」, 電気学会産業応用部門誌 (投稿予定)

International conference

1. Sehoon Oh and Yoichi Hori, "TCSC Controller Design Considering Torsional Vibration Suppression in Turbine-Generator System", Proc. of IPEC-2000, Vol.3, pp.1357-1362, 2000.4

2. Nobutaka Bando, Sehoon Oh and Yoichi Hori: "External Disturbance Rejection Control Based on Identification of Transfer Characteristics from the Acceleration Sensor for Access Control of Hard Disk Drive System", Proc. of AMC 2002, pp.52-56, 2002.7.3-5, Maribor

3. Nobutaka Bando, Sehoon Oh and Yoichi Hori: "Acceleration Feedforward Control based on Adaptive Identification of Transfer Characteristics for Hard Disk Drives", IIP/ISPS Joint MIPE'03, pp. 28-29, 2003.

4. Sehoon Oh and Yoichi Hori: "A Novel Control Method for Power-assisted Wheel Chair", Proc. of 6th SNU-UOT Joint Seminar on Electrical Engineering, 2003.11, Seoul

5. Sehoon Oh, Naoki Hata, and Yoichi Hori: "Development of Various Observers for Intelligent Power Assist Control of a Wheelchair", SICE Annual Conference 2004

6. Sehoon Oh and Yoichi Hori: "Development of a Gravity Compensated Controller for Power Assisted Wheelchairs Using a Novel Instantaneous Speed Observer", Proc. 4th International Conference on Power Electronics and Motion Control (IPEMC 04), 2004.8.14-16, Xi'an, China

7. Sehoon Oh, Naoki Hata, Yoichi Hori: "Proposal of Human-friendly Motion Control - Control Design for Power Assistance Tools and its Application to Wheelchair", IECON 2004, 2004.11.2-7, Pusan (Best Presentation Award)

8. Sehoon Oh and Yoichi Hori : "Development of Noise Robust State Observer for Power Assisting Wheelchair and its Applications", IPEC-Niigata 2005, 2005.4.4-8, Niigata

9. Sehoon Oh, Naoki Hata, Yoichi Hori: "Control Developments for Wheelchairs in Slope Environments", ACC 2005, 2005.6.8-10, Portland, Oregon (Best Paper Presentation)

10. Sehoon Oh and Yoichi Hori : "Sensor Free Power Assisting Control Based on Velocity Control and Disturbance Observer", ISIE 2005, 2005.6.20-23, Dubrovnik, CROATIA (Student Forum, Second Prize)

11. Sehoon Oh and Yoichi Hori : "Lateral Disturbance Rejection and One Hand Propulsion Control of a Power Assisting Wheelchair", IECON 2005 (to be submitted)

Domestic conference

1. 呉 世訓, 堀 洋一, 「軸ねじれ振動抑制を考えたTCSC制御器設計」, 平成11年電気学会産業応用部門大会, 長崎, 1999.8

2. 呉 世訓, 堀 洋一, 「TCSCの非線形性を考慮したSSR振動抑制制御器の設計」, 電気学会産業計測制御研究会, IIC-00-21, 2000.3

3. 坂東信尚, 呉　世訓, 堀　洋一, 「加速度センサからの伝達特性に基づいた外部外乱抑圧制御器の磁気ディスク装置への応用」, 電気学会産業計測制御研究会, IIC-02-88, 2002.8

4. 渡邊 信哉, 畠 直輝, 呉 世訓, 堀 洋一, 「傾斜環境を考慮したパワーアシスト車椅子制御の高機能化」, 電気学会産業計測制御研究会, IIC-04-29, 2004.3

5. 呉 世訓, 堀 洋一: 「やわらかい外乱抑制を利用した人間親和型制御法の一提案」, 平成16年電気学会産業応用部門大会, 高松, 2004.9

6. 呉 世訓, 堀 洋一:「外乱オブザーバを利用した速度ベースのパワーアシスト制御器設計とロボットや車椅子への応用」, IIC-05-12, 2005.3

7. 呉 世訓, 堀 洋一:「環境適用を目指した車椅子の運転状況オブザーバの設計と応用」, 平成17年電気学会産業応用部門大会, 福井, 2005.8

8. 呉 世訓, 堀 洋一:「車椅子における 2 次元制御を応用した片手漕ぎの実現」, 第 23 回日本ロボット学会学術講演会, 2005.9 (投稿中)